AN ABSTRACT OF THE THESIS OF

GEORGE GARY ICE for the degree of DOCTOR OF PHILOSOPHY

in FOREST ENGINEERING presented on January 12, 1978

Title: REAERATION IN A TURBULENT STREAM SYSTEM

Abstract approved: _____
George W. Brown

The oxygen concentration in a stream is an important parameter of water quality. Changes in oxygen concentrations can affect various stream organisms including fish. Foresters have become concerned with predicting the impacts of forest activities on oxygen levels in streams. Slash, which accumulates in streams as a result of harvesting activities, is a food source for stream organisms. During aerobic respiration, oxygen is utilized. Under some conditions the oxygen concentration can be depleted below acceptable levels. Large, fish bearing streams are generally well protected by forest practice regulations. For smaller streams without fish populations, the issue is one of downstream impairment of water quality as deoxygenated water enters fish-bearing reaches.

A natural process counteracting oxygen depletion is reaeration. Reaeration is the exchange of gases between the atmosphere and water. This process operates to maintain oxygen near the saturation concentration. The change in the

oxygen deficit in a stream is a function of the existing deficit and the reaeration rate coefficient.

The objective of this study was to develop a predictive equation for the reaeration rate coefficient based on the hydraulic characteristics of stream channels. This is a a first step in developing guidelines to regulate harvesting residues in streams. Seven natural stream sites were selected in Oregon. These sites represented a wide range of hydraulic conditions. The stream reaches were segregated into segments of uniform hydraulic characteristics. Sodium sulfite was injected into the stream to artificially deplete the oxygen concentration. The recovery of the oxygen concentration was used to determine the reaeration rate coefficient.

Several models for the reaeration process were tested using regression techniques. Some were models proposed by other investigators and some were developed independently. The predictive equation which fit the data best is a function of the maximum unit energy dissipation rate (E_D) and a depth parameter (H_D):

$$K2_{20} = 37 \frac{E_D^{1/2}}{H_D^{2/3}}$$

This equation is consistent with theoretical descriptions of gas exchange phenomena. As the rate of energy dissipation increases in a segment, the turbulence in the

segment also increases. Turbulence promotes an increase in the liquid-atmosphere interface area and in the exchange rate of volume elements in the interface. Reaeration is stimulated when deaerated water from the bulk flow of the stream replaces the oxygen saturated water in the surface film. As the area of liquid-atmosphere contact increases, the total flux of oxygen molecules into the depleted fluid volume increases. As the fluid volume increases, the change in concentration for a specific flux of molecules decreases. The depth term (H_D) can be used to describe the ratio of the surface area to the volume of fluid in the segment. In this study, the depth term used was the discharge divided by the mean width and maximum velocity. This approach adjusts for dead zones that do not actively mix with the bulk flow.

For field applications, predicting the reaeration coefficient for any temperature (T) requires that the slope (s), active width (W_D), maximum velocity (U_D), and discharge (Q), be measured for uniform stream segments. These variables are combined in the following equation:

$$K2_T = 1.016^{(T-20)} \; 37 \; \frac{W_D^{2/3} s^{1/2} g^{1/2} U_D^{7/6}}{Q^{2/3}}$$

Using the predicted reaeration rates, estimates of mean segment velocities, biochemical oxygen demand loading, and rates of oxygen demand decay, it is possible to predict the

oxygen concentration of a stream moving through and downstream from a harvesting site. The reaeration rate influences the maximum deficit and time required for recovery and can be used to evaluate the risks that debris accumulations pose to water quality.

REAERATION IN A TURBULENT STREAM SYSTEM

by

George Gary Ice

A THESIS

submitted to

Oregon State University

in partial fulfillment of
the requirements for the
degree of

Doctor of Philosophy

June 1978

APPROVED:

Professor of Forest Engineering
in charge of major

Head of Department of Forest Engineering

Dean of Graduate School

Date thesis is presented January 12, 1978

Typed by Deanna L. Cramer for George Gary Ice

ACKNOWLEDGEMENTS

I wish to thank the many friends, fellow students, and professors who provided me with moral support and assistance during my years at Oregon State University and University of California at Berkeley. I especially want to thank Dr. George Brown who provided invaluable support and guidance throughout this study. Thanks also to my committee, Dr. Hank Froehlich, Dr. Jim Hall, Dr. Ken Williamson, Dr. Dave Bella, Dr. Bob Krahmer, and Dr. Roy Brooks, for their efforts in my research and education.

The financial assistance provided by the Oregon State University School of Forestry, Forest Research Laboratory, and Water Resources Research Institute is gratefully acknowledged.

I owe a special thanks to my family. My parents, George and Rubye Ice and brother, Gene, always provided me with encouragement. My wife, Catherine Roberts, not only supported and encouraged me but also helped in the field work and in the preparation of the text.

TABLE OF CONTENTS

Table of Contents -- continued

LIST OF TABLES

LIST OF FIGURES

REAERATION IN A TURBULENT STREAM SYSTEM

INTRODUCTION

The harvesting and removal of timber provides an important economic base to the Pacific Northwest. These same silvicultural activities can endanger water quality by modifying associated forest stream ecosystems. In the Pacific Northwest, small forest streams are often valuable spawning and rearing sites. Even when streams provide no fish habitat, they may influence water quality downstream where it is critical for fish habitat. Because of these conflicts, it is necessary to be able to predict the impact of forest activities on water quality in a wide range of stream systems.

The dissolved oxygen concentration is an important component of the water quality. The suitability of a stream as a fish habitat is dependent on adequate oxygen concentrations. Changes in stream oxygen concentrations can affect the development, growth, activity, reproductive capacity, and survival of a variety of stream organisms.

The concentration of oxygen in a stream is a function of the solubility of oxygen and the various sources and sinks that modify the oxygen concentration. Harvesting can affect each of these factors. For example, harvesting activities can increase the load of organic debris in the

stream, modify streambed characteristics, and alter the physical environment of the stream system causing large changes in stream temperature.

Accelerated accumulations of organic debris are a major concern of foresters. Debris deposited in a stream is available to organisms as a food source. The oxygen concentration of a stream can be depleted as the organic matter is oxidized during respiration of these organisms.

Reaeration is a process that counteracts oxygen depletion in small streams. During this process gas is exchanged between the atmosphere and the water. This physical process operates to modify the oxygen concentration in a stream towards its saturation value. The difference between the saturation concentration and actual concentration is the oxygen deficit. Molecular diffusion causes a flux of oxygen molecules into a solution with a deficit. The change in the deficit of a gas in a body of liquid is a function of the existing deficit and a rate constant. This relationship can be expressed as a first order kinetic reaction.

Stream segments with large reaeration rates can assimilate greater amounts of organic debris before the deficits become unacceptable. The time required for the stream to recover from a deficit is also shorter for streams with larger reaeration rates. For these reasons, foresters need to be able to predict the reaeration rate for a stream in

order to model the impact of forest operations on the stream environment.

Implementation of the Federal Water Pollution Control Act Amendments of 1972 (Public Law 92-500) calls for identification of "silviculturally related nonpoint sources of pollution" and development of "procedures and methods including land use requirements to control to the extent feasible such [pollution] sources." The Oregon Forest Practices Act and Public Law 92-500 require that streams important to fisheries be protected and that water quality be maintained at high levels.

Much of the controversy about developing best management practices for forest sites is associated with small first and second order streams. These small streams are classified as class II streams in the Oregon Forest Practices Act. These are streams that have not been identified as directly important for fish habitat, recreation, or domestic use. The concern, however, is that deaerated water, leachates, and organic debris from class II streams can be transported downstream to adversely impact class I streams which have important fish resources.

Data on reaeration rates in these typically small and turbulent streams is limited. Direct measurement of reaeration for all sites would be ideal. Unfortunately, direct measurement of reaeration would be a difficult and costly technique to apply to all forest streams near North-

west harvesting sites. Further, the reaeration rate is related to the hydraulic properties of the stream. Therefore, directly measured values become invalid with changes in discharge rates and streambed characteristics.

A predictive equation for the reaeration rate which is based on stream hydraulic characteristics would allow foresters to evaluate where potential oxygen problems might occur. Using a predicted reaeration rate coefficient, the projected organic loading, and decay rate constants, the oxygen concentration within and downstream from a harvesting site can be calculated.

It is important that foresters be able to discriminate between sites that may have oxygen problems and sites that can tolerate organic inputs. Where a stream cannot assimilate large amounts of organic debris, it may be necessary to prescribe buffer strips or streamside management zones around the streams. This could be a costly reduction of the timber available for havesting on a site. The clean-up of debris deposited in the stream and special felling techniques are alternative procedures for treating sensitive sites. Buffer strips, stream clean-up, and special harvesting techniques generally increase operation costs, thus reducing revenues. Streamside zones are often the most productive. The removal of these sites from commercial wood production conflicts with society's needs for future wood supplies. Therefore, the social cost of reduced

future timber revenues must be considered. On the other hand, the economic and social consequences of allowing practices which adversely deplete oxygen are fish mortality and habitat reduction.

The purpose of this study is to develop a predictive method for estimating reaeration rate coefficients that could be used to predict reaeration downstream from harvest units. One of the criteria for the method is that it be suitable for use in the field. Using the predicted reaeration rate, foresters can estimate the distance required for a stream to recover from organic debris inputs and oxygen deficits, and the maximum deficit that could be expected. The relative sensitivity of streams to organic loads can also be evaluated.

LITERATURE REVIEW

Solubility

> Gasses dissolve in liquids to form true solutions with the degree of solubility depending on the nature of the gas, the nature of the solvent, the pressure, and the temperature (Landine 1971).

Solutions are homogeneous mixtures in a similar phase. In stream systems, water acts as a solvent for many substances. All gases, including oxygen and carbon dioxide, dissolve in water to become components or solutes in the solution. The solubility of a gas defines the concentration at which an equilibrium exists between the gas in solution and the gas in the atmosphere. From a molecular viewpoint, oxygen molecules in the water and in the atmosphere are constantly in random motion. At saturation, oxygen molecules enter and leave the solution at the same rate. The relative rate at which gas molecules move from the atmosphere to the water can be related to the pressure of the gas species in the atmosphere. Maron and Prutton (1965) suggest that one can consider "the gas as a solute which vaporizes to establish a vapor pressure above the solution." Under these conditions:

$$a_s = f \cdot k \qquad (1)$$

where f is the fugacity of the gas above the solution, a_s is the activity of the gas in solution, and k is a constant.

For an ideal gas phase, the fugacity is equal to the partial pressure of the gas above the solution. For an ideal solution, the activity is equal to the mole fraction. If temperature remains constant, the mole fraction and weight of a gas per unit volume of solution can be related. This approach yields Henry's Law which states:

> The weight of any gas that will dissolve in a given volume of a liquid, at constant temperature, is directly proportional to the pressure that the gas exerts above the liquid (Sawyer and McCarthy 1967).

Henry's Law is expressed as:

$$C_s = H_L \cdot P_{gas} \qquad (2)$$

where C_s is the saturation concentration in mg/l, H_L is the Henry's Law constant in mg/l · mm Hg (or mg/cm^3 · pascal), and P_{gas} is the partial pressure of the gas species in mm Hg (or pascals).

The partial pressure of oxygen can be determined using the principles of Dalton's Law.

> In a mixture of gases, such as air, each gas exerts pressure independently of the others. The partial pressure of each gas is proportional to the amount (percent by volume) of the gas in the mixture, or in other words, it is equal to the pressure which that gas would exert if it were the sole occupant of the volume available to the mixture (Sawyer and McCarthy 1967).

Since oxygen remains at a relatively constant proportion in the atmosphere, the partial pressure of oxygen is proportional to the barometric pressure. The volumetric

proportion of oxygen reported in the literature ranges from 20.90% to 21.00%, with 20.95% being the most widely accepted figure (Landine 1971). Saturation values are usually reported for 1 atm barometric pressure (760 mm Hg or 101,308 pascals). Conversion of standard pressure saturation values to actual saturation values can be made using the equation:

$$C_s = C_s' \frac{P - p}{P_{st} - p} \qquad (3)$$

where (in SI units) P_{st} is 101,308 pascals, P is the barometric pressure in pascals, p is the vapor pressure of the water at the given water temperature in pascals, C_s' is the saturation concentration of oxygen in kg/m^3 at 101,308 pascals (1 atm) and a given water temperature, and C_s is the actual saturation concentration in kg/m^3. Expressed in more conventional units, P_{st} is 760 mm Hg, P and p are measured in mm Hg, and C_s' and C_s are measured in mg/l.

The solubility of a gas in water is inversely related to water temperature. Maron and Prutton (1967) note:

> If a substance dissolves at saturation with evolution of heat, then solubility decreases with rising temperature. On the other hand, if a substance dissolves with absorption of heat, the solubility increases as the temperature is raised.

The solubility of oxygen for different temperatures and at a standard pressure has been measured in several studies (Whipple and Whipple 1911; Truesdale 1955; Churchill et al. 1962; Montgomery 1964). Both Holtje (1971) and

and Landine (1971) reviewed oxygen saturation values and concluded that the values used by "Standard Methods"[1] were the least accurate. Landine concludes that Montgomery's values are, in theory, the most accurate. Holtje suggests that the experimental techniques used in the Churchill study make that data the most acceptable. Saturation values developed by the Churchill and Montgomery studies are very close, particularly over the range of 5°C to 15°C. Appendix III lists empirical equations developed from four temperature-saturation studies and includes a table listing the corresponding saturation values between 0°C and 30°C.

Modeling Dissolved Oxygen

Dissolved oxygen is an important component in the physical environment of aquatic organisms. The dissolved oxygen concentration in a stream is vulnerable to significant changes due to natural shifts and man-made disturbances. Modeling the impacts of human activities on dissolved oxygen has become an important tool for controlling detrimental changes in water quality and aquatic habitats.

In order to model the behavior of dissolved oxygen in streams, it is necessary to determine how dissolved oxygen enters streams and how it is removed. The processes that

---

[1] Standard Methods for the Examination of Water and Wastewater, published by the American Public Health Assoc., Inc., New York.

contribute or remove oxygen are known as sources and sinks. Some processes can be either sources or sinks depending on stream conditions. One such process is the exchange of oxygen between the atmosphere and stream. The movement of oxygen into solution is called reaeration.

Pioneering work on reaeration was done by Adeney and Becker in 1914. In their study they used the concept of a gas deficit which is the difference between the saturation and actual gas concentration in a solution. Working with oxygen and nitrogen gases, they found that the change in the gas deficit in a body of liquid was a function of its existing deficit and a rate constant. The rate constant is now referred to as the reaeration rate constant, reaeration coefficient, or exchange coefficient. The change in the gas deficit is expressed as a first order kinetic reaction:

$$\frac{dD}{dt} = -K_2 D \tag{4}$$

where D is the deficit in mg/l (or kg/m^3), t is time in days (or s), and K_2 is the reaeration coefficient in $days^{-1}$ (or s^{-1}).

A second major step in oxygen modeling resulted from the Streeter and Phelps (1925) study of natural purification in the Ohio River. They assumed that the only sink for oxygen in the Ohio River was the oxygen demand of organisms and chemicals that were oxidizing organic matter

in the water. This oxygen sink, called the biochemical oxygen demand, could be modeled (like the reaeration process) as a first order kinetic equation. The biochemical oxygen demand (BOD) is the amount of oxygen organisms require to oxidize organic matter to a non-reactive state. The rate at which oxygen is utilized for oxidation is a function of the total biochemical oxygen demand and a rate constant.

The rate of BOD utilization is expressed as:

$$\frac{dL}{dt} = -K_1 L \tag{5}$$

where L is the BOD in mg/l (or kg/m^3), t is time in days (or s) and K_1 is the BOD rate constant in $days^{-1}$ (or s^{-1}).

The oxidation of organic matter results in a decrease in the BOD. The oxidation also utilizes dissolved oxygen and therefore increases the dissolved oxygen deficit. Since both the deficit and BOD are expressed in units of mg/l (or kg/m^3) of oxygen, the equations for atmospheric reaeration and biochemical oxygen demand can be combined. Streeter and Phelps combined equations (4) and (5) to yield:

$$\frac{dD}{dt} = -\frac{dL}{dt} \tag{6}$$

From equation 6, the equation for the oxygen sag curve was developed:

$$D = \frac{K_1 L_0}{K_2 - K_1} e^{-K_1 t} + \left[D_0 - \frac{K_1 L_0}{K_2 - K_1}\right] e^{-K_2 t} \qquad (7)$$

where L_0 is the initial BOD in mg/l (or kg/m^3) and D_0 is the initial deficit in mg/l (of kg/m^3).

The development of the oxygen sag curve allowed prediction of a future oxygen deficit if information on the K_1, K_2, L_0, D_0, and t were available. It also enabled calculation of any one of these variables from measurements of the others.

More detailed models based on the work of Streeter and Phelps have been proposed to account for additional oxygen sources and sinks. Figure 1 diagrams the possible sources and sinks of oxygen in surface water. Oxygen sources that can be modeled include reaeration, inflowing oxygenated water, and photosynthesis. Oxygen sinks can include biochemical oxygen demand, respiration of photosynthetic organisms, inflowing deoxygenated water, deaeration of supersaturated water and benthic oxygen demand. Most oxygen models assume that the river approaches a uniform and steady state condition with the stream cross section being completely mixed. This allows one-dimensional modeling of dissolved oxygen concentrations along a reach and simplifies the equation. Additional complexity is required where significant diurnal or tidal fluctuations occur, where longitudinal dispersion modifies dissolved oxygen and BOD concentrations, where other mechanisms

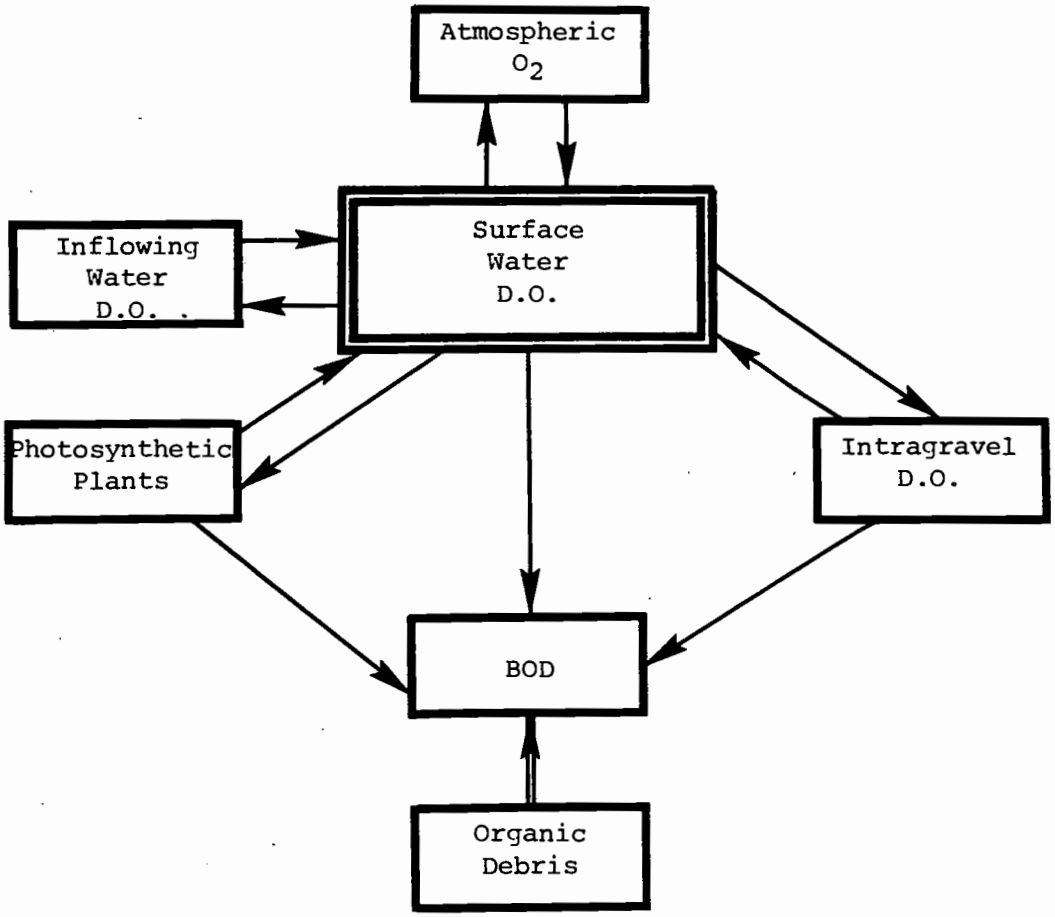

Figure 1. Sources and sinks of dissolved oxygen in a small stream system.

contribute to BOD inputs and removal, and where other factors invalidate the model assumptions.

Several more detailed models using the balancing approach of Streeter and Phelps have been found to be appropriate under various stream conditions.

The Streeter and Phelps model accounted for the processes of reaeration and biochemical oxygen demand. Camp (1963) presented an oxygen balance which also accounted for constant additions of BOD along the study reach, settling of the BOD to the stream bottom, and photosynthesis. Camp's equations were originally developed using base 10 constants for the atmospheric reaeration rate constant (k_2), the deoxygenation rate constant (k_1), and the BOD settling rate constant (k_3) in days^{-1} (or s^{-1}). When converted to base e constants, Camp's balance for the change in the oxygen deficit and BOD are shown as:

$$\frac{dD}{dt} = (-K_2D + K_1L) - a \qquad (8)$$

$$\frac{dL}{dt} = (-K_1 + K_3)\ L + P_B \qquad (9)$$

where a is the rate of photosynthesis by algae in mg/l/day (or kg/m^3/s), and P_B is the rate of BOD additions to the stream from bottom deposits in mg/l/day (or kg/m^3/s).

Dobbins (1964) developed oxygen balance equations for many of the same processes that Camp had modeled and

included consideration of longitudinal dispersion. Dobbins uses the following equations:

$$\frac{\partial C}{\partial t} + U \frac{\partial C}{\partial x} = D_x \frac{\partial^2 C}{\partial x^2} + K_2 D - K_1 L - a \qquad (10)$$

$$\frac{\partial L}{\partial t} + U \frac{\partial L}{\partial x} = D_x \frac{\partial^2 L}{\partial x^2} - (K_1 + K_3) L + P_B \qquad (11)$$

where U is the mean velocity in miles/day (or m/s), C is the concentration of oxygen, x is the longitudinal distance in miles (or m), and D_x is the longitudinal dispersion coefficient in miles^2/day (or m^2/s). Dobbins notes that a is the net effect of plant respiration and photosynthesis and that it can be either a source (negative) or a sink (positive).

For a steady state and uniformly flowing stream, $\frac{\partial L}{\partial t}$ and $\frac{\partial C}{\partial t}$ become zero. As the coefficient for longitudinal dispersion becomes small, the Dobbins equation becomes equivalent to that of Camp. If photosynthesis, BOD additions and settling become unimportant, then the simplified equation is equal to the Streeter and Phelps model.

Simplified modeling of English streams by Edwards and Owens (1962) and Owens and Edwards (1966) assumed that the rates of processes were independent of time and longitudinal position. The basic equation they used is:

$$Q_{ox} = P_{ox} \pm D_{ox} - R_{ox} \qquad (12)$$

where Q_{ox} is the rate of change of dissolved oxygen in g/m^2/day (or $kg/m^2/s$), P_{ox} is the rate of oxygen production by photosynthesis in g/m^2/day (or $kg/m^2/s$), D_{ox} is the rate of oxygen transfer through the stream surface in g/m^2/day (or $kg/m^2/s$), and R_{ox} is the rate of oxygen utilization by respiration in g/m^2/day (or kg/m^2/day).

A more detailed model was later proposed in which the respiration and photosynthetic units of the oxygen system were more completely segregated. This model is expressed as:

$$Q_{ox} = P_B + P_P - R_M - R_B - R_P + D_{ox} \qquad (13)$$

where P_B is the rate of photosynthesis by bottom plants, P_P is the rate of photosynthesis by phytoplankton, R_M is the respiration rate of bottom deposits, R_B is the respiration rate of attached bottom plants, and R_P is the respiration rate of unattached phytoplankton. All terms are in units of g/m^2/day (or $kg/m^2/s$).

Bennett and Rathbun (1972), in reviewing this equation, noted that the term R_{BOD} should be added in polluted streams. Bennett and Rathbun also noted that the term D_{ox} can be related to the Streeter and Phelps term $\frac{dD}{dt}$ if the assumptions made by Owens and Edwards are correct. D_{ox} is defined by the equation:

$$D_{ox} = f_{ox}(\bar{C}_s - \bar{C}) \qquad (14)$$

where f_{ox} is the exchange coefficient in m/day (or m/s).

Under the special conditions of a steady state, uniform stream where the process rates remain constant, the deficit would also remain constant and therefore $\bar{C}_s - \bar{C}$ could be replaced by $C_s - C$ in equation 14. When the left side of equation 14 is divided by the mean depth of the stream, it becomes equivalent to the change in the oxygen concentration over time. Comparison of equation 14 with equation 4 shows that the term f_{ox} divided by the mean depth of the stream becomes equivalent to the reaeration coefficient (K_2).

From studies on the biochemical oxygen demand created by logs, needles, and leaves, Schaumburg and Atkinson (1970), Atkinson (1971), and Berry (1974) concluded that BOD additions could not realistically be modeled as either slug or constant inputs. Berry noted that the BOD leaches from the slash before it is available for rapid oxidation. Soluble organics, once released from the slash, are then oxidized according to the process described by equation 4. Berry visualized the leaching process as a linear first order decay reaction. Equation 15 represents the leaching process:

$$\frac{dS}{dt} = -K_4 S \qquad (15)$$

where S is the potential BOD remaining as slash in mg/l (or kg/m^3) and K_4 is the leaching rate constant in $days^{-1}$ (or s^{-1}).

Using the varying addition rate expressed in equation 15, Berry solved for the rate change of the soluble BOD (L):

$$\frac{dL}{dt} = K_4 S_0 \, e^{-K_4 t} - K_1 L \qquad (16)$$

where S_0 is the initial slash BOD in mg/l (or kg/m^3).

In cases concerned with logging debris in streams, Berry showed that equation 16 can be substituted for equation 9. The dissolved oxygen deficit is then found using equation 17:

$$D = \frac{K_1}{K_2 - K_4} \left(L_0 - \frac{K_4 S_0}{K_1 - K_4}\right)\left(e^{-K_4 t} - e^{-K_2 t}\right) + \frac{K_1}{K_2 - K_4} \left(\frac{K_4 S_0}{K_1 - K_4}\right)\left(e^{-K_4 t} - e^{-K_2 t}\right) + D_0 e^{-K_2 t} \qquad (17)$$

Equation 17 is applicable for forest streams where there is steady and uniform flow, uniform debris loading, constant temperature, and no scouring, deposition, or photosynthesis.

Atmospheric Reaeration

With the development of models to simulate oxygen processes in streams, it has become necessary to estimate the parameters and coefficients in the various models. Atmospheric reaeration acts to adjust gas concentrations in solutions toward saturation as defined by equation 4. When stream temperature and barometric pressure are known, it has

been shown that the saturation concentration of oxygen can be calculated. Measuring the actual dissolved oxygen concentration permits determination of the deficit. Knowing the deficit allows calculation of the rate of gas exchange when the reaeration rate constant (K_2) is known or can be predicted.

Several different approaches to predicting reaeration coefficients have been used. Early research and practical observations showed that the rate of gas transfer between the atmosphere and a solution is much more rapid in agitated fluids than in quiescent fluids. As internal motions or turbulence increase, the rate of gas transfer increases. Turbulence results where the viscous forces of adhesion and cohesion become small compared to inertial forces. Volume elements are swirled and mixed within the bulk motion in an irregular and unpredictable spectrum of motions. Because turbulence arises from the physical interaction of the stream and its channel, the accepted approach has been to predict reaeration rates using stream flow and channel parameters. This overall approach which links the rate of reaeration to physical and hydraulic parameters has been examined in two different types of studies: those which concentrate on gas exchange theories, and those which are empirical or semi-empirical in nature.

Gas Exchange Theories

An attempt to explain reaeration on a theoretical basis was made by Whitman (1923) and Lewis and Whitman (1924). They theorized that a laminar layer of gas and a laminar layer of liquid existed at the gas-liquid interface. If the reaeration process operates through these laminar layers then the transport of oxygen through the films to the bulk of the liquid can be defined by the equation:

$$N = k_L(C_i - C_L) = k_G(p_G - p_i) \qquad (18)$$

where N is the mass of oxygen moving through the films in mg/cm^2s (or kg/m^2s), C_L and C_i are the concentrations of oxygen in the bulk water phase and interface in mg/l (or kg/m^3), p_G and p_i are the partial pressures in the gas phase and at the interface in mm Hg (or pascals), k_L is the liquid film coefficient in $days^{-1}$ (or s^{-1}), and k_G is the gas film coefficient in mg/mm/Hg days (or kg/pascal/s).

It is not possible to measure the concentration or pressure within the surface films, but it is possible to measure the concentration in the bulk of the liquid and the partial pressure in the atmosphere, and to determine the saturation value for the liquid. Using these bulk values, equation 19 defines the transport of oxygen:

$$N = K_L(C_s - C_L) = K_G(p_G - p_s) \qquad (19)$$

where C_s is the saturation concentration in mg/l (or kg/m^3), p_s is the partial pressure of oxygen at saturation in mm Hg (or pascals), and K_L and K_G are the overall liquid film and gas film coefficients in cm/day (or m/s).

Combining Henry's Law (equation 2) with equation 19 yields:

$$\frac{1}{K_L} = \frac{1}{H_L k_G} + \frac{1}{k_L} \tag{20}$$

Bennett and Rathbun note that for sparingly soluble solutions, such as oxygen and carbon dioxide, H_L is extremely large so that the term $\frac{1}{H_L k_G}$ becomes extremely small. It was therefore determined that K_L is approximately equal to k_L and that the liquid film exerts the most control over the rate of oxygen exchange (see Appendix II).

Mass transfer across the liquid film is visualized as occurring by molecular diffusion. This process can be modeled using Fick's first law of diffusion, which states that the total flux of mass across a boundary (N) is a function of the concentration gradient, area of interface, and a diffusion coefficient. For the Lewis and Whitman model, the process can be expressed using the equation:

$$N = D_m \frac{C_s - C_L}{\chi} \tag{21}$$

where D_m is the molecular diffusivity in ft^2/day (or m^2/s), and χ is the film thickness in ft (or m).

From the definition of N, Lewis and Whitman showed that:

$$N(\frac{A}{V}) = \frac{dC}{dt} \tag{22}$$

Combining equations 4, 21 and 22 they derived the equation:

$$K_2 = \frac{N}{D}(\frac{A}{V}) = (\frac{D_m}{\chi})(\frac{A}{V}) \tag{23}$$

where D is the deficit in mg/l (or kg/m^3). Isaacs and Gaudy (1968) note that this equation proved impractical because of the problems in measuring χ. Furthermore, the concept of laminar layers becomes less realistic as stream turbulence increases. This theory did show that both the solvent characteristics accounted for by D_m and the hydrodynamic characteristics accounted for by χ were important.

Higbie (1955) and Danckwerts (1951) also visualized the water surface as being bounded by a laminar liquid film. In their models, an attempt was made to account for the role of turbulence in increasing the rate of gas exchange.

Higbie's penetration theory proposed that K_2 was a function of the contact time of turbulent surface eddies at the interface. Fick's second law of diffusion is represented by the equation:

$$\frac{\partial C}{\partial t} = D_m \frac{\partial^2 C}{\partial y^2} \tag{24}$$

where y is the depth in ft (or m) from the surface. Higbie assumed an infinitely deep film. This is a good assumption when film thickness is large relative to the depth penetrated by diffusing molecules. Higbie defined the following boundaries:

$$C = C_L \text{ when } t = 0, \quad y = 0$$

$$C = C_L \text{ when } t > 0, \quad y = \infty$$

$$C = C_s \text{ when } t > 0, \quad y = 0$$

He assumed that the surface elements were mixed with the bulk volume after a uniform time (t_e) within the surface film. He was then able to solve for the concentration change and rate of exchange. When equation 24 is solved according to Higbie's assumptions, equation 25 results:

$$C = C_L + (C_s - C_L)\ \text{erfc}\left(\frac{y}{2\sqrt{tD_m}}\right) , \qquad (25)$$

where C is the concentration of the fluid after time t in mg/l (or kg/m^3). For the contact period of t_e, the gas absorbed per unit surface area can be expressed as:

$$N\ t_e = 2(C_s - C_L)\sqrt{\frac{D_m t_e}{\pi}} \qquad (26)$$

If the left side of equation 26 is divided by $(C_s - C_L)\,t_e$, an equation for the liquid film coefficient K_L results:

$$K_L = 2\sqrt{\frac{D_m}{\pi t_e}} \qquad (27)$$

Multiplying the liquid film coefficient by the stream surface area (A) and dividing by the volume of the stream segment (V) yields the reaeration rate coefficient:

$$K_2 = 2 \frac{A}{V} \sqrt{\frac{D_m}{\pi t_e}} \tag{28}$$

Danckwerts concluded that the films and laminar boundary layers proposed by Lewis, Whitman, and Highbie could not exist in a unified form under turbulent conditions. Instead of assuming a single liquid film with one contact period (t_e), Danckwerts modeled a surface film, parts of which are constantly being renewed. Replacement of volume elements at the surface is assumed to be independent of the age of the elements. Portions of the surface film are constantly being replaced by new volume elements at the rate of r (in s^{-1}). Using these assumptions, Danckwerts derived equation 29:

$$\phi = r\, e^{-r\theta} \tag{29}$$

where θ is the age of the surface in s and ϕ is the surface age distribution function.

The absorption of gas into those surface elements of age θ is represented by the equation:

$$N\theta = \theta(C_s - C_L) r\, e^{-r\theta} \sqrt{\frac{D_m}{\pi\theta}}\, d\theta \tag{30}$$

The mean rate of absorption per unit area of turbulent surface is represented by equation 31:

$$N = (C_s - C_L) \sqrt{D_m} \int_0^\infty \frac{r\, e^{-r\theta}}{\sqrt{\pi\theta}}\, d\theta \qquad (31)$$

which can be simplified to equation 32:

$$N = (C_s - C_L) \sqrt{D_m r} \qquad (32)$$

The equation for the liquid film coefficient can be derived from equations 19 and 32:

$$K_L = \sqrt{D_m r} \qquad (33)$$

Multiplying by the surface area and dividing by the segment volume yields the reaeration rate equation:

$$K_2 = \frac{A}{V} \sqrt{D_m r} \qquad (34)$$

The models of both Higbie and Danckwerts recognized the role of turbulence in reaeration. Unfortunately, the parameters t_e and r are unmeasurable.

Dobbins (1956, 1964, 1965) and O'Connor and Dobbins (1956) developed a model in which a laminar film of thickness χ overtops the turbulent bulk flow. Using the age distribution assumed by Danckwerts (equation 29), Fick's second law of diffusion (equation 24), and the boundary conditions:

$$C = C_L \text{ when } t = 0, \quad 0 < y \leq \chi$$

$$C = C_s \text{ when } t \geq 0, \quad y = 0$$

$$C = C_L \text{ when } t \geq 0, \quad y = \chi$$

a solution for the liquid film coefficient was developed:

$$K_L = \sqrt{D_m r} \coth \left(\frac{r\chi^2}{D_m}\right)^{\frac{1}{2}} \tag{35}$$

Another model, which does not assume a film at the liquid surface, but does assume periods of quiescence in vertical columns was also proposed:

$$K_L = \sqrt{D_m r} \tanh \left(\frac{rH^2}{D_m}\right)^{\frac{1}{2}} \tag{36}$$

where H is the hydraulic depth of the stream in ft (or m). Since the terms $\coth \left(\frac{r\chi^2}{D_m}\right)^{\frac{1}{2}}$ and $\tanh \left(\frac{rH^2}{D_m}\right)^{\frac{1}{2}}$ approach 1 for most stream conditions, Dobbins suggested that equations 35 and 36 be simplified to:

$$K_2 = K_L \frac{A}{V} \frac{(D_m r)^{\frac{1}{2}}}{H} \tag{37}$$

It should be noted that equation 34 solved by Danckwerts and equation 37 are identical. As in Danckwerts' model, the problem of estimating the renewal rate (r) and its relationship to stream turbulence remains.

O'Connor and Dobbins noted that velocity fluctuations occur along the x, y, and z axes. The velocity of the fluid in one of these directions at any time can be

expressed by considering the mean velocity in that direction and any velocity fluctuation. For example, the downstream velocity at any time can be defined by the term U ± u, where U is the mean velocity in the x direction and u is the difference between the observed and mean velocities. If the velocity fluctuations along the separate axes are not correlated, then the turbulence is considered isotropic. Isotropic turbulent flow is found in cases where there is no shearing stress or velocity gradient. In nonisotropic turbulence, found in shallow open channels, there is a significant correlation between the velocity fluctuations. For Chezy coefficients less than 17, nonisotropic turbulence is assumed to exist.

O'Connor and Dobbins used Prandtl's mixing length hypothesis to describe the scale of turbulence. According to Prandtl's hypothesis:

$$|\bar{u}| = l \frac{dU}{dy} \tag{38}$$

where $|\bar{u}|$ is the mean absolute velocity fluctuation in the x direction in ft/s (or m/s), $\frac{dU}{dy}$ is the velocity gradient in the y direction, and l is the mixing length in ft (or m). The parameter l represents the distance a water particle departs from the mean motion before it returns to the main body. Dobbins and O'Connor suggested that l is a measure of the average size of an eddy. Increases in $|\bar{u}|$ imply that turbulence is becoming more intense and that the rate of

renewal will increase. An increase in l means that the eddy size is increasing, thus retarding renewal. It was therefore proposed that the ratio $\frac{|\bar{u}|}{l}$ be used to define the rate of surface renewal (r). Substituting r for $\frac{|\bar{u}|}{l}$, equation 38 becomes:

$$r = \frac{dU}{dy} \tag{39}$$

The von Karman universal logarithmic velocity law was used to define the velocity gradient $\frac{dU}{dy}$ and the renewal rate (r):

$$r = \frac{dU}{dy} = \frac{(Hgs)^{\frac{1}{2}}}{K_o H} \tag{40}$$

where K_o is the von Karman constant, g is the gravitational constant, and s is the slope of the energy gradient in ft/mile. Assuming a constant value of 0.4 for K_o, the solution to equation 36 can be derived:

$$K_2 = \frac{480}{0.434} \frac{D_m^{\frac{1}{2}} s^{\frac{1}{4}}}{H^{5/4}} \tag{41}$$

O'Connor and Dobbins note that the assumptions of 0.4 for the von Karman constant is not always valid. This is particularly true where the scale of the bed roughness approaches the stream depth (H).

In isotropic turbulence, the velocity gradient approaches zero. Therefore, the velocity gradient cannot be used to predict the vertical velocity fluctuations. In

order to predict renewal rates under isotropic conditions, O'Connor and Dobbins used Kalinske's measurements of vertical velocity fluctuations and mixing lengths in the Mississippi River. From this data it was shown that equation 42 was appropriate for isotropic turbulent conditions:

$$r = \frac{U}{H} \tag{42}$$

The reaeration rate constant could then be defined as:

$$K_2 = \frac{D_m^{\frac{1}{2}}}{H} \left(\frac{U}{H}\right)^{\frac{1}{2}} \tag{43}$$

Dobbins based a later study (1964) on many of the same assumptions that he and O'Connor had used to develop equation 36. Dobbins suggests that it is the "small eddies by which most of the conversion of kinetic energy into heat takes place." At the surface, small eddies are dissipating energy generated from bottom shear. Dobbins assumed that the potential energy loss per unit mass of liquid (E) in ft/s (or m/s) was proportional to the turbulent energy per unit mass of liquid at the surface (E_S). Accounting for the effect of surface tension (σ) in ft·lb/ft^2 (or pascal · m) and density (ρ) in slugs/ft^3 (or kg/m^3), he theorized that the renewal rate could be expressed as:

$$r = \frac{c_1 \rho \chi E}{\sigma} \tag{44}$$

where c_1 is a constant.

Dobbins assumed that the effective film thickness was related to the minimum size of eddy that could form. Kolmogoroff described the limiting eddy size as a function of the stream kinematic viscosity (ν) in ft^2/s (or m^2/s) Using this relationship, Dobbins expressed the film thickness as:

$$\chi = \left(\frac{\nu^3}{E}\right)^{\frac{1}{4}} c \qquad (45)$$

where c is a proportionality constant.

Dobbins noted that stream turbulence can deform the water surface from a smooth plane. The actual surface area (A) exposed to atmospheric gas exchange can be significantly different from the area calculated by measuring the stream width and length. Using the new definitions for A, r, and x and accounting for temperature effects, Dobbins rewrote equation 35 as:

$$K_2 = \frac{0.12\ C_A A E^{3/8}\ \coth\left(\frac{B E^{1/8}}{C_4^{\frac{1}{2}}}\right)}{0.434\ C_4^{3/2} H} \qquad (46)$$

where:

$$C_A = 1.0 + F^2$$

$$C_4 = 0.9 + F$$

$$A = 9.68 + 0.054(T-20)$$

$$B = 0.976 + 0.0137(30-T)^{3/2}$$

$$E = 30.0(sU)$$

$F = \frac{U}{\sqrt{gH}}$ = the Froude number

U = velocity in ft/s

s = slope of energy grade line in ft/1000 ft

T = temperature in °C

H = depth of stream in ft

K_2 = reaeration constant in $days^{-1}$

Metzger and Dobbins (1967) and Metzger (1968) presented an improved version of equation 46 in which they substituted the surface compression modulus (M_s) for the surface tension (σ). Using this substitution, the equation accurately predicts the rate-retarding effects of surface-active agents on reaeration. In waters not polluted by detergents, the renewal rate can be expressed using the equation:

$$r = \frac{1.3\ \rho\ \nu^{3/4}\ E^{3/4}}{C_4{}^3} \qquad (47)$$

where $C_4 = 0.9 + F$. Dobbins states that the coefficient C_4 "reflects to a large degree the fraction of the total energy dissipation which occurs near the surface."

Isaac and Maag (1969) criticize equations 41 and 43 for incorrectly evaluating r and χ. Parkhurst and Pomeroy (1972) praise the work but note its dependence on the concept of a limiting eddy size. Wilson and MacCleod (1974), in reviewing predictive equations for reaeration coefficients, state:

> Of all correlations examined, those of Dobbins (1965) and of Parkhurst and Pomeroy (1972) give the most reliable prediction over the whole range of sewer and river data...

Thackston and Krenkel (1969) assumed that the reaeration coefficient was a function of the surface renewal and was inversely proportional to the depth of the stream. In the Danckwerts and O'Connor and Dobbins models, the reaeration coefficient was found to be proportional to $r^{\frac{1}{2}}$. Thackston and Krenkel proposed that K_2 should be proportional to r.

Krenkel (1960) suggested that r was proportional to the longitudinal mixing coefficient (D_L) in ft/day (or m/s). D_L averages turbulent effects and was assumed to be proportional to the average eddy diffusivity (k_y) in ft/day (or m/s). In nonuniform streams, D_L proved to be a poor prediction of K_L and r.

According to Krenkel, the momentum transfer coefficient (ε_y) in ft^2/day (or m^2/s) "... is often considered to be equal to, or proportional to ..." the eddy diffusivity (k_y). Data from Al-Saffar showed that the shear velocity (U*) in ft/s (or m/s) could be calculated from the mean momentum transfer coefficient ($\bar{\varepsilon}_y$):

$$U^* = \frac{6\bar{\varepsilon}_y}{K_o H} \tag{48}$$

where K_o is von Karman's constant.

Thackston and Krenkel combined equation 48 with the equation:

$$\varepsilon_y = K_o U^* \left(1 - \frac{Y}{H}\right) \tag{49}$$

which is based on the Vanoni modification of the von Karman universal velocity distribution. This yielded the equation:

$$\varepsilon_y = 6\bar{\varepsilon}_y \frac{Y}{H}\left(1 - \frac{Y}{H}\right) \tag{50}$$

The authors noted that equation 50 required ε_y at any relative depth $(\frac{Y}{H})$ to be linearly proportional to $\bar{\varepsilon}_y$. $\bar{\varepsilon}_y$ was found to be proportional to shear velocity (U*) and depth (H). Using these principles, the solution for the vertical mass transfer coefficient (k_y) at the surface is:

$$k_{y_{surface}} = C_1 \frac{K_o}{6} HU^* = C_2 HU^* \tag{51}$$

where C_1 and C_2 are constants. The vertical mass transfer coefficient at the surface $(k_{y_{surface}})$ was assumed to be proportional to the renewal rate (r). The reaeration rate coefficient (K_2) is therefore expressed by the equation:

$$K_2 = C_4 \frac{C_2 HU^*}{H^2} = C_5 \frac{U^*}{H} \tag{52}$$

Reducing equation 52 to its most fundamental form yields the equation:

$$K_2 = \frac{0.000125}{0.434} \left[1 + \left(\frac{\bar{U}}{\sqrt{gH}}\right)^{\frac{1}{2}}\right] \sqrt{\frac{sg}{H}} \qquad (53)$$

This equation also accounts for an increased area of interface due to surface deformation.

Miyamoto (1932) and Tsivoglou (1967) suggested reaeration models which are based on the movement of gas molecules at the stream surface. The Miyamoto model is:

$$K_2 = \frac{A}{0.434\ H} \frac{R\ T_K^{\frac{1}{2}}}{2\ M} e^{(-M/2R\ T_K)(\nu_m)} \qquad (54)$$

where R is the ideal gas constant in liter-atmospheres/°K, T_K is the temperature in °K, M is the molecular weight of the gas (oxygen) in g/mole, and ν_m is the velocity (perpendicular to the interface) that a solute molecule must attain in order to leave the liquid.

Bennett and Rathbun, in reviewing this model, state that the escape velocity term (ν_m) reflects the role of turbulence in reaeration. The term $M(\nu_m)^2/2$ is the activation energy necessary for escape from the liquid. Local shear stress can influence the activation energy, and shear stress is also related to turbulence. The variable ν_m has not been measured.

Tsivoglou developed his model using the steady state condition of saturation. At saturation the rate of movement of gas molecules into the water (r_e in mg/s) is equal to the rate of movement of gas molecules out of the water

(r_o in mg/s). The rate at which molecules move into solution is a function of the gas concentration in the atmosphere. The rate of molecules moving out of solution is a function of the concentration of the dissolved gas in the liquid at the interface. Tsivoglou modeled r_o as:

$$r_o = b(hC_w n_s A) \tag{55}$$

where h is the thickness of liquid available for loss of gas, b is the percent of molecules being lost from h, C_w is the concentration of dissolved gas at the surface, n_s is the number of fresh surfaces exposed at the interface, and A is the area of interface. At saturation, r_e equals r_o:

$$r_e = r_o = b(hC_w n_s A) = b(hC_s n_s A) \tag{56}$$

where C_s is the concentration of dissolved gas at saturation. The rate of molecules entering the solution remains constant even when the solution is not at saturation. Equation 57 describes the flux of molecules across the interface:

$$r_e - r_o = bhn_s A(C_s - C_w) \tag{57}$$

The quantity $(C_s - C_w)$ is the deficit at the surface. Assuming that the surface deficit and bulk deficit can be related, then the reaeration coefficient (K_2) can be expressed by the equation:

$$K_2 = (bhn_s A/V) \tag{58}$$

For equation 58 to be valid, it is not necessary for a segregated film to exist.

Fortescue and Pearson (1967) and Lamont and Scott (1970) have developed predictive models based on eddy movements at the surface. Fortescue and Pearson modeled stream flow as consisting of a series of square rolling cells of dimension L_e. The velocity of an eddy in the longitudinal or vertical direction was modeled as a function of size of the eddy cell, spatial position within the cell, and average kinetic energy of the cell. Using appropriate boundary conditions to solve for a two dimensional representation of Fick's second law of diffusion, the liquid film coefficient may be expressed as:

$$K_L = \frac{1.46}{0.434} \frac{D_m u}{L_e} \tag{59}$$

O'Connor and Dobbins showed that $u/L_e = U/M$. The predictive equation for the reaeration rate coefficient is:

$$K_2 = \frac{1.46}{0.434} \left(\frac{1}{H}\right) \left(\frac{D_m U}{H}\right)^{\frac{1}{2}} \tag{60}$$

Lamont and Scott (1976) modeled stream flow at the surface as consisting of large eddies with small eddies superimposed upon them. They considered the form of eddies to be similar to the square cell used by Fortescue and

Pearson. The local transfer rate of solute across the interface is dependent on eddy size, energy, and molecular diffusivity. Using an energy spectrum based on a Fourier decomposition of a turbulent velocity field, a variety of eddy conditions could be estimated. The overall transfer coefficient is the sum of gas transfer rates from all eddy sizes. The equation for reaeration is:

$$K_2 \alpha \frac{1}{H} \left(\frac{\nu}{D_m}\right)^{-\frac{1}{2}} (E\nu)^{\frac{1}{4}} \qquad (61)$$

where E is the rate of energy dissipated by turbulence per unit mass in cm^2/s^3 (or m^2/s^3). This model has not been evaluated for open channel conditions because it was developed for industrial applications.

Empirical Equations

Many attempts have been made to measure hydraulic parameters and correlate them directly to the reaeration coefficient.

Streeter and Phelps correlated measured reaeration rates against several streamflow characteristics in the Ohio River. They proposed that the reaeration rate constant could be predicted using the equation:

$$K_2 = \frac{C}{0.434} \frac{U^n}{H_m^2} \qquad (62)$$

where the coefficient C is a function of stream surface slope, H_m is the depth above the minimum flow in ft (or m), U is the velocity in ft/s (or m/s), and η is a function of the mean relative increase in velocity with a 5 ft increase in depth. This formula is applicable only for those reaches of the Ohio River studied and only during periods in which the discharge levels are comparable to those studied (Wilson and Macleod 1974). Bennett and Rathbun noted that the parameters used by Streeter and Phelps were artificial.

In 1962 Churchill et al. studied reaeration below dams. This investigation is frequently cited because it was made under almost ideal field conditions. The water released from the dam was deoxygenated but free of biological oxygen demand. The equation developed and recommended by Churchill et al. is:

$$K_{2(T)} = 5 \frac{U}{R_h^{5/3}} (1.0241)^{T-20} \quad (63)$$

where R_h is the hydraulic radius in ft (or m) and T is the temperature in °C.

Several studies by Isaacs et al. (1968, 1969a, 1969b), 1970) developed predictive equations for reaeration. The basic form of the equations is:

$$K_2 = c \frac{U}{H^{3/2}} \quad (64)$$

Many factors, including the streambed configuration and bottom roughness, were considered. The coefficient c is defined by the equation:

$$c = c' \ (D_m^{\frac{1}{2}} \ \nu^{1/6} \ g^{-1/6}) \tag{65}$$

where c' changes with the shape of the channel, D_m is the molecular diffusivity, ν is the kinematic viscosity, and g is the gravitational constant. This definition of c means that equation 64 is dimensionally constant. Isaacs et al. evaluated the data of Churchill et al. and found c to be equal to 3.739. The study channels used by Isaacs had values for c of 3.051 and 2.440.

Isaacs showed that if the bottom shape and velocity distribution for a stream are known, then the reaeration coefficient can be more accurately described by integrating equation 64 over the cross section. Equation 66 accounts for variation in shape and velocity over the stream cross section while using overall velocity and depth parameters:

$$K_{2_T} = \bar{c} \ \phi_S \ \phi_U \ \frac{U}{H^{3/2}} \ (1.0241)^{T-20} \tag{66}$$

where ϕ_S and ϕ_U are constants for shape and velocity.

Parkhurst and Pomeroy (1972) developed a predictive equation for the "superficial exchange coefficient for oxygen" from the general formula:

$$K_L = \phi_{UN}, \ \phi_F C_A \phi_P \phi_S \phi_T \ (sU)^m \ R_h^n \tag{67}$$

where ϕ_{UN}, ϕ_F, C_A, ϕ_P, ϕ_S, and ϕ_T are coefficients adjusting the equation for units, general fit, the ratio of actual interface to hydraulic width, water purity effects, channel shape effects, and temperature effects, respectively. The exponent n which controls the role of the hydraulic radius has been used in a number of studies and assigned values from -5/3 to +0.34. Parkhurst and Pomeroy defined C_A as the ratio of "the area of actual air-water interface to the superficial area of a stream." Dobbins estimated that:

$$C_A = 1 + 0.3\ F^2 \tag{68}$$

where F is the Froude number. Parkhurst and Pomeroy suggest that an analysis of sewer data yields the following improved equation:

$$C_A = 1 + 0.17\ F^2 \tag{69}$$

Thackston and Krenkel estimated C_A from the equation:

$$C_A = 1 + F^{0.5} \tag{70}$$

Parkhurst and Pomeroy analyzed the energy dissipation term $(sU)^m$ in relation to sewer data and estimated m at 0.375. Solving for the coefficients ϕ_N, ϕ_F, ϕ_P, and ϕ_S yields the following solution:

$$K_L = 0.96\ (1 + 0.17\ F^2)\ \phi_T\ (sU)^{3/8} \tag{71}$$

where U is in m/s and K_L is in m/hr (or m/s). Velocity (U) can be predicted from the slope and discharge of the channel. Using the equation:

$$U = c\ s^{0.41}\ Q^{0.24} \tag{72}$$

where Q is the discharge in m/s, s is the slope, and c is a constant, Parkhurst and Pomeroy developed the equation:

$$K_2 = K_L \frac{A}{H} = 24(0.96)c^{3/8}(1 + 0.17F^2)\ \phi_T\ s^{0.53}\ Q^{0.09} \tag{73}$$

where K_2 is in $days^{-1}$.

Owens, Edwards, and Gibbs (1964) developed an empirical equation for small English streams by artificially depleting dissolved oxygen. Using data from their own study and the Churchill study, the English group proposed that the reaeration coefficient could be estimated by the equation:

$$K_2 = \frac{9.41}{0.434}\ U^{0.67}\ H^{-1.85} \tag{74}$$

Isaacs and Maag criticized the use of data sets that were not continuous and noted that the equation was biased in favor of sites where reaeration was rapid.

Holtje (1971) studied reaeration rates in a small Oregon stream using procedures similar to those employed by Owens, Edwards and Gibbs. Holtje recommended the equation:

$$K_{2(T)} = 1.016^{(T-20)}\ (181.6\ sUg - 1657\ s + 20.86)\ \ (2.304) \tag{75}$$

as the best predictor of reaeration rates in small, turbulent mountain streams. Although Holtje's equation showed a correlation coefficient of 0.9920, it is strongly influenced by a few large K_2 values and shows substantial variations where K_2 values are small. Critical oxygen problems are more likely to occur where reaeration is slow. The general use of this equation must also be questioned because it is based on data from a single stream site.

Extreme Turbulence Effects

Most of the equations discussed above for predicting the reaeration rate coefficient were developed under the assumption that the surface remains continuous. In many small streams this is not the case. Where turbulence is severe, entrainment of bubbles, free fall, and droplet formation may contribute to an increasing rate of reaeration.

Physical descriptions of extremely turbulent flow have been presented by Straub and Anderson (1958), Gangadharaiah et al. (1970), and Lakshmana Rao et al. (1970). Straub and Anderson, using experimental channels, found that self-aerated flow had two regions of aeration:

> ... an upper region consisting primarily of independent droplets and larger agglomerations of water that move independently of the stream proper and a lower region in which discrete air bubbles are suspended in a turbulent stream and are distributed by the mechanism of turbulence.

The volume of entrained air was shown to be dependent on the depth of the channel and on the intensity of the turbulent fluctuations generated at the bottom of the channel. The mean concentration of air in the water (by volume) was correlated to $U^*/d_T^{2/3}$ or $s'/q^{1/5}$ where d_T is the transitional depth between the upper and lower zones of flow, s' is the sine function of the slope angle and q is unit discharge.

Gangadharaiah et al. concluded:

> For inception of air entrainment to occur, it is shown that the surface eddies should leave the free surface, besides the whole fluid becoming fully developed turbulent flow.

They refined work by Straub and Anderson, relating the mean air concentration to the Froude number and to energy loss.

Reaeration in Falls

Small drops and falls are sites of rapid reaeration. Holtje found the highest K_2 values in small drops. The hydraulic conditions of a drop differ significantly from those found in riffles, rapids, or pools. Under the most extreme conditions, the water will leave the streambed entirely and then dissipate energy in a hydraulic jump at the bottom of the drop.

A study by Gameson and Barrett (1978) defined the reaeration process at a weir as:

$$\frac{D_1}{D_2} = W_c(Ht_1 - Ht_2) + 1 \qquad (76)$$

where D_1 and D_2 are the upstream and downstream oxygen deficits in mg/l (or kg/m^3), Ht_1 and Ht_2 are the water surface elevations in m, and W_c is the weir reaeration constant. Parkhurst and Pomeroy suggested that the equation:

$$-\frac{dD_0}{d(Ht_1 - Ht_2)} = K_H D_O \qquad (77)$$

might be used if reaeration is assumed to be proportional to change in the potential energy ($mgH_1 - mgH_2$). The term m is the mass of the water flow over the drop and g is the gravitational constant. Equation 76 provides a linear fit to data, whereas equation 77 is logarithmic. In studying sloping passages and turbulent streams, Gameson found K_H values of only 0.088. K_H values for weirs with unpolluted water were 0.54.

Tebbutt (1972) reports studies on cascades (a series of drops) in which a deficit ratio (r_D) was used to evaluate reaeration characteristics. The deficit ratio defined by Tebbutts is expressed by the equation:

$$r_D = \frac{1 - \frac{D_1}{C_{s(1)}}}{1 - \frac{D_2}{C_{s(2)}}} \qquad (78)$$

where $C_{s(1)}$ and $C_{s(2)}$ are the saturation values in mg/l (or kg/m^3) above and below the cascade and D_1 and D_2 are the corresponding deficits in mg/l (or kg/m^3). Tebbutt found that r_D could be calculated from the expression:

$$r_D = 1 + \frac{a' \, b_f \, \Delta Ht}{2} \tag{79}$$

where a' is a coefficient for pollutant interference with reaeration, b_f is a coefficient for the fall pattern (free or step) and ΔHt is the height of the drop. Expressed in terms of the weir coefficient (from equation 76):

$$W_C = \frac{r_D - 1}{\Delta Ht} \tag{80}$$

Tebbutt's studies indicated that there may be an optimum step size for maximum reaeration and that increasing discharge over a drop will reduce the reaeration coefficient.

Another indication that mechanisms differ between normal turbulent flow and flow in falls is found in the influence of temperature on reaeration rates. Parkhurst and Pomeroy found that temperature affects free fall reaeration in a linear rather than logarithmic manner:

> The principal disparate information is from the measurements of the effects of weirs and waterfalls. Extrapolating from the observations in streams, a low temperature coefficient would be expected, but the coefficient found by Gameson, Vandyke, and Ogden is similar to that expected from slow streams and the temperature dependence

> appears to be linear rather than exponential. Perhaps the different aeration mechanisms in waterfalls alters the temperature effect.

Bubble Mass Transfer

Much theoretical work has been done in the field of industrial engineering to describe and quantify the process of mass transfer between bubbles and liquids. Even under controlled conditions with the release of uniformly sized bubbles, the liquid mass transfer coefficient (K_L) is not constant. Calderbank and Lochiel (1964) state: "Since the size, shape, and velocity of a bubble change appreciably as it rises and dissolves, its mass transfer coefficient should also vary accordingly." Deindoerfer and Humphrey (1961) indicate that as the age of a bubble increases, the mass transfer coefficient decreases. In natural streams, the relative oxygen concentrations of the bubble and the liquid will determine whether bubbles decrease in size (as in a deaerated liquid) or increase (as in a supersaturated liquid).

Equations predicting the liquid mass transfer coefficient from a single bubble have been developed from both theoretical and empirical studies. Higbie (1935), Calderbank and Lochiel, and Johnson et al. (1969) developed similar equations in the form:

$$K_L = c \left(\frac{D_m U_b}{de}\right)^{\frac{1}{2}} \qquad (81)$$

where D_m is the molecular diffusivity in cm^2/s (or m^2/s), de is the equivalent spherical diameter of the bubble in cm (or m), and U_b is the velocity of the rising bubble in cm/s (or m/s). Values assigned to c range from 1.13 to 1.36.

Haberman and Morton (1954) developed an equation for the velocity of a rising bubble in water:

$$U_b = 1.02 \ (g \ \frac{de}{2})^{\frac{1}{2}} \tag{82}$$

where g is the gravitational constant in cm/s^2 (or m/s^2). Baird and Davidson (1962), using equation 82, developed the equation:

$$K_L = 0.975 \ de^{-\frac{1}{4}} \ D_m^{\frac{1}{2}} \ g^{\frac{1}{4}} \tag{83}$$

Johnson et al., accounting for bubble shape distortion and transfer from the frontal surface only, developed the equation:

$$K_L = 1.13 \ (\frac{U_b D_m}{de})^{\frac{1}{2}} \ (\frac{de}{0.58 + 0.23 \ de})^{\frac{1}{2}} \tag{84}$$

Equation 84 was adjusted to fit experimental data and account for exchange at the rear surface of the bubble:

$$K_L = 1.13 \ (\frac{D_m U_b}{0.45 + 0.2 \ de})^{\frac{1}{2}} \tag{85}$$

Equation 85 closely fits data measured by Baird and Davidson, Leonard and Houghton (1963), Calderbank and Lochiel, and Johnson et al.

Droplet Reaeration

Studies on droplet reaeration evolved from work done on bubble mass transfer.

Lewis and Whitman (1924) studied gas absorption from bubbles using the equation:[1]

$$\ln \left(\frac{C_s - C_0}{C_s - C_t}\right) = \frac{10^6}{\omega} K_L A t \qquad (86)$$

where ω is the weight of the water column in lb (or kg), A is the area of the bubble surface in ft^2 (or m^2), t is the time in hrs (or s), C_s is the oxygen saturation of the water column in ppm (or kg/m^3), C_0 is the initial concentration, C_t is the concentration at time t, and K_L is the oxygen transfer coefficient in lbs of oxygen per hour of exposure, per ft^2 of bubble surface, and per ppm deficit (or m/s). From equation 86 it can be shown that:

$$K_2 = \frac{K_L}{H} = \frac{10^6}{\omega} K_L A \qquad (87)$$

where H is the mean depth of the column in ft (or m), and K_2 is in units of $days^{-1}$ (or s^{-1}).

Ippen *et al.* (1952) showed that K_L could be calculated by modifying equation 86 to the form:

$$K_L = \frac{dC}{dt} \left(\frac{\omega}{10^6}\right) \frac{1}{A(C_s - C_t)} \qquad (88)$$

---

[1] Equation 86 has been adjusted to base e.

Carver used equation 88 to evaluate the gas transfer process of droplets. In his study, the properties of droplets were substituted for the properties of the liquid column. ω became the weight of the droplet and C_s, C_0, and C_t became the oxygen concentrations of the droplet.

Two separate tests were conducted. In tests with deaerated droplets, the oxygen transfer coefficient (K_L) decreased as the size of the droplet increased. In tests with fully aerated droplets in a nitrogen atmosphere, K_L was found to increase with the size of the droplet. No explanation of this discrepancy was presented; however, the data for deaerated droplets was collected over a very small range of droplet sizes (0.47 to 0.54 cm^2). Tests in the nitrogen atmosphere used a much larger size range (0.15 to 0.50 cm^2) and may be subject to less error. In the tests with deaerated droplets, K_L became independent of droplet size as the oxygen concentration of the droplet approached saturation.

Banks and Herrera (1977), in considering the influences of wind and rain on the reaeration rate in lakes and lagoons, discussed the role of rain droplets in reaeration. Using data collected by the Thames Survey Committee and Water Pollution Research Laboratory (1964), Banks and Herrera were able to show that rain droplets increased oxygen transfer both through direct addition of oxygen from the aerated droplets (as in measurements by Carver) and through

increased circulation at the surface resulting from droplet bombardment. The Thames investigators used a tank stirred by an impeller to measure the overall reaeration rate when rainfall and mixing unassociated with the rainfall occur simultaneously. They found that the overall equation for oxygen transfer could be defined as:

$$K_L = K_I + R_r(a_1 - a_2K_I) \tag{89}$$

where K_I is the oxygen transfer coefficient due to the impeller mixing in cm/s (or m/s), a_1 and a_2 are constants dependent on tank characteristics, and R_r is the total rainfall rate in cm/s (or m/s). When no forces other than rainfall are contributing to oxygen transfer, the equation for K_L would be simply:

$$K_L = K_D = R_r a_1 \tag{90}$$

where K_D is the oxygen transfer rate resulting from droplet disturbances. For uniform droplet size and uniform velocity, the power of the rainfall (P_r) in ergs/s·cm^2 (or watts) can be expressed by the equation:

$$P_r = \tfrac{1}{2}\rho R_r U_d^2 \tag{91}$$

where U_d is the velocity of the falling droplet in cm/s (or m/s) and ρ is the density of the water droplet in slug/ft^3 (or kg/m^3). Banks and Herrera noted that because both P_r

and K_D are proportional to R_r, K_D could be assumed to be a function of P.

Reaeration Measurement Techniques

Three general methods can be used to measure the reaeration rate coefficient. In streams where the oxygen concentration is depleted below saturation (or elevated above saturation), the reaeration rate coefficient can be calculated from a balance of sources and sinks of oxygen. Streeter and Phelps, using equation 7, were able to solve for K_2 by measuring K_1, L_0, D_0, D_t, and t.

In streams where natural or man-caused deficits do not occur, artificial deficits can be created by chemical reduction of the dissolved oxygen. Using this procedure under pollution-free conditions eliminates the need to measure K_1 and L_0. Owens et al. (1964) used this method for their study. This disturbed equilibrium method will be discussed in greater detail under "Procedures."

Another technique measures the loss of a radioactive gas from solution. Tsivoglou (1967) showed that:

$$\frac{K_a}{K_b} = \frac{Dm_a}{Dm_b} = \frac{d_b}{d_a} \qquad (92)$$

where K_a and K_b are the gas exchange constants for gas species a and b, Dm_a and Dm_b are molecular diffusivities, and d_a and d_b are diameters of the gas molecules. If a

reaeration rate coefficient is determined for any gas species, the coefficient can be calculated for any other gas. Tsivoglou injected a slug of the radioactive noble gas krypton^{85} and tritiated water. Dispersion was accounted for by measuring the ratio of the krypton^{85} to the tritiated water at times 0 and t. The gas exchange constant for krypton^{85} can be calculated using the equation:

$$K_{kr} = \frac{\ln\left(\frac{C_{kr}}{C_{tr}}\right)_0 - \ln\left(\frac{C_{kr}}{C_{tr}}\right)_t}{t} \qquad (93)$$

where C_{kr} is the concentration of krypton^{85} in mg/l (or kg/m^3), C_{tr} is the tritium concentration in mg/l (or kg/m^3), t is the time in days (or s), and K_{kr} is the krypton^{85} rate coefficient. Combining the results of equation 93 with equation 92, the oxygen reaeration coefficient for a stream can be determined. Tsivoglou has used this procedure in polluted streams in order to make a measurement of K_2 that is independent of other oxygen-modifying sources and sinks.

STUDY SITES

Seven streams were selected for field testing. These sites were chosen because they represent a range of hydraulic conditions that would typically be found in small first or second order Oregon streams. Two streams are in the Willamette Valley, two are in the Coast Range, and three are in the Cascade Range (Figure 2).

Oak Creek

The Oak Creek site is located in the Willamette Valley, 6.5 km (4 miles) north of Corvallis. Oak Creek is a tributary of the Marys River. joining it near the confluence of the Willamette River. The Oak Creek study site is near the south entrance of McDonald Forest, an experimental tract owned and managed by Oregon State University. Immediately downstream is an experimental vortex weir and gaging station. Upstream about 200 m is an experimental flume. Discharge measured during the study varied from less than 0.006 m^3/s (0.2 cfs) to nearly 0.03 m^3/s (1 cfs). At the top of the study reach elevation is about 146 m (480 ft) above msl.

The study section is a natural channel. Along this stretch of Oak Creek the streambed has long pools separated by riffles. The streambed varies from silty in the pools to rocky in the steep sections. Surrounding vegetation

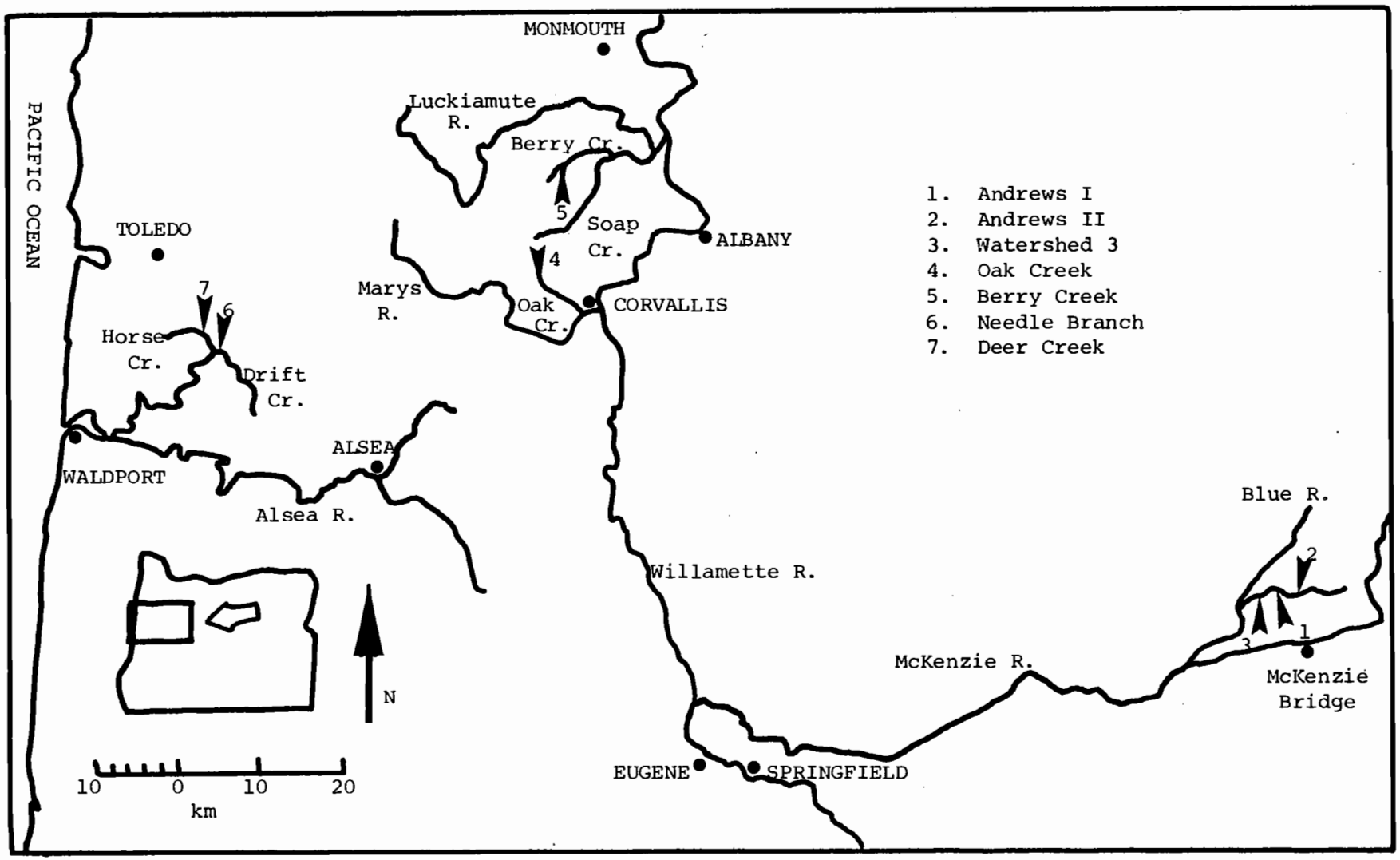

Figure 2. Map of study sites in western Oregon.

includes red alder (Alnus rubra Nutt.), bigleaf maple (Acer macrophyllum Pursh.), black cottonwood (Populus trichocarpa Torr. and Gray), Pacific serviceberry (Amelanchier alnifolia Nutt. var. semiintegerifolia (Hook) C. L. Hitchc.), mountain snowberry (Symphoricarpos mollis Nutt.), Himalaya blackberry (Rubus procerus Muell.), and poison oak (Rhus diversiloba Torr. and Gray).

Six segments were recognized as hydraulically distinct in the study reach. Segments 1, 2, and 4 are pools with very low gradients and velocities of flow. Segments 3, 5, and 6 are riffles with exposed rock. The six segments total 87.5 m (287 ft) in length. Total drop over the study reach is about 1.2 m (4 ft).

Berry Creek

Berry Creek is located about 16 km (10 miles) north of Corvallis in Dunn Forest, another tract owned by Oregon State University. Berry Creek is a tributary of Soap Creek which flows into the Luckiamute River. The Luckiamute is a tributary of the Willamette River.

The study site is surrounded by second growth Douglas-fir (Pseudotsuga menziesii (Mirb) Franco) and the steep banks are lined with red alder. Berry Creek is a small, moderate to swiftly flowing stream; the streambed is rocky. Discharge in Berry Creek varies from 0.003 m^3/s (0.1 cfs) in the summer to a peak of 0.57 m^3/s (20 cfs) in the winter

or spring (Warren et al. 1964). The elevation of the study site is about 135 m (450 ft) above msl.

In 1971 Holtje studied reaeration in Berry Creek about 270 m (900 ft) downstream from the present site. Although hydraulic modifications to the earlier test site prevented closer replication, the use of the same stream allows a comparison of results between these two studies.

Four segments totaling 64 m (210 ft) in length were selected. The total drop for the four segments is nearly 2 m (6 ft). A section of dissected streambed between segments 2 and 3 was excluded from the study. Segment 1 is a pool; the other three are riffles of moderate gradient.

Needle Branch

Needle Branch is a coastal stream in the Alsea River basin. The study site is located 16 km (10 miles) east of the Pacific Ocean near Toledo. Needle Branch is a tributary of Drift Creek which flows into the Alsea River.

The study site was clearcut in 1966 as part of the Alsea Watershed Study. No buffer strip was left during the clearcutting but a dense thicket of red alder, willow (Salix spp. L.), and salmonberry (Rubus spectabilis Pursh) now shades the stream. Understory components of the vegetation include sword fern (Polystichum munitum (Kaulf) Presl. var. munitum), vine maple (Acer circinatum Pursh), and bracken fern (Pteridium aquilinum (L.) Kuhn var.

lanuginosum (Bong.) Fernald). Douglas-fir seedlings planted after harvesting are restocking the site away from the stream.

Needle Branch is a very small and slow flowing stream. Discharge is reported to vary from 0.0003 m^3/s (0.01 cfs) to winter peaks of 1.81 m^3/s (64 cfs). The streambed is a composite of gravels. The elevation of the study site is about 134 m (440 ft) above msl.

Two segments of 30.5 m (100 ft) and 24.4 m (80 ft) in length were tested. Both sections have a low gradient; the second section is deeper and narrower. Total drop for the test segments is 0.64 m (2.1 ft).

Deer Creek

Deer Creek is located about 3.2 km (2 miles) northwest of Needle Branch Creek. It is a tributary of Horse Creek which flows into Drift Creek. The drainage was part of the Alsea Watershed Study and parts of it were clearcut in 1966. A buffer strip was left to protect the stream. Red alder, salmonberry, vine maple, and sword fern are common near the study site.

The section of Deer Creek used in this study is a steep and rocky channel. Discharge and velocity of flow are much greater than in Needle Branch Creek. Discharge is reported to range from 0.004 m^3/s (0.15 cfs) to 5.6 m^3/s (201 cfs). The creek drains an area of 300 hectares (1.17

miles^2); elevation of the study site is about 188 m (625 ft) above msl.

Five segments totaling 74.7 m (245 ft) in length were isolated; total drop is 1.70 m (5.59 ft). Sections 2 and 5 have the least gradient. Section 5 is a large pool. Sections 1, 3, and 4 are turbulent riffles with exposed rocks.

Watershed 3

Watershed 3 is located in the H.J. Andrews Experimental Forest, 72 km (45 miles) east of Eugene. The stream draining Watershed 3 is a tributary of Lookout Creek, which flows into Blue River. Blue River is a tributary of the McKenzie River which joins the Willamette near Eugene. Watershed 3 is an experimental basin that has been used in several water quality studies (Brown 1967; Rothacher et al. 1967). The site used in this study was scoured to bedrock by a debris torrent. The resulting streambed has several sections with virtually no particle roughness. The rock underlaying the basin is largely greenish breccias and tuffs (Rothacher et al.). Vegetation in the basin includes Douglas-fir, red alder, vine maple, red huckleberry (Vaccinium parvifolium Sm.), thimbleberry (Rubus parviflorus Nutt.), trailing blackberry (Rubus ursinus Cham. and Schlect. var. macropectolus (Dougl.) Brown), and blackcap raspberry (Rubus leucodermis Dougl.).

Discharge is reported by Rothacher to have varied from minimums below 0.006 m^3/s (0.2 cfs) to a maximum of 1.2 m^3/s (40 cfs). Elevation of the study site is about 564 m (1850 ft) above msl. The total change in elevation for the 44.2 m (145 ft) of streambed studied is 5.14 m (16.85 ft).

Four segments were identified. Segment 1 is a fast-dropping, narrow channel of smooth bedrock. Segment 2 is deeper but drops even more rapidly over bedrock and rock debris. The third segment is flatter with more bed material; the fourth is a waterslide dropping more than 2 m (6 ft).

Andrews I

Andrews I is an unnamed stream less than 1.6 km (1 mile) east of Watershed 3. It flows into Lookout Creek. Andrews I is a steep and turbulent stream; both upstream and downstream from the study segment are numerous small waterfalls and drops. The study segment is relatively narrow and shallow. The streambed is stair-stepped with uniform small drops totaling 2.9 m (9.5 ft) over the 27.4 m (90.4 ft) section studied. No data on discharge is available, but frequent measurements and observations indicate flow patterns similar to those of Watershed 3. The streamside vegetation and elevation are also comparable.

Andrews II

Andrews II is a small stream about 4.8 km (3 miles) east of Andrews I. It also is a tributary of Lookout Creek. The upper section of Andrews II is similar to Andrews I, and the lower section is similar to segments in Berry Creek and Oak Creek. The streambed material ranges from large rocks in the steep upper portions to small pebbles in the flat lower section. Vegetation is similar to that of the other Andrews sites, although elevation is slightly higher.

Five segments were used, totaling 33 m (110 ft) in length. A portion of the channel within the study reach was excluded from measurements because it was highly dissected. The total drop is 1.84 m (6.04 ft), most of which occurs in the upper 15 m (50 ft) of the test reach.

PROCEDURES

The disturbed equilibrium method was used to determine the reaeration rate coefficient in natural streams. The procedures used by Holtje were closely followed.

Creating an Artificial Oxygen Deficit Using Sodium Sulfite

Method

Dissolved oxygen was artificially depleted by releasing a reducing agent, sodium sulfite (Na_2SO_3), into the stream. Oxygen combines with sodium sulfite to form sodium sulfate (Na_2SO_4) in the presence of the catalyst cobaltous chloride ($CoCl_2$).

$$2Na_2SO_3 + O_2 \xrightarrow{CoCl_2} 2Na_2SO_4 \qquad (94)$$

The concentration of sodium sulfite necessary to create a desired deficit in the dissolved oxygen concentration of a stream can be calculated with the equation (developed by Holtje):

$$C_{ss} = \frac{1.335 \times 10^4 \, DQ}{I} \qquad (95)$$

where C_{ss} is the concentration of sodium sulfite in g/l, D is the desired dissolved oxygen deficit in mg/l, Q is the discharge in ft^3/s (cfs), and I is the injection rate in ml/min.

A Mariotte injection vessel was constructed from a 5 gallon (20 l) glass carboy. A 25 l rigid polyethylene container was substituted for the glass carboy in later tests. The Mariotte vessel has the advantage of delivering fluid at a constant rate despite changes in the level of the solution. The air inlet tube and solution outlet tube were made of 3/16 inch (0.005 m) rigid plastic tubing. A 1 m length of flexible tubing was connected to the top of the outlet tube. The rate of flow was controlled by raising the vessel above the stream and adjusting the end of the tubing to a level below the outlet opening. A siphon was created by blowing into the air inlet tube.

Sources of Error

Although sodium sulfite provides a convenient means of depleting the dissolved oxygen in a stream, Benedek (1971) notes that this technique can introduce additional sources of error. Three possible errors introduced by the use of sodium sulfite are: a slow reaction causing a residual oxygen demand downstream; interference by the Co^{++} catalyst with chemical measurements of dissolved oxygen; and modification of stream reaeration properties due to the contamination by sodium sulfate. None of these problems proved to be significant in this study.

Reaction Time

Rapid and complete reaction of the sodium sulfite is necessary for accurate measurement of K_2 values. A solution containing 5 mg of cobaltous chlorite per 1 of sodium sulfite solution was suggested by previous studies. In field tests, it was found that substances in natural waters tie up the catalyst so that it must be used in greater strengths. The cobalt demand seems to vary with the stream and season. In order to insure that an adequate but minimum amount of catalyst was injected, Co^{++} was titrated into a mixture of stream water and sodium sulfite. A 500 ml sample of stream water with approximately 40 mg of Na_2SO_3 was titrated with a solution of 50 mg/l of $CoCl_2$. A Yellow Springs Instruments Model 54 Dissolved Oxygen Meter was used to monitor the dissolved oxygen concentration. During the titration, little or no change in dissolved oxygen is observed until a break-point is reached where free cobalt is available. A small additional quantity of cobalt results in a complete and rapid reduction of the dissolved oxygen. The g/l of cobaltous chloride (C_{cc}) needed for a rapid reaction can be calculated from the equation:

$$C_{cc} = 170 \cdot \frac{Ti\ Q}{T} \qquad (96)$$

where Ti is the amount of titrants in ml used to achieve the break point, Q is the discharge of the stream in cfs, and I is the injection rate in ml/min. Use of the

indicated quantity of catalyst resulted in rapid deaeration without residual oxygen demand.

Chemical Measurement of Dissolved Oxygen

The sodium sulfite/catalyst mixture did not interfere with chemical determination of dissolved oxygen because samples were taken before injection. Chemical determinations of dissolved oxygen were used only to standardize the Dissolved Oxygen Meter.

Modification of Stream Reaeration Properties

Benedek states that the presence of sodium sulfate (or any electrolyte) in water will influence the viscosity and surface tension of the water. Consequently, the solubility of oxygen and reaeration rate in the solution will also be modified.

The reduction in the solubility of oxygen that results from additions of sodium sulfate to the water does not affect the calculations of K_2 if the final saturation concentration is measured. In any case, the low concentrations of sodium sulfate used in this study produced no observable differences in oxygen solubility.

Additions of sodium sulfate to water may, however, change the value of K_2 because both diffusivity (D_m) and area of atmospheric-liquid interface (A) can be affected by changes in the viscosity and surface tension.

Ratcliff and Holdcroft (1963) report that the decrease in diffusivity resulting from the addition of an electrolyte can be predicted from the depression of viscosity. They use the equation:

$$\log_{10} \left(\frac{D_{m_o}}{D_m}\right) = 0.637 \log_{10} \left(\frac{\mu}{\mu_o}\right) \qquad (97)$$

where D_{m_o} and μ_o are the diffusivity and viscosity of pure water.

Tsivoglou, in his development of a reaeration model, proposed that molecular diffusivity could be predicted using the equation:

$$D_m = \frac{RT_K}{No\ 3\pi\ \mu\ d} \qquad (98)$$

where R is the universal gas constant (0.08205 l · atm/mole · °K), T_K is the temperature in °K, No is Avagadro's number (6.023×10^{23} molecules/mole), μ is the viscosity of the liquid, and d is the diameter of the gas molecule. From equation 98, the ratio of the molecular diffusivity for a liquid with and without an electrolyte in solution can be shown to be:

$$\frac{D_m}{D_{m_o}} = \frac{\mu_o}{\mu} \qquad (99)$$

Although equations 97 and 99 are different, they both show

that molecular diffusivity can be influenced by changes in viscosity.

Most researchers recognize that D_m is an important parameter in determining the gas exchange coefficient. Both Tsivoglou and Dobbins compared gas species and found that the ratio of gas diffusivities was directly proportional to the ratio of exchange coefficients:

$$\frac{K_a}{K_b} = \frac{D_{m_a}}{D_{m_b}} \qquad (100)$$

where K_a and K_b are the gas exchange coefficients for gas species a and b in m/s. Any change in the molecular diffusivity will therefore change the oxygen exchange coefficient (K_L).

In equations 44 and 47, Dobbins theorizes that the renewal rate (r) is another factor influenced by surface tension and viscosity. A change in r would, in turn, affect the value of K_L.

No measurable change in D_m, r, or K_L would be predicted for the concentrations of solute used in this study.

Interface area is theoretically increased with the addition of solutes because of increases in both surface tension and viscosity. Increased surface tension is reported to prevent coalescence of bubbles and could possibly prevent surface films from uniting. Calderbank found that bubble surface area increased in fluids with greater

viscosity. This may represent the tendency of viscous liquids to maintain deformed shapes.

From tests of different concentrations of sodium sulfite, Benedek reports that "the error resulting from the addition of 100 mg/l of Na_2SO_3, in a non-steady state reaeration test, would be negligible." The maximum concentration of sodium sulfite used in this study was less than 90 mg/l.

Environmental Considerations of Test Chemicals

Sodium Sulfite

An important consideration in any study that releases chemicals into the environment is the impact of those chemicals. The use of large quantities of the salt sodium sulfite as a reducing agent for dissolved oxygen was of particular concern despite its accepted use in several reaeration studies.

Under test conditions, sodium sulfite was released into streams in the presence of the catalyst Co^{++}. Streams usually contain some trace metal ions capable of acting as catalysts, and Chen and Morris (1972) report that under natural conditions sodium sulfite is rapidly oxidized to sodium sulfate.

The hydrated form of sodium sulfate, sodium sulfate decahydrate, is a naturally occurring salt. Pure deposits are found in Horseshoe Lake, Saskatchewan, and mixed

deposits are found in Searles Lake, California. Sodium sulfate decahydrate is commonly known as Glauber's salt after Rudolf Glauber who produced it from sulphuric acid and sodium chloride. Glauber's salt was first used as a laxative and is now commercially used in pulp and textile processes. It is a normal salt, exhibiting the characteristics of neither a base nor an acid. Sodium sulfite and sodium sulfate are both highly soluble and quickly flush through the stream system. Physical absorption and biological uptake of these salts have not been studied.

Cobaltous Chloride

The cobaltous chloride injected with the sodium sulfite as a catalyst is added only in minute concentrations; but because cobalt is reported to be potentially toxic to sheep and cattle, careful evaluation and monitoring of cobalt levels is desirable.

Cobaltous chloride is used industrially in the preparation of paints and as an indicator of humidity. Soluble forms of cobalt such as cobaltous chloride have been reported to produce both therapeutic and toxic effects on sheep and cattle depending on the concentration of cobalt. In low concentrations cobalt, which is a component of vitamin B-12, serves as an antianemic. Cobalt is noncummulative; it is rapidly eliminated from the body.

Church and Pond (1974) reported that sheep can tolerate 3 mg of Co^{++} per kg body weight for a period of 8 weeks with no toxic reaction. Clark-Hewley (1974) claims that doses of 50 mg of Co^{++} per day cause no toxic reaction in livestock. At very high levels cobalt can cause excessive formation of hemoglobin with resulting hyperplasma. Doses of 300 mg Co^{++} per kg body weight are reported to be fatal in sheep.

Concentrations of cobaltous chloride in test streams were raised a maximum of 1 mg/l during testing periods. That concentration of cobalt corresponds to about 0.42 mg/l. A 1000 lb cow, heat stressed at 100°C, could consume up to 55.5 l of water (an amount equivalent to 12% of its body weight). The resultant dose of Co^{++} from the stream would be 23.3 mg, assuming that the cow drank from test water all day.

The longest injection period used in this study was 4 hr. At most sites the test stream was rapidly diluted with water from other streams joining it below the test site. Where possible, the Co^{++} concentrations used were well below the 1 mg/l maximum.

Field Measurements

Hydraulic parameters measured for the selected stream segments included discharge, width, depth, length, travel time, and change in elevation.

Discharge was measured near the study sites. Needle Branch, Deer Creek, and Watershed 3 are equipped with experimental weirs. Culverts are located on Berry Creek, Andrews I, and Andrews II. When discharge was low, flow could be collected and timed. Splitting of flow was necessary at larger discharges. An experimental vortex weir and bypass flume are located downstream from the Oak Creek site. Discharge was measured by determining the flume cross section and velocity of flow. At each stream, discharge could be confirmed by measuring the injection rate and artificial oxygen deficit created by the addition of sodium sulfite. From equation 95:

$$Q = \frac{CI}{1.335 \times 10^{4} D} \qquad (101)$$

The value of Q, calculated from the oxygen deficit, provided a good check on the upper limit of discharge.

At the study site, stream segments with uniform characteristics were isolated and marked with stakes. The segment length between stations was measured along the centerline of the stream. Stream width was measured at the stations and at 10 ft (3.05 m) intervals between stations. Where unusually irregular cross sections were located within a segment, the interval was altered to obtain a more representative measurement. At each measurement point, the depth of the stream at 1 ft intervals across the channel was

recorded. Where the cross-channel line intersected rock and organic debris above the surface of the water, the length of these intersections was noted.

Time of travel within a segment was calculated by dropping Rhodamine B dye into the stream at an upper station and measuring the time required for the leading edge of the dye cloud to reach the next station.

The elevational change occurring within a segment was measured with a transit or level and a surveyor's rod. The elevational change was measured as the difference between the water surface at the upper and lower stations.

The dissolved oxygen concentration was measured with a membrane electrode probe. The probe was standardized according to an idometric determination of dissolved oxygen concentrations. Stream water was collected for the idometric determination with a sampler similar to the APHA type design shown in "Standard Methods." The sampler was constructed of 1/4 inch (0.006 m) plexiglass and is diagrammed in Figure 3. The upper gasket was made of 1/8 inch (0.003 m) neoprene and the air outlet and water inlet tubes were pieces of 3/8 inch (0.010 m) plexiglass tubing. An elastic cord held the cap and cylinder together during sampling. This design allows overflow of the bottles with minimum air contact.

Two 300 ml BOD bottles were filled and allowed to overflow for 10 seconds. Hach Chemical Company Reagents®

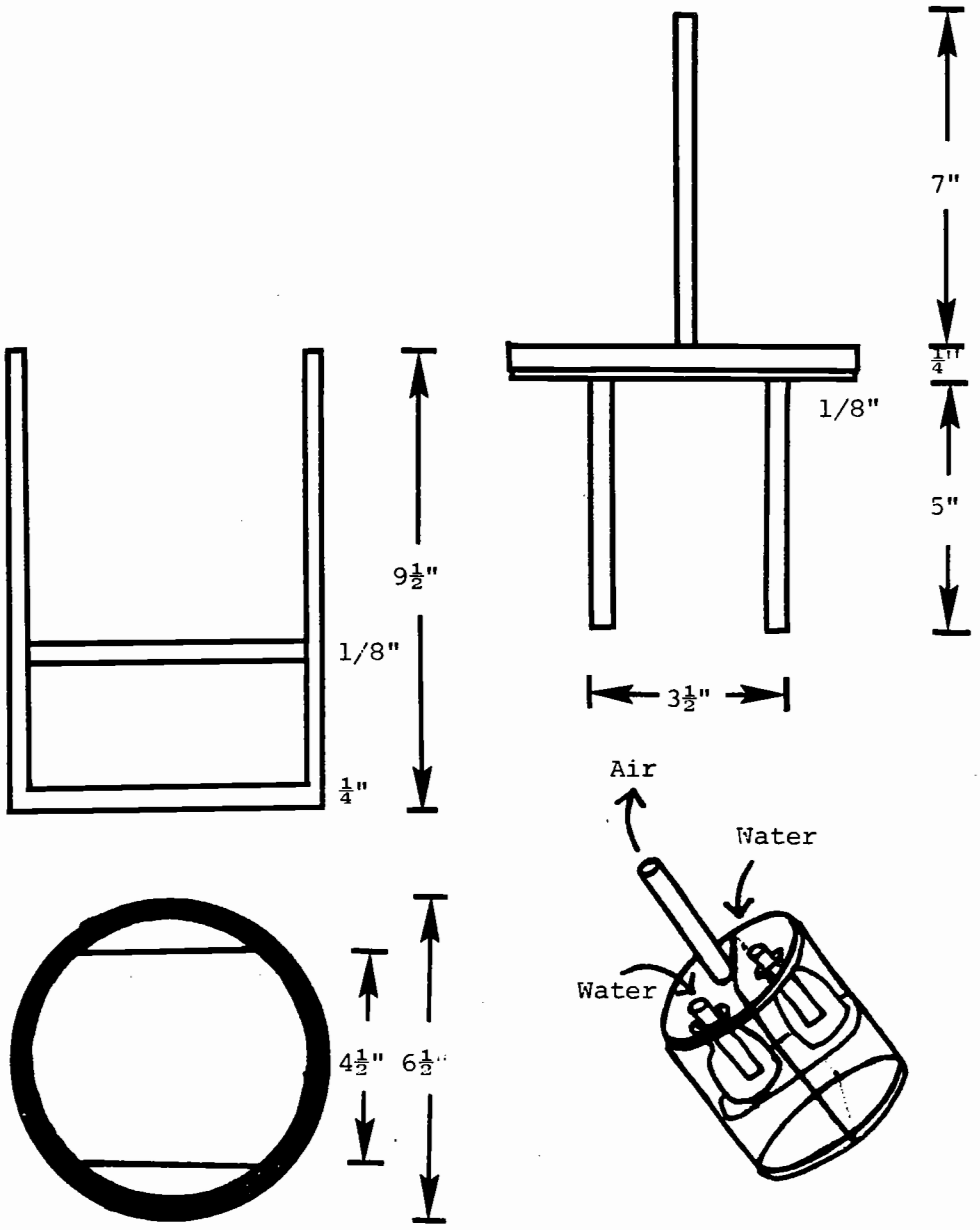

Figure 3. Dissolved oxygen sampler for idometric determination.

conveniently packaged in pre-measured "pillows," were used to determine dissolved oxygen concentration according to the azide modification of the Winkler Method. The contents of a manganous sulfate pillow and an alkaline iodide-azide powder pillow were added to each BOD bottle. The manganous sulfate added to the sample releases Mn^{++}. The alkaline iodide-azide pillow adds sodium hydroxide (NaOH), potassium iodide (KI), and sodium azide (NaN_3). The Mn^{++} is oxidized in the reaction:

$$Mn(OH)_2 + \tfrac{1}{2}O_2 \longrightarrow MnO_2 + H_2O \qquad (102)$$

When sulfamic acid is added to the bottles, the iodide ion (I^-) is oxidized to free iodine (I_2^0) in reaction:

$$MnO_2 + 2\ I^- + 4H^+ \longrightarrow Mn^{++} + I_2^0 + 2H_2O \qquad (103)$$

The sodium azide, added earlier with the potassium iodide and sodium hydroxide, combines with nitrite (NO^-_2) under acid conditions to stop it from oxidizing I^- to I_2^0.

Titration was made with phenylarsine oxide (PAO) solution rather than the usual sodium thiosulfate ($Na_2S_2O_3$). PAO solution is reported to be more stable than sodium thiosulfate. The addition of PAO solution results in the reduction of I_2^0 to I^-. The presence of I_2^0 can be determined using a starch indicator. When I_2^0 has been removed, the titration is complete. Because the full 300 ml sample was used in determining the oxygen concentration, the mg/l

of oxygen in the sample was calculated as two-thirds of the ml of titrant used.

This determination of dissolved oxygen concentration was used to calibrate a Yellow Springs Instruments Model 54 Oxygen Meter (YSI-54). The YSI-54 is a Clark-type, membrane-covered, polarographic probe. A membrane permeable to gases allows oxygen to enter the sensor chamber. A polarizing voltage is applied which causes the oxygen to be reduced at the cathode and a current to flow across the sensor cell. The current is a function of the rate oxygen enters the sensor. Automatic adjustments are made for changes in the pressure of the dissolved oxygen due to changes in temperature. The YSI-54 can also be used to measure temperature directly.

Temperature and dissolved oxygen concentration were measured at all stations prior to deaeration. After deaeration was begun, the YSI-54 was monitored until the dissolved oxygen concentration had stabilized. Temperature and dissolved oxygen concentration were then remeasured at all stations.

PRELIMINARY DEVELOPMENT OF AN EQUATION FOR PREDICTING THE REAERATION COEFFICIENT IN SMALL TURBULENT CHANNELS

The reaeration coefficient (K_2) has been previously defined in the equation:

$$\frac{dD}{dt} = -K_2 D \tag{4}$$

where dD/dt is the change in the oxygen deficit with time. The value of K_2 is determined by the rate at which gas is exchanged between the atmosphere and liquid for a unit area of interface (K_L), the total area of surface exposed (A), and the volume of water being reaerated (V). Hydraulic parameters determine the intensity of turbulent mixing, which controls the gas transfer coefficient (K_L). The mean hydraulic depth (H) can be used to characterize the area and volume. These relationships can be expressed as:

$$K_2 = \frac{A}{V} K_L = \frac{K_L}{H} \tag{104}$$

Equation 104 shows that A, V, and K_L must be determined in order to accurately predict K_2.

Volume

The volume of flow in a stream segment undergoing reaeration can be closely approximated using the segment

length and average cross-section. Errors are introduced by nonuniform channel characteristics, entrainment of bubbles, and the presence of non-mixing "dead zones." Numerous measurements of stream depth will minimize errors caused by bottom and surface irregularities. (See the Discussion.) Inception of bubbles can occur where the velocity of turbulence normal to the surface creates enough kinetic energy to overcome surface tension. Gangadharaiah et al. (1970) report that the concentration of bubbles entrained can be calculated with the equation:

$$1 - \bar{C} = \frac{1}{1 + C'nF^{3/2}} \qquad (105)$$

where $\bar{C}$ is the mean concentration of entrained air (by volume), n is Manning's roughness coefficient, F is the Froude number, and C' is a channel shape constant. Using data from Straub and Anderson, Gangadharaiah found that C' ranged from 1.35 in rectangular channels to 2.16 in trapezoidal channels. Using this relationship, the true volume of water can be calculated from the formula:

$$V = V_o \frac{1}{1 + C'nF^{3/2}} \qquad (106)$$

where V_o is the observed stream volume. The change in volume can become a very significant factor in artificial spillways. In natural channels bubbles are entrained but

are usually a very minor component of the volume. This is particularly true in less turbulent conditions.

The presence of non-mixing "dead zones" has been reported in studies dealing with both stream temperature and reaeration. Thackston and Krenkel (1969) placed bricks in an artificial channel to create vertical eddies which were somewhat isolated from the main flow. No difference was found between the predicted K_2 values (based on average hydraulic characteristics) and observed K_2 values. In contrast, Brown (1972) found that prediction of maximum stream temperatures was greatly improved when isolated eddies could be eliminated from the calculations:

> All pools are not fully mixed. Only the flowing portion of the pool should be included in the calculation of surface area. The average width of a reach can best be estimated by following a dye cloud through the reach taking frequent measurements of its width.

The different conclusions drawn from these two studies can be explained by the nature and degree of isolation. In the Thackston and Krenkel study, the "dead zones and flow discontinuities" were probably still mixing and influencing the stream. Small discontinuities in the streambed probably do not cause complete isolation. This is particularly true of an artificial channel where the flow is confined. Dye observations made during Brown's study indicated that the portions of the stream eliminated from calculations were definitely isolated. When a pool can become thermally

or hydraulically isolated it is appropriate to eliminate the unmixed portion from the calculations.

Interface Area

The liquid-atmosphere interface of a stream segment with laminar flow can be defined as the product of the average width and length. Dobbins (1964), Thackston and Krenkel, and Parkhurst and Pomeroy (1972) have shown that in turbulent flow it is necessary to account for an increase in the surface area caused by rippling and deformation. The relationships developed by these authors used the Froude Number to calculate the proportional increase in surface area.

Equations 68 and 69 were developed for turbulent flow without bubble entrainment. It seems reasonable to assume that the forces which cause bubbles to be entrained in flow are the same as those causing surface distortion. If this is the case, the total increase in surface area due to both surface distortion and entrainment of bubbles may be predicted from one equation. Gangadharaiah's equation can be used for this purpose if the following assumptions are made: the bubble concentration ($\bar{C}$) is inversely proportional to depth; a characteristic or average radius (R_b) for the bubbles can be used to describe the relationship between entrained bubble volume and entrained bubble surface area; the average bubble size always remains constant

for different conditions; and surface distortion can be related to the same physical properties that cause bubble entrainment.

The ratio of the volume of flow containing entrained bubbles to flow without bubbles can be expressed using Gangadharaiah's equation:

$$\frac{1}{1 - \bar{C}} = C'nF^{3/2} + 1 \qquad (107)$$

From this equation and the assumptions made above, it is possible to develop an equation for the coefficient C_A which accounts for the increase in surface area resulting from turbulence and bubble entrainment. This equation is:

$$C_A = c_1(1 + c_2nF^{3/2}) \qquad (108)$$

where c_1 and c_2 are constants. If a stream or experimental channel were evaluated under conditions where n remained nearly constant and c_1 was included with other constants, then C_A could be expressed as:

$$C_A = (1 + c_3F^{3/2}) \qquad (109)$$

which is very similar to equations 68 and 69, but now includes bubble entrainment as a component.

Gas Transfer Coefficient

A model of reaeration must account for the roles of both molecular diffusion and turbulent mixing. An increase in either process has been shown to increase the rate of reaeration. It is through the gas transfer coefficient (K_L) that molecular diffusion and turbulent mixing influence the reaeration rate constant (K_2).

Molecular diffusion results from the inherent kinetic energy of gas molecules. The average kinetic energy of a perfect gas molecule is represented by the equation:

$$\overline{KE} = 3/2\ \kappa T \qquad (110)$$

where κ is Boltzmann's constant (1.38042×10^{-16} ergs/°K) and T is in °K. The average relative speed of molecular movement can be determined from the equation:

$$\overline{KE} = \tfrac{1}{2}Mv^2 \qquad (111)$$

where M is the mass of the gas molecule and v is its velocity.

From equations 110 and 111 it can be seen that as temperature increases, there is a corresponding increase in molecular velocity. With elevated molecular velocities, molecular diffusivity (D_m) increases. Other variables, including surface tension and viscosity, are temperature dependent, influencing both molecular diffusivity and hydraulic characteristics of water. However, the change in

reaeration rate with a temperature change has been modeled using D_m as the only temperature-dependent variable.

The molecular diffusivity of a solute in a given solvent is dependent on properties of both. Each gas species will have a unique D_m in water. Reaeration rates of different gases in water are related to their molecular diffusivities, which further supports the importance of D_m in determining K_L.

In formulating the equation to predict K_L, it becomes necessary to consider whether a laminar film develops at the gas-liquid interface. Any change in the concentration of dissolved oxygen in a fluid which results from physical reaeration must occur due to a flux of gas molecules across a gradient at the air-liquid interface. Several of the studies discussed in the Literature Review section assume that a film exists at the surface of the water. Film theories suggest that adhesion, cohesion, and surface tension hold a film of water in isolation from the bulk flow. If the film can be considered deep relative to the distance a molecule can penetrate into it, if the rate of gas transfer at the surface is rapid, and if the diffusivity of the gas in water is slow, then a gradient will form in the film. Diffusion will occur across this gradient according to Fick's first law of diffusion:

$$J = -D_m \frac{dC}{dI} \qquad (112)$$

where $\frac{dC}{dl}$ is the concentration gradient and J is the flux of molecules per unit area and time. In the film penetration model, volume elements are exchanged between the film and bulk flow. This results in fresh elements being presented at the surface, promoting gas exchange.

Tsivoglou notes that the existence of a film has never been confirmed. He proposed that the dependence of the gas exchange coefficients on D_m is explained because gas concentrations in volume elements of the bulk flow must equalize simultaneously with the influx of molecules through the surface. Equalizing the gas concentrations in the bulk flow does not provide a mechanism by which D_m can control the rate that molecules move into the liquid. For the film penetration model to successfully account for the role of D_m, it must be assumed that the volume elements are withdrawn from the surface before they are fully reaerated. Under this assumption, D_m would control the mean concentration in the volume elements withdrawn from the surface.

O'Connor and Dobbins developed an equation for the gas exchange coefficient which accounts for the influence of D_m without the existence of a film:

$$D_L = \sqrt{D_m r} \quad \tanh \left(\frac{rH^2}{D_m}\right)^{\frac{1}{2}} \tag{35}$$

Using the film penetration model, they showed that:

$$K_L = \sqrt{D_m r} \coth \left(\frac{r\chi^2}{D_m}\right)^{\frac{1}{2}} \quad (36)$$

where K_L is the gas exchange coefficient in ft/day (or m/s), r is the renewal rate in $days^{-1}$ (or s^{-1}), H is the stream depth in ft (or m), χ is the film thickness in ft (or m), and D_m is molecular diffusivity in ft^2/s (or m^2/s). For a small turbulent stream, r would be very large. When $r\chi^2$ or rH^2 is large relative to D_m, then the functions $\coth \left(\frac{r\chi^2}{D_m}\right)^{\frac{1}{2}}$ and $\tanh \left(\frac{rH^2}{D_m}\right)^{\frac{1}{2}}$ approach 1 and equations 35 and 36 can be simplified to:

$$K_L = \sqrt{D_m r} \quad (37)$$

It is apparent from this equation that turbulent mixing acts to control the gas transfer coefficient through the renewal rate. Turbulence has been previously described as the sum of instantaneous divergences from the mean motion of flow. Turbulence is a process, internal to the stream-flow system, that dissipates energy. From these relationships it follows that the renewal rate is related to the rate at which energy is dissipated.

During laminar flow, the internal motion of water is a sliding of water layers across or between adjacent layers. Energy is efficiently converted from potential to kinetic energy in the form of stream velocity. The potential energy change can be calculated as:

$$PE = mg\Delta Ht \tag{113}$$

where m is the mass of the fluid, g is the gravitational constant, and ΔHt is the change in head. The change in kinetic energy of the stream can be calculated as:

$$KE = \tfrac{1}{2}m(U_2^2 - U_1^2) \tag{114}$$

where U_1 and U_2 are the velocities at stations 1 and 2. For this idealized case the potential energy change should be equal to the change in kinetic energy, assuming there is no loss of energy through friction.

Laminar flow is very rare and does not occur naturally in forest streams. As the viscous forces of water become small compared to the inertial forces, the flow becomes turbulent. The Reynolds number is defined as:

$$\mathbb{R} = \frac{UR_h}{\nu} \tag{115}$$

where U is the velocity of flow in ft/s (or m/s), R_h is the hydraulic radius in ft (or m), and ν is the kinematic viscosity in ft^2/s (or m^2/s). When $\mathbb{R}$ is large, the flow is turbulent. No definite upper limit is defined for the change from laminar to transitional flow, or from transitional to turbulent flow. This suggests that $\mathbb{R}$ is an incomplete parameter for describing the state of the flow.

Dobbins (1964), Krenkel and Orlob (1962), and Holtje (1971) computed the rate of energy dissipation (E) using

the equation:

$$E = U \cdot S \cdot g \qquad (116)$$

where U is the mean velocity in ft/s (or m/s), g is the gravitational constant in ft/s^2 (or m/s^2), and S is slope. The product of velocity and slope is the change in head per unit time in ft/s (or m/s). E is the rate of the change in potential energy per unit mass of water. Dobbins states:

> The energy is withdrawn from the main flow to create the kinetic energy of turbulence that finally is dissipated by viscous action into heat. For the flow as a whole, the rates of withdrawal, creation of turbulent energy, and dissipation are equal.

One of the assumptions implicit in using the energy dissipation (E) is that flow in the stream section being studied is steady and uniform. It is important that the incoming and outgoing velocities be equal, or the change in the potential energy will have to account for both the kinetic energy of turbulence and the kinetic energy of velocity. Over a long stream section, the difference in the kinetic energy of velocity would become small relative to the potential energy drop and $U \cdot S \cdot g$ would become an increasingly good measure of the energy available for turbulent mixing.

Temperature Dependence

Although the solubility of oxygen decreases as temperature increases, the reaeration rate has been shown to

increase with temperature, due primarily to the greater kinetic energy of the oxygen molecules. Tsivoglou, using his model of the reaeration process, suggested that the theoretical temperature correction can be calculated using the equation:

$$\frac{K_{2(T_2)}}{K_{2(T_1)}} = \frac{C_{S(T_1)}}{C_{S(T_2)}} = \phi_T^{T_2-T_1} \qquad (117)$$

With this relationship, ϕ_T is 1.022 ± 0.004. Several of Tsivoglou's assumptions have been criticized (Bennett and Rathbun 1972).

Measured values for ϕ_T commonly used to convert reaeration rates to the equivalent rate at 20°C are:

ϕ_T = 1.016 Streeter, Wright and Kehr (1936)

ϕ_T = 1.0241 Churchill, et al. (1962)

Both these measured values have been widely used in reaeration studies. The Streeter et al. value is used in this study because it is supported by Krenkel and Orlob (1963), Metzger and Dobbins (1967), and Metzger (1968).

The validity of using a single equation to measure the responses of stream reaeration to temperature has been questioned. It has been suggested, through stirring-tank experiments, that ϕ_T is affected by turbulence. No theoretical basis seems evident for this conclusion. It seems more probable that these studies have failed to

completely account for surface distortion, molecular diffusivity, film depth, and surface renewal.

In this study, the equation from Streeter et al. will be used for temperature corrections:

$$K_{2(T)} = 1.016^{(T-20)} K_{2(20)} \qquad (118)$$

where $K_{2(T)}$ and $K_{2(20)}$ are the reaeration rates in $days^{-1}$ (or s^{-1}) for stream temperatures T and 20°C.

Complete Model

When the factors of molecular diffusivity, energy dissipation, true active volume, surface area increase, and temperature are all considered, the following formula can be used to predict the reaeration rate of a stream:

$$K_2 = 1.016^{(T-20)} c_1(1 + c_2 n F^{3/2}) \frac{(D_{m20} E)^{\frac{1}{2}}}{H} \qquad (119)$$

According to Tsivoglou's development of ϕ_T, the expression $1.016^{(T-20)}$ is dimensionless. The term for increased surface area $(1 + c_2 nF)$ is also dimensionless if n is treated as a dimensionless variable.[3] This is reasonable since it expresses the ratio of actual surface area to the

[3]Manning's n is usually treated as having the dimension of either $TL^{-1/3}$ or $L^{-1/6}$. Chow (1959) notes that n can be treated as a dimensionless variable if the constant 1.49 is assumed to have the dimension $L^{1/3}T^{-1}$. The value for n is therefore the same in both English and metric units.

product of measured width and length. F is the Froude number for the segment. The molecular diffusivity in ft/day (or m/s) and energy dissipation rate in ft^2/s^3 (or m^2/s^3) are used to determine the gas exchange coefficient component of the equation. The mean hydraulic depth of the active stream (H) is in ft (or m). Therefore, c_1 is expressed in units of days/ft (or s/m).

DATA ANALYSIS

The basic parameters measured in the field tests were manipulated into composite parameters. Predictive equations for the reaeration coefficient (K_2), using stream hydraulic parameters, were then compared to measured values for K_2 using linear and nonlinear techniques.

Measured Stream Parameters

The length, elevational change, discharge, and dye travel time were measured for each stream segment. Measurements of the width and depth were also made at intervals along the length of the segment. From the field data for each segment, weighted averages were calculated for the width, depth, wetted perimeter, and cross-sectional area. The weighting was based on the proportion of the segment bracketed by measurement points. The active stream width was defined as the stream width observed to be discolored by dye.

The average hydraulic radius (R_h) in ft (or m) was calculated from the average wetted perimeter (W_p) in ft (or m) and the cross-sectional area (A_w) in ft^2 (or m^2):

$$R_h = \frac{A_w}{W_p} \tag{120}$$

The stream slope (s) was calculated as the elevational change (ΔHt) in ft (or m) divided by the stream segment length (X) in ft (or m):

$$s = \frac{\Delta Ht}{X} \tag{121}$$

The average stream velocity (U) in ft/s (or m/s) was calculated using the equation:

$$U = \frac{Q}{A_w} \tag{122}$$

where Q is the discharge in ft^3/s (or m^3/s).

The velocity (U_D) in ft/s (or m/s) of a florescent dye introduced into the stream was also calculated:

$$U_D = \frac{X}{t_D} \tag{123}$$

where X is the length of the segment in ft (or m) and t_D is the travel time in s^{-1} required for the leading edge of the dye to travel through the segment. Brown (1972) and Holtje (1971) both used dye to characterize velocities in small streams. This method measures the maximum velocity in the stream segment.

When cross-sectional area is calculated from the width and depth measurements it is assumed that all the water is actively mixing. When this is not the case, dye velocity can be used to obtain a more realistic estimate of active cross-sectional area. If it is assumed that the active

portion of the stream is moving at the velocity of the dye (near maximum), then the depth of active water (H_D) in ft (or m) can be calculated using the equation:

$$H_D = \frac{Q/U_D}{W_D} \tag{124}$$

where Q is the discharge in ft^3/s (or m^3/s), U_D is the dye velocity in ft/s (or m/s), and W_D is the active width of the stream in ft (or m). The parameter H_D is a simple way of correcting for the presence of stagnant water that contributes very little to the net oxygen exchange.

Several other important composite parameters were computed from the average field measurement values. These parameters include the Froude number, the Reynolds number, the rate of energy dissipation, Manning's n, and Chezy's C. Additional stream parameters were generated by substituting the dye velocity (U_D) for the average cross-sectional velocity (U).

The Froude number (F) is a dimensionless parameter that is the ratio of inertial forces to gravitational forces. The Froude number was calculated using the equation:

$$F = \frac{U}{(gH)^{0.5}} \tag{125}$$

where U is velocity in ft/s (or m/s), g is the gravitational constant in ft/s^2 (or m/s^2), and H is the average depth in

ft (or m). The maximum Froude number (F_D) was calculated using the equation:

$$F_D = \frac{U_D}{(gH_D)^{0.5}} \tag{126}$$

where U_D is the dye velocity in ft/s (or m/s), g is the gravitational constant, and H_D is the active stream depth in ft (or m). When F is greater than 1.0, the flow is supercritical and inertial forces are greater than gravitational forces. Chow (1959) describes supercritical flow as "rapid, shooting, and torrential."

The Reynolds number (ℝ) is the dimensionless ratio of viscous to inertial forces. The Reynolds number was calculated using equation 115. In order to calculate ℝ, the kinematic viscosity (ν) in ft^2/s must be determined. It was approximated using the empirical equation cited by Dean (1973):

$$\nu = \frac{0.0010076391042}{2.1482(T) - 8.435 + \sqrt{8078.4 + (T-8.435)^2} - 120} \tag{127}$$

where T is temperature in °C.

The rate of energy dissipation (E) in ft^2/s^3 (or m^2/s^3) was determined using equation 116. The maximum energy dissipation rate for a segment was calculated as:

$$E_D = sU_Dg \tag{128}$$

where s is the slope in ft/ft (or m/m), U_D is dye velocity, and g is the gravitational constant. E has been used by several researchers as a parameter for predicting K_2 values.

Manning's and Chezy's formulas are both used to predict stream velocities. Manning's formula is sometimes considered to be a special case of Chezy's equation. Manning's n and Chezy's $\mathbb{C}$ are coefficients which indicate stream resistance to flow.

Manning's roughness coefficient (n) is calculated using the equation:

$$n = \frac{1.49}{U} R_h^{0.67} s^{0.5} \qquad (129)$$

where U is velocity in ft/s, R_h is the hydraulic radius in ft, and s is the slope in ft/ft. As n increases, the resistance to flow becomes greater. Manning's formula is commonly used for natural streams.

Chezy's equation is another commonly used predictive formula. Chezy's resistance factor ($\mathbb{C}$) in $ft^{0.5}/s$ (or $m^{0.5}/s$) is calculated using the equation:

$$\mathbb{C} = \frac{U}{(R_h s)^{0.5}} \qquad (130)$$

as $\mathbb{C}$ increases, the resistance to flow decreases.

Reaeration Coefficients

Reaeration rate constants were calculated for each stream segment from observed oxygen deficits below the sodium sulfite injection stations. The reaeration rate constant (K_2) in $days^{-1}$ for a segment is calculated using the equation:

$$K_2 = 86400(\ln D_0 - \ln D_t)/t \qquad (131)$$

where D_0 and D_t are the upstream and downstream deficits in mg/l (or kg/m^3) and t is the time of flow in seconds between the upstream and downstream stations.

The time between stations (t) was calculated from the mean velocity (U) in ft/s (or m/s) and the length of the segment (X) in ft (or m):

$$t = \frac{X}{U} \qquad (132)$$

(The travel time of dye between stations (t_D) could also be used to calculate K_2. This method was used by Holtje.)

The deficit (D) in mg/l (or kg/m^3) is calculated from the observed oxygen concentration (C) and the saturation concentration (C_s) in mg/l (or kg/m^3):

$$D = C_s - C \qquad (133)$$

The concentration of oxygen in each stream was measured prior to deaeration using the Winkler method (described under "Procedures"). These streams were assumed to be at

saturation. In order to test that assumption, measured oxygen concentrations were compared to values calculated using equation 3:

$$C_s = C_s' \frac{P - p}{P_{st} - p} \tag{3}$$

where C_s' is the solubility of oxygen at a given temperature and a standard pressure (P_{st}), P is the observed pressure, and p is the vapor pressure of water in mm Hg.

Churchill's equation was used to predict the solubility of oxygen in water at standard pressure:

$$C_s' = 14.632 - 0.41022(T) + 0.007991(T^2) - 0.000077774(T^3) \tag{134}$$

where T is the stream temperature in °C.

Barometric pressures near the study areas were obtained from the National Weather Service and the O.S.U. Marine Science Center. Corrections for differences in pressure due to differences in elevation between measurement stations and study sites were made using an equation cited by Trewartha (1954):

$$P_{Ht} = P_o - (0.02667\Delta Ht) \tag{135}$$

where P_{Ht} is the barometric pressure in mm Hg at the study site, P_o is the barometric pressure in mm Hg at the measurement station, and ΔHt is the difference in elevation in ft between the study site and the measurement station.

The calculated saturation values agreed very closely with the observed values. Therefore, the initial oxygen concentrations measured before deaeration were used for C_s (Appendix V).

Data Modifications

Several early experiments were conducted with insufficient cobaltous chloride catalyst. This resulted in a sustained oxygen demand through all or part of the test reach. In segments with low reaeration rates, a reduction in the dissolved oxygen concentration was observed from upstream to downstream stations. In segments with low reaeration rates, the reaeration rate coefficients calculated from observed deficits were depressed. All data sets collected on streams injected with insufficient cobaltous chloride were eliminated from analysis.

In two of the 51 test segments, no change was observed in the dissolved oxygen concentration. In both cases, the segments were short and positioned at the lower end of the test reach. Deficits and changes in oxygen concentrations would be expected to be small for segments in this position. Rather than bias the total stream response by eliminating these segments, they were combined with the segment immediately upstream.

For four segments, the observed reaeration rates seem unusually high. All of these segments are short pools

or quiescent reaches below riffles. It appears that energy is advected into the pools from upstream drops in the form of velocity and turbulence. The dissipation of energy and subsequent increased renewal rate appears to be higher in these segments than would be predicted from their slopes. For this reason, these four segments were combined with the segments immediately upstream. Although these segments were originally thought to be hydraulically distinct, they must be combined with the riffles above to fully account for the effects of energy dissipation on the reaeration rate.

Model Testing

K_2 values measured in the field tests were compared with values estimated by reaeration models using least squares regression techniques.

Linear Regression

At Oregon State University, the Statistical Interactive Program System (SIPS) is available for multiple linear regression. Regression analysis is used to fit a mathematical model to the relationship between a dependent variable and independent variables. The general model for a linear regression is:

$$Y_i = \alpha + \beta x_i + \gamma z_i + e_i \qquad (137)$$

where Y_i is the observed value for the dependent variable; α, β, and γ are regression coefficients; x_i and z_i are the observed independent variables; and e_i is the difference between the observed value (Y_i) and the predicted value ($\hat{Y}_i$) of the dependent variable. The error term e_i is the result of errors in measuring the variables and stochastic errors inherent in trying to model physical phenomena.

The regression coefficients are selected so that the squared deviation between the vectors of the observed and predicted dependent variables are minimized. This procedure is supported by the Gauss-Markov Theorem (as stated by Wonnacott and Wonnacott 1972):

> Within the class of linear unbiased estimators of [the regression coefficients], the least squares estimator has minimum variance.

Non-Linear Regression

At Oregon State University, analysis of non-linear models is possible using the program CURFIT, which is based on a Gauss-Newton non-linear least squares method. The CURFIT program is an iterative approximating procedure. The user must supply partial derivatives of the model with respect to the regression coefficients. (This is done automatically for linear models in SIPS.) Initial estimates of coefficients are necessary to begin the computation. If the initial coefficients selected are sufficiently close to those which will best fit the model according to the least

squares estimators, then the program will converge on those best-fit values.

Selecting the Regression Model

The SIPS program was used to conduct multiple linear regression tests. In the initial tests, variables were selected for their entering F-test values. Guthrie et al. (1973) note that this procedure "... selects the single variable to enter the regression model which makes the greatest contribution to reducing the residual variability below that of the current model." Variables were added until they no longer satisfied the F-test criterion at the 0.95 level. The t statistics, entering F values, analysis of variance table, and multiple correlation coefficients for the models were evaluated.

The t statistic tests the null hypothesis that the regression coefficient is zero. When the t statistic is large, the hypothesis can be rejected. The multiple correlation coefficient (R^2) is the ratio of the variance of Y_i explained by the model to the total variation. When the explained variation nearly equals the total variation, the model closely fits the observed variables.

For non-linear models using CURFIT, it was necessary to develop an accurate estimate of the regression coefficients. A non-linear model in the form:

$$Y_i = \alpha x_i^{\beta} z_i^{\gamma} + e_i \qquad (138)$$

can be linearized to the form:

$$\ln Y_i = \ln \alpha + \beta \ln x_i + \gamma \ln z_i \qquad (139)$$

in order to estimate the regression coefficients. The coefficients β and γ can be determined directly from the linearized model using SIPS. The coefficient α was estimated as $e^{\ln\alpha}$. Because of linearization errors, the fit between the actual and predicted values of K_2 might not have a slope of 1.0.

The regression coefficients developed using this SIPS procedure were used in the CURFIT program in selection of the final coefficient values. These coefficients were selected by evaluating the R^2 of the model and the slope of the relationship between the actual and predicted values of K_2. When both R^2 and the slope were near 1.0, the model satisfactorily evaluated the observed data.

RESULTS

The field data from 45 study reaches were used to develop equations predicting reaeration rate constants for small turbulent streams. The analytical techniques described in the previous chapter were used for this purpose. Several model forms were examined including linear, multiplicative, and non-linear. Models proposed by other workers were also evaluated using data from this study. These models included functions specifically designed to account for turbulent effects. Predictive equations that use only the slope and width of the stream were also compared to the data since these variables are more easily obtained by technicians in the field. Finally, oxygen sag curves were developed for the study streams using field observations and were compared with those predicted by the model which best described the reaeration process.

Linear Equation

Holtje (1971) proposed an equation in a simple linear form for the prediction of reaeration rates in small streams. This equation was derived from a multiple linear regression analysis of several hydraulic variables. A linear equation was developed with the field data from this study according to this same regression procedure. For all regression models, the measured reaeration

coefficients were adjusted to the expected reaeration coefficient at 20°C according to equation 118. The linear model was chosen using the entering F-values as the selecting criterion. The size of the F-value determines whether the residual of the model to the data is significantly reduced by the entering variable. Variables were included if they significantly improved the model at the 0.95 level. Eighteen variables were tested and only four of those were selected for the linear equation. This technique yielded the linear model:

$$K_{2_{20}} = 29.475 - 602.97\ U + 1727.9\ F - 297.53\ E + 219.7\ E_D \quad (140)$$

where $K_{2_{20}}$ is the reaeration rate coefficient at 20°C in $days^{-1}$, U is the mean velocity in ft/s, F is the Froude number, E is the mean energy dissipation in ft^2/s^3, and E_D is the maximum energy dissipation in ft^2/s^3. From the t-values listed for the coefficients in Table 1, the hypothesis that the regression coefficients are zero can be rejected at the 0.99 probability level. The next entering F value, for slope of the stream, fell below the 0.95 F-test criterion. Slope was therefore rejected as a parameter because it did not significantly reduce the residual. Figure 4 shows the relationship between the reaeration coefficients measured (adjusted for a standard temperature of 20°C) and the values of $K_{2_{20}}$ predicted by equation 140. (The R^2

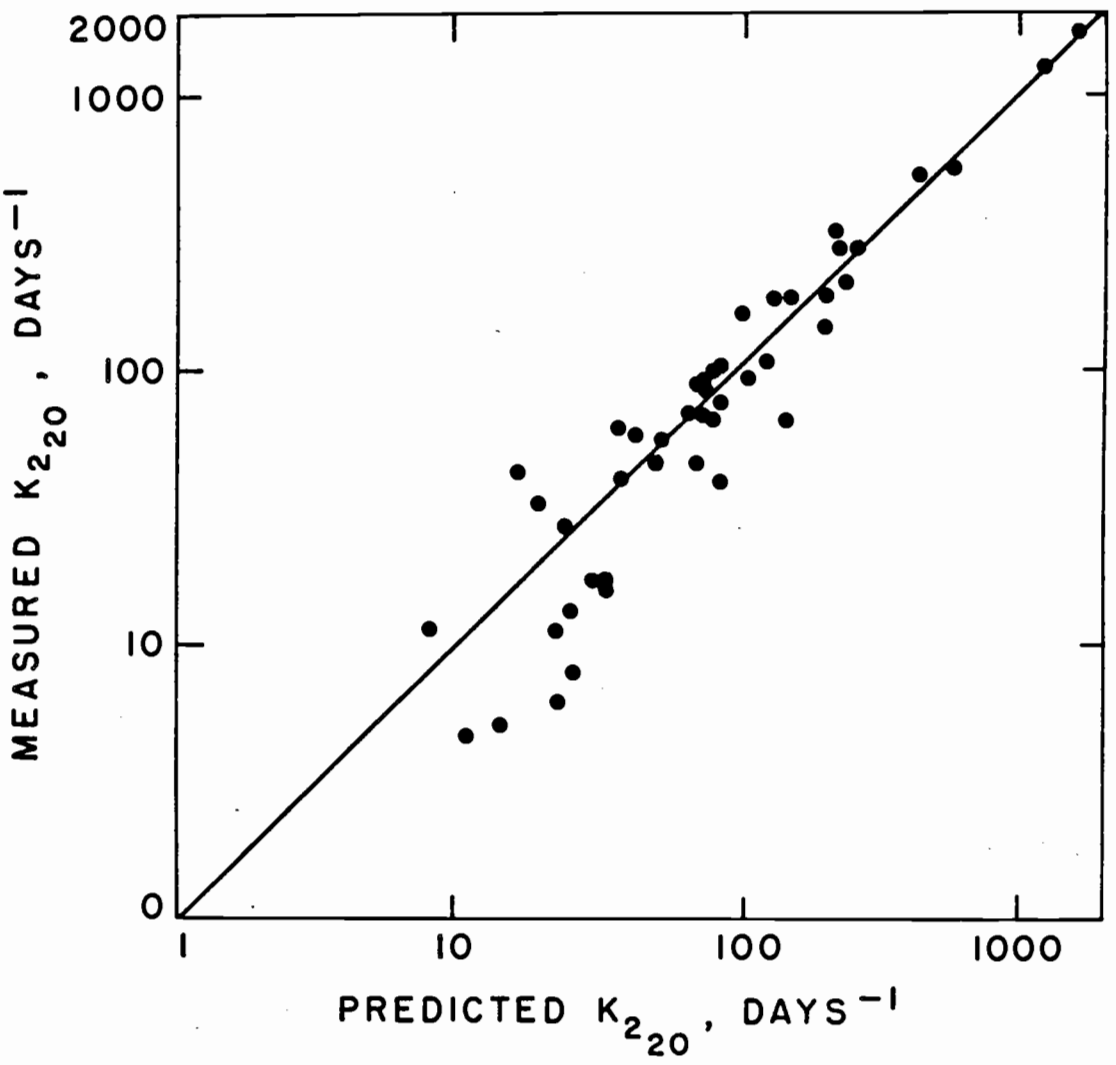

Figure 4. Measured versus predicted values of $K_{2_{20}}$ from equation 140.

$$K_{2_{20}} \text{ (predicted)} = 29.475 - 602.97\ U + 1727.9\ F - 297.53\ E + 219.7\ E_D$$

values reported for this model and for the other models developed in this section are for the measured and predicted $K_{2_{20}}$ values.) The equation provides a reasonably good fit for the large reaeration values. In the lower range, the equation becomes less reliable.

Table 1. Regression variables and statistical information for the linear model.

Variable	Coefficient Value	Standard Error of Regression Coefficients	t-values for Coefficients
Constant	29.475	8.9273	3.3017
U	-602.97	72.045	-8.3693
F	1727.9	161.76	10.682
E	-297.52	23.465	-12.679
E_D	219.7	9.4115	23.344
	slope = 1.000		
	R^2 = 0.990		

Multiplicative Models

Multiplicative models were developed that are similar to the form suggested by Krenkel and Orlob (1963), Owens, Edwards, and Gibbs (1964) and Isaacs (1968). Regression techniques were again utilized to obtain the coefficients for the variables selected, and the F-test criterion was used to select the significant variables. The log transformations of the measured reaeration rate constants and 18

hydraulic parameters were analyzed for this solution. This approach was used to develop the model shown below:

$$K_{2_{20}} = 35.04 \frac{E_D^{0.4447}}{H_D^{0.3472} R_h^{0.3592}} \quad (141)$$

where H_D is a depth parameter in ft and R_h is the hydraulic radius of the stream channel in ft. The depth parameter H_D is defined by the equation:

$$H_D = Q/(W_D \cdot U_D) \quad (124)$$

where Q is the discharge in ft^3/s, W_D is the active stream width in ft, and U_D is the dye velocity in ft/s.

The regression variables and coefficients for the model are listed in Table 2. The slope and R^2 values are

Table 2. Regression variables and statistical information for the multiplicative model.

Variable	Coefficient Value*	Standard Error of Regression Coefficients	t-values for Coefficients
R_h	-3.5921	0.13081	-2.7460
H_D	-3.4719	0.12214	-2.8427
E_D	4.4468	0.02999	14.830
Constant	3.5566	0.19504	18.236
	Slope = 1.026		
	R^2 = 0.985		

*Values reported in logarithmic form to permit testing of coefficient significance.

taken directly from equation 141. The t-values listed were obtained using the coefficient values in the logarithmic form.

The hydraulic radius requires numerous measurements of the stream depth. The field application of equation 141 can be simplified if R_h is not used as a variable for the predictive equation. For smooth, shallow, wide streams, the value of the hydraulic radius (R_h) approaches the value of the hydraulic depth (H). The denominator of equation 141, which uses both H_D and R_h, describes the stream depth in terms of both the surface contact and streambed contact. The parameter H_D is an expression of the ratio of surface area available for oxygen transfer to the active segment volume. The parameter R_h can be considered the ratio of the stream volume to the streambed surface available for shear stress. For a smooth, wide, shallow stream where the average and maximum velocities are equal, R_h and H_D become equal.

For equation 141, R_h is the last variable to enter the equation using the F-test criterion. Because of these considerations a simplified multiplicative model was tested where R_h was eliminated. The resulting simplified multiplicative equation is:

$$K_{2_{20}} = 36.98 \frac{E_D^{0.4967}}{H_D^{0.6078}} \qquad (142)$$

The R^2 values for equations 141 and 142 were both 0.985. However, the slope of equation 142 was 1.249 which indicates that this equation is less accurate in predicting the reaeration rate.

If the multiplicative model is developed according to linear multiple regression techniques such as those used to develop equations 141 and 142, the residuals of the natural logarithms become the fitting criteria. This procedure reduces the dominance of the larger values. However, when the equation is transposed back from the logarithmic form, the slope between the observed and predicted reaeration rates often diverges from 1.0.

In order to avoid this divergence and develop an accurate equation, a non-linear fitting procedure was used. This non-linear iterative estimation procedure requires that the equation form and coefficient values be estimated. The coefficients developed in equation 142 were used as starting values for the simplified non-linear model estimate. The resulting equation is

$$K_{220} = 24.91 \frac{E_D^{0.4995}}{H_D^{0.7811}} \qquad (143)$$

Equation 143 is both accurate and precise (Table 3). The standard errors of the regression coefficients are very small, indicating that these parameters are important.

Table 3. Regression variables and statistical information for the simplified multiplicative model.

Variable	Coefficient Value	Standard Error of Regression Coefficients	t-values for Coefficients*
Constant	24.91	4.144	6.011
E_D	0.4994	0.0297	16.82
H_D	0.7811	0.0602	12.98
	slope = 1.000		
	R^2 = 0.992		

*The t-values are not an exact measurement for the non-linear extimation procedure but are accepted as close approximations.

Equation 143 is similar in form to an equation derived by Krenkel and Orlob (1963):

$$K_{220} = 56.83 \frac{E^{0.408}}{H^{0.660}} \qquad (144)$$

where E is the average unit energy dissipation rate in ft^2/s^3, and H is the hydraulic depth in ft. As will be discussed later, E and H may be comparable to E_D and H_D under some conditions.

Krenkel and Orlob used a 1 ft wide circulating flume. This configuration may bias predictions for larger streams due to sidewall effects, but it is probably appropriate for small streams. Small streams are frequently dissected by rocks. This dissection of the channel can influence the apparent roughness of the streambed in a manner similar to

the sidewalls of a small flume. If the stream data from the current study are expressed in the form of equation 144, using E and H rather than E_D and H_D as used in equation 143, the resulting equation is:

$$K_{2_{20}} = 57.95 \frac{E^{0.273}}{H^{0.738}} \qquad (145)$$

Equation 145 has a slope of 1.000 and a regression coefficient of 0.947 (Table 4).

Table 4. Regression variables and statistical information for multiplicative model using mean segment parameters.

Variable	Coefficient Value	Standard Error of Regression Coefficients	t-values for Coefficients*
Constant	57.95	21.48	2.698
E	0.2726	0.0787	3.464
H	0.7381	0.1457	5.066
	slope = 1.000		
	R^2 = 0.947		

*The t-values are not an exact measurement for the non-linear estimation procedure but are accepted as close approximations

The velocity of flow could be expected to be more uniform in a flume than in a natural channel. The mean velocity in a flume would probably be very near the maximum velocity. If it is assumed that the zones of maximum energy dissipation largely determine the reaeration rate,

then the most accurate predictions should be made using the variables E_D and H_D, which are derived from the maximum velocity. This is, in fact, illustrated by the results of this study. The regression analysis shows that equation 143 is a more precise estimator of the measured reaeration rates than equation 145.

The fit of equation 143 to the stream data is shown in Figure 5. The fit of the predicted reaeration rates to those measured is reasonably consistent throughout the range of values measured. Relative scatter for lower reaeration rate coefficient values is comparable to that found in the middle reaeration range. The R^2 value for the entire data set is 0.992. The R^2 value for the measured coefficients below 100 $days^{-1}$ is 0.792. The R^2 value for the measured coefficients below 10 $days^{-1}$ is 0.667.

Equations Designed to Account for Increased Surface Area Due to Turbulence

The next step in the model development was intended to include the additional complexity of the surface distortion that results from turbulence. The internal motion of turbulent eddies can increase the liquid-atmosphere contact area by stimulating surface waves. Where turbulence is extreme, bubbles can be entrained in the flow to further increase the liquid-atmosphere contact area.

Several reaeration studies have attempted to account for the role of increased surface area in reaeration.

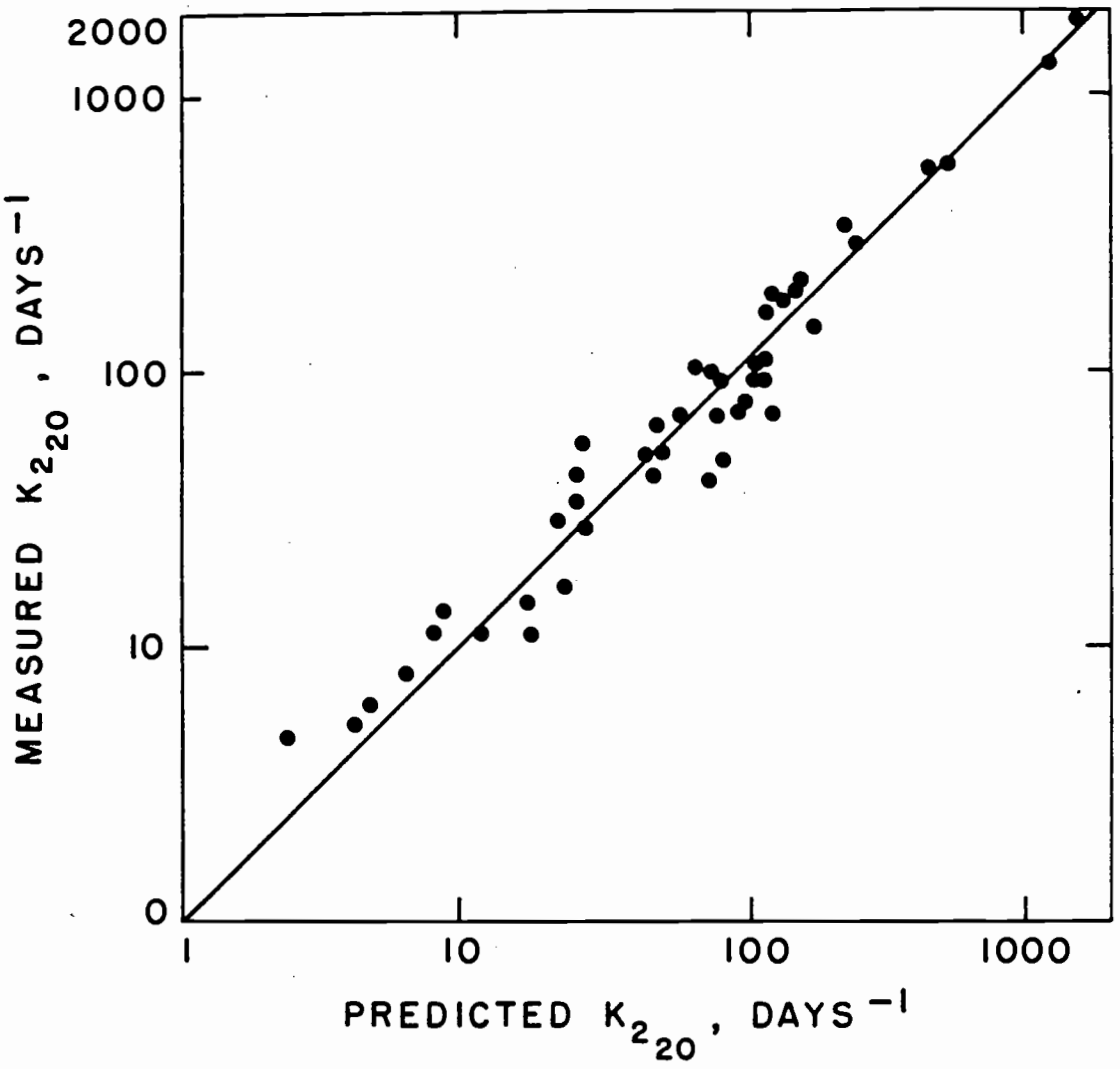

Figure 5. Measured versus predicted values of $K_{2_{20}}$ from equation 143.

$$K_{2_{20}} \text{ (predicted)} = 24.91 \frac{E_D^{0.4995}}{H_D^{0.7811}}$$

Examples include the models proposed by Dobbins (1964), Thackston and Krenkel (1969), and Parkhurst and Pomeroy (1972). The term C_A is used to describe the ratio of the actual surface area to the planar surface area. The general form of the equations that have been used to predict C_A is:

$$C_A = (1 + C_2 F^{C3}) \tag{146}$$

where F is the Froude number.

For model testing, it was assumed that surface renewal effects were accounted for by the energy dissipation and depth parameters. Effects of surface area increases were assumed to be proportional to the form of the function shown in equation 146. The composite form of the equation used to fit the data is:

$$K_{220} = C_1(1 + C_2 F^{C3}) \frac{E_D^{C4}}{H_D^{C5}} \tag{147}$$

The functions proposed by the authors cited above were tested by holding C_2 and C_3 constant at the suggested values. The coefficients C_1, C_4, and C_5 were allowed to move to their best fit values. The precision of all three equations is similar (Table 5).

The standard errors for some of the coefficients in equations 148, 149, and 150 were large enough so that the hypothesis that some of the coefficients are zero could not be rejected.

Table 5. Reaeration equations which account for increased surface area based on proposed equations for C_A.

	Equation	R^2	Equation Number
After Thackston and Krenkel	$K_{2_{20}} = 19.11\ (1 + F^{0.5})\ \frac{E_D^{0.346}}{H_D^{0.753}}$	0.983	148
After Dobbins	$K_{2_{20}} = 18.51\ (1 + 0.3\ F^{2.0})\ \frac{E_D^{0.326}}{H_D^{0.869}}$	0.967	149
After Parkhurst and Pomeroy	$K_{2_{20}} = 20.84\ (1 + 0.15\ F^{2.0})\ \frac{E_D^{0.388}}{H_D^{0.838}}$	0.979	150

When all the coefficients including C_2 and C_3 were allowed to float freely and values were derived for all five coefficients, the best-fit equation was unrealistic (i.e., the Froude number was raised to the fifteenth power). The standard errors for some of the coefficients were again too large to reject the hypothesis that the coefficients were zero.

Thus, because the precision of the equation was not improved by including surface disturbance considerations and because the standard errors of the coefficients were statistically less sound, these equations were rejected for use in small forest streams.

Another equation for C_A was developed after studies by Gangadharaiah et al. (1970). The form of the equation for

C_A is:

$$C_A = C_1(1 + C_2\ n\ F^{C_3}) \tag{108}$$

where n is the Manning n. This form would account for the role of both streambed roughness and inertial energy in generating surface disturbances. The composite test equation:

$$K_{2_{20}} = C_1(1 + C_2F^{C_3})\ \frac{E_D{}^{C_4}}{H_D{}^{C_5}} \tag{151}$$

can be shown to be equivalent to equation 119 when the square root of the molecular diffusivity at 20°C ($D_{m_{20}}$) is accounted for by C_1, C_3 is equal to 1.5, C_4 is equal to 0.5, C_5 is equal to 1.0, and the parameters E_D and H_D are equivalent to E and H. The terms E and H are the average unit energy dissipation rates and depth, respectively.

The values of C_2 and C_3 were initially fixed at the values suggested by Gangadharaiah, and equation 151 was solved for C_1, C_4 and C_5. A solution for all five coefficients was also attempted. The R^2 values for these models were considerably smaller than those developed in the previous equations and the standard errors of the coefficients were large. For these reasons, this more complex equation was also rejected.

Selecting the Final Model

The exponents for the energy dissipation and depth terms derived for equations 143 and 145 were similar to values suggested by other studies and were theoretically justifiable. Three sets of exponents were tested to determine if they would yield satisfactory predictive equations. For each of these sets of exponents regression techniques were used to derive the value of the coefficient C.

Krenkel and Orlob (1962), using dimensional analysis, suggested that an equation in the form:

$$K_{2_{20}} = C \frac{E_D^{1/3}}{H_D^{2/3}} \qquad (152)$$

could be justified. When C is a dimensionless coefficient, both sides of this equation are in the units of time^{-1}.

The reaeration rate coefficient has been theoretically described by Thackston and Krenkel (1969) as proportional to the renewal rate and by O'Connor and Dobbins (1956) as proportional to the square root of the renewal rate. The renewal rate is a function of surface turbulence. The unit energy dissipation rate has been used to describe the scale of turbulence. Because of energy transfer considerations, the reaeration rate has been described as proportional to a function of the unit energy dissipation rate within a specified range of exponents. The exponents used in predictive

equations for K_2 have ranged from 0.25 by Lamont and Scott (1970) to 1.0 by Holtje (1972). Theoretical developments by Danckwerts (1951) and O'Connor and Dobbins (1956) indicate that reaeration is proportional to the square root of the surface renewal for small turbulent streams. If the unit energy dissipation rate is assumed to be proportional to stream turbulence and to renewal rate at the surface then the exponent for the energy function should be 0.5.

The predictive equation derived by Krenkel and Orlob (1962) from channel tests suggests that K_2 is proportional to $H_D^{-2/3}$. Field data from the current study confirms this. If these relationships are used, the form of the predictive equation becomes

$$K_{2_{20}} = C \frac{E_D^{1/2}}{H_D^{2/3}} \tag{153}$$

The coefficient C now has units of:

$$\frac{\text{time}^{1/2}}{\text{length}^{1/3}} .$$

When the square root of the molecular diffusivity is accounted for in the coefficient, the remaining units are:

$$\frac{\text{time}}{\text{length}^{4/3}}$$

If the reaeration rate is assumed to be proportional to the square root of the energy dissipation, if the

surface area exposed to gas exchange is planar, and if K_2 is inversely proportional to the active depth, then the equation becomes:

$$K_{2_{20}} = C \frac{E_D^{1/2}}{H_D} \qquad (154)$$

When the square root of the molecular diffusivity is accounted for in the coefficient C, the remaining units are time/length.

The results of the regression analysis of these equations are shown in Figures 6, 7, and 8. The energy and depth functions were treated as a composite variable and the coefficient C was determined. A comparison of the fit of these three equations to the stream data is shown in Table 6.

Table 6. Comparison of simplified theoretical equations.

Equation Number	Coefficient	R^2	Slope
152	50	0.945	1.0
153	37	0.990	1.0
154	11	0.956	1.0

A model in the form of equation 153 was selected as the best fitting equation. The R^2 and slope values show that this equation is a precise and accurate predictor for the range of reaeration coefficients measured. The fit is particularly good for the lower K_2 values where oxygen

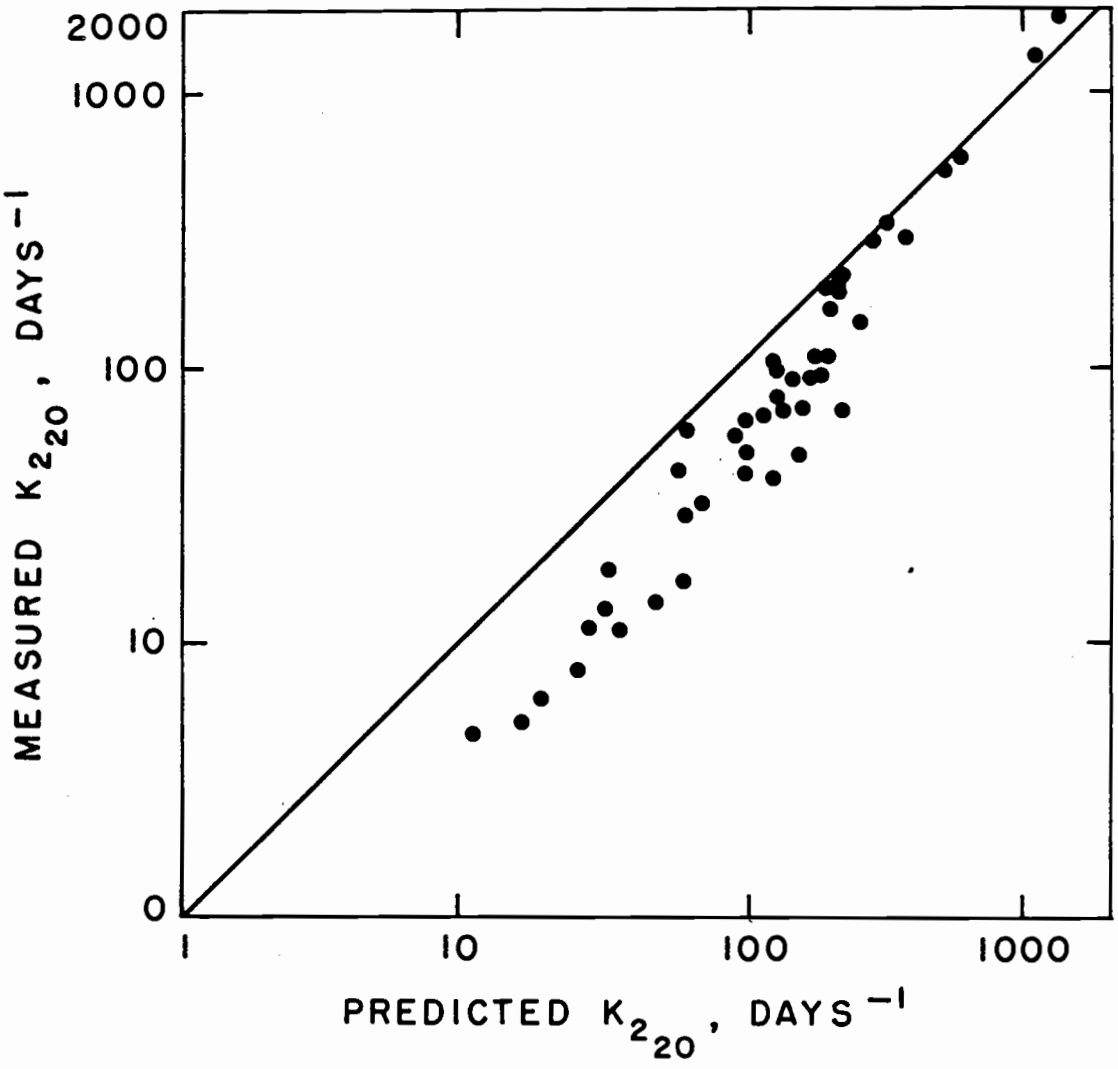

Figure 6. Measured versus predicted values of $K_{2_{20}}$ from equation 152.

$$K_{2_{20}} \text{ (predicted)} = 50 \frac{E_D^{0.333}}{H_D^{0.667}}$$

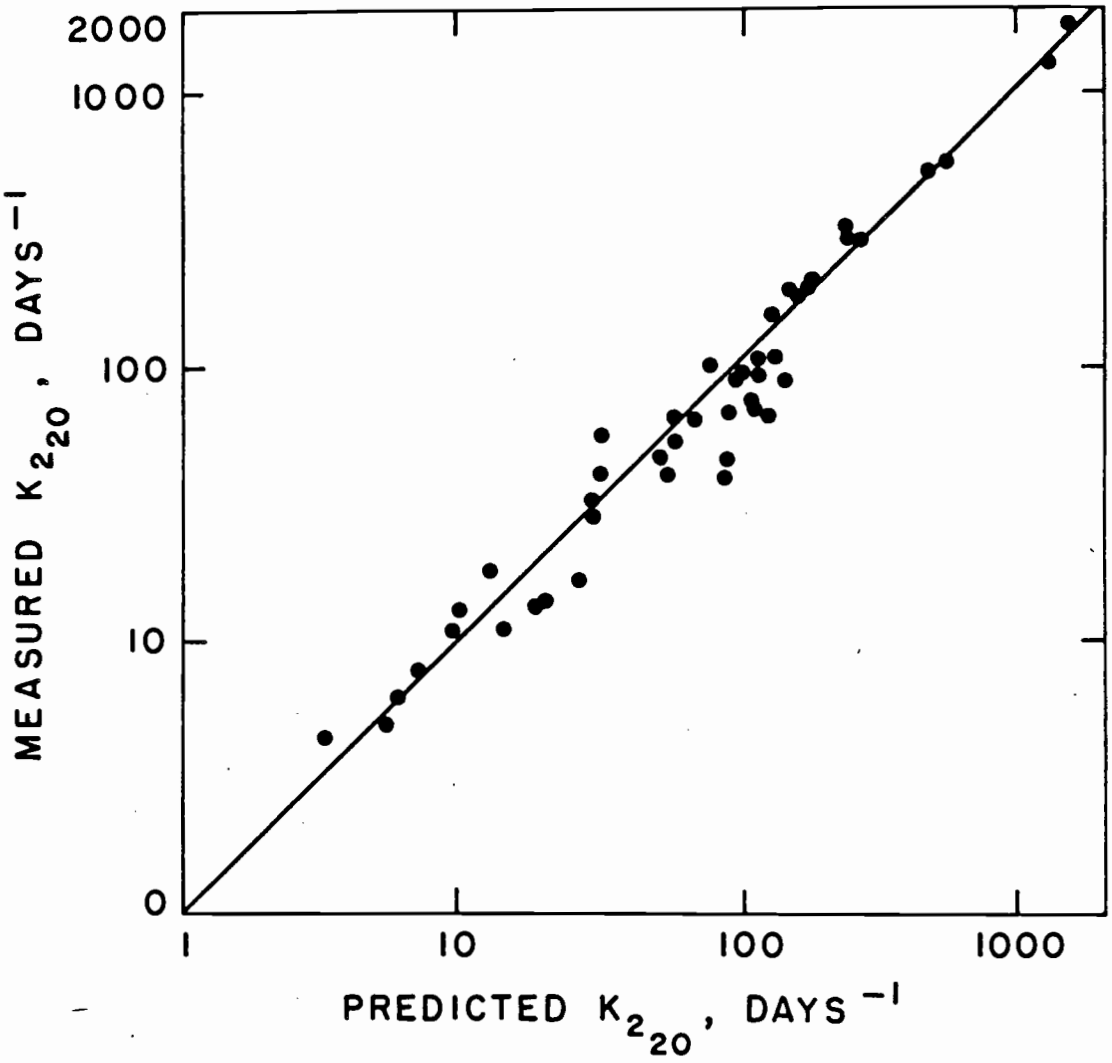

Figure 7. Measured versus predicted values of $K_{2_{20}}$ from equation 153.

$$K_{2_{20}} \text{ (predicted)} = 37 \frac{E_D^{0.5}}{H_D^{0.667}}$$

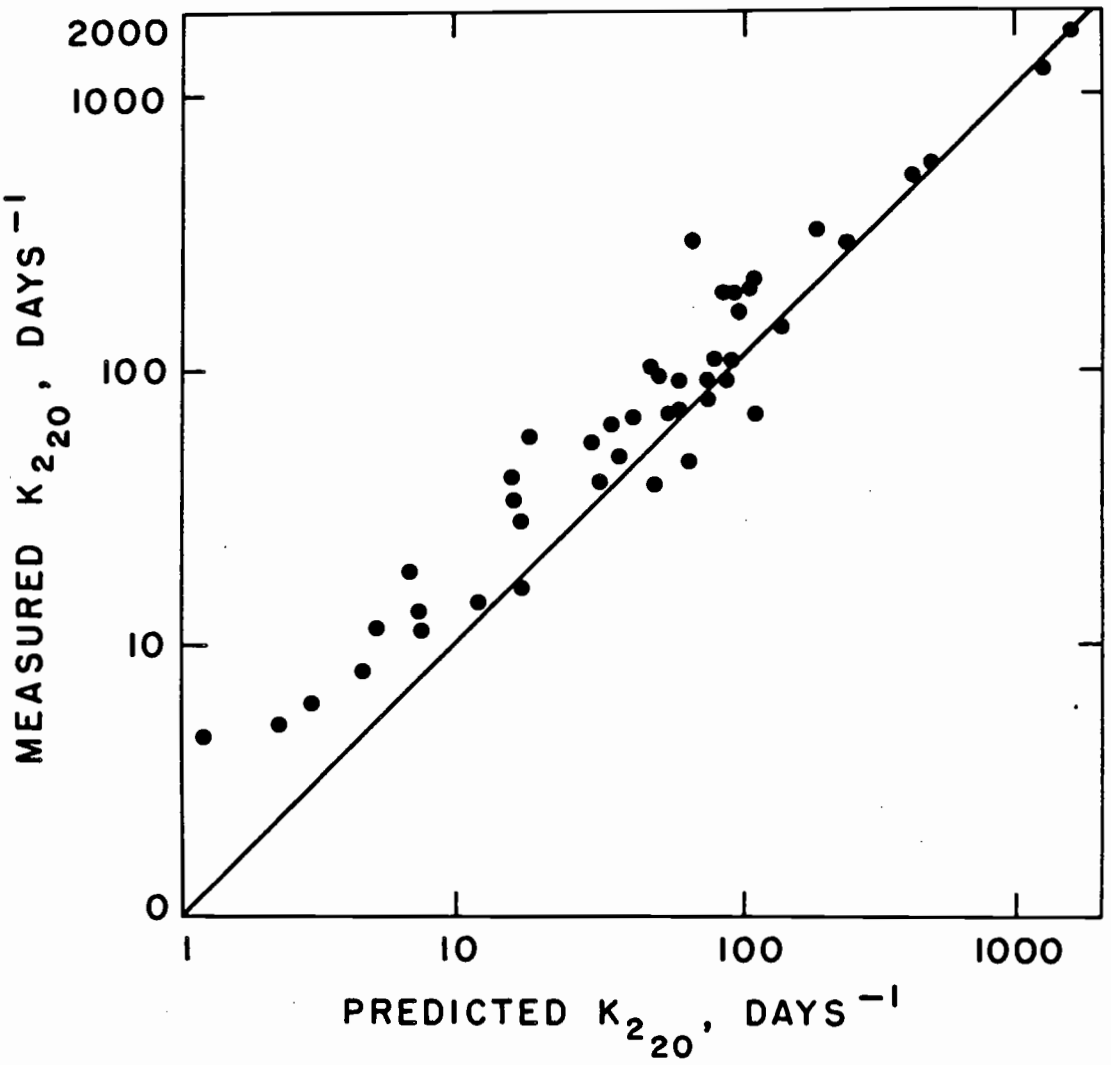

Figure 8. Measured versus predicted values of $K_{2_{20}}$ from equation 154.

$$K_{2_{20}} \text{ (predicted)} = 11 \frac{E_D^{0.5}}{H_D^{1.0}}$$

deficits are most likely to occur. The final form of this equation is:

$$K_{2_{20}} = 37 \frac{E_D^{1/2}}{H_D^{2/3}} \qquad (155)$$

Simplified Reaeration Model Based on Stream Width and Slope

For many timber sales, the collection of field data for harvest planning is done by technicians who do not have extensive training in hydrology, fluid mechanics, and water chemistry. Furthermore, the time and funding required to make detailed measurements of streamflow and bed characteristics is often not available. These problems could be avoided if the reaeration model includes only parameters which are easy to measure.

The field data from this study were therefore fit to some very simple models with easily measured parameters. Regression analysis was used to test the hypothesis that acceptable predictions of reaeration could be made using only stream slopes and the width of the stream surface as independent variables.

Under many conditions, slope will be the only parameter known. Since slope is an important component of the unit energy dissipation rate (E) and is also important in determining velocity, it is potentially an effective parameter for estimating reaeration rates. Because slope does

not provide information on surface or streambed contact area, volume, or roughness, the relationship between slope and reaeration rate is approximate. If only the slope of the streambed is known, the reaeration rate coefficient can be predicted using the following equation which was derived using a simple linear regression:

$$K_{2_{20}} = 4861\ s \tag{156}$$

where s is the slope in ft/ft. The regression coefficient for this equation is 0.79866; the slope between the predicted and measured values is 1.000.

If the stream width and slope are known, then the reaeration rate can be estimated with the equation:

$$K_{2_{20}} = 110.7\ \frac{s^{0.5}}{W} \tag{157}$$

Equation 157 is a simplified multiplicative model. Although this equation fits the measured data quite well (R^2 = 0.93774; slope = 1.000), its application to other streams may be inappropriate because of the influence of pools in this study. For example, when stream depth and velocity are included in the model, the reaeration rate coefficient is proportional to the width of the stream. With a simplified model, that relationship is influenced by the presence of pools. In the pools found in this study, increases in width were associated with increases in depth and decreases

in stream velocity. This accounts for the inverse relationship expressed in equation 157. The applicability of this simplified model may be largely determined by the presence or absence of pools of this same nature. In a stream where increased width is due to the presence of shallow riffles, equation 157 would become inappropriate. Under these same conditions, equation 155 would still be expected to provide a meaningful estimate of the reaeration rate.

Dissolved Oxygen Sag Curve

Reaeration coefficients were calculated for the stream segments on Oak Creek, Needle Branch, and Watershed 3 from equation 155 and the field data used to derive the reaeration model. The coefficients were then used to calculate dissolved oxygen concentrations through the study reaches by means of the oxygen sag method described by equation 7. The calculated values can be compared to the measured values at each station. Two reaeration runs are shown for each stream reach as a means of replicating the sag curve calculations. The observed and predicted concentrations for Oak Creek, Needle Branch, and Watershed 3 are shown in Figures 9, 10 and 11. Oak Creek provides a good comparison of the predicted and observed dissolved oxygen concentrations because it is a long test reach with several segments that vary in their reaeration rates. Watershed 3 and

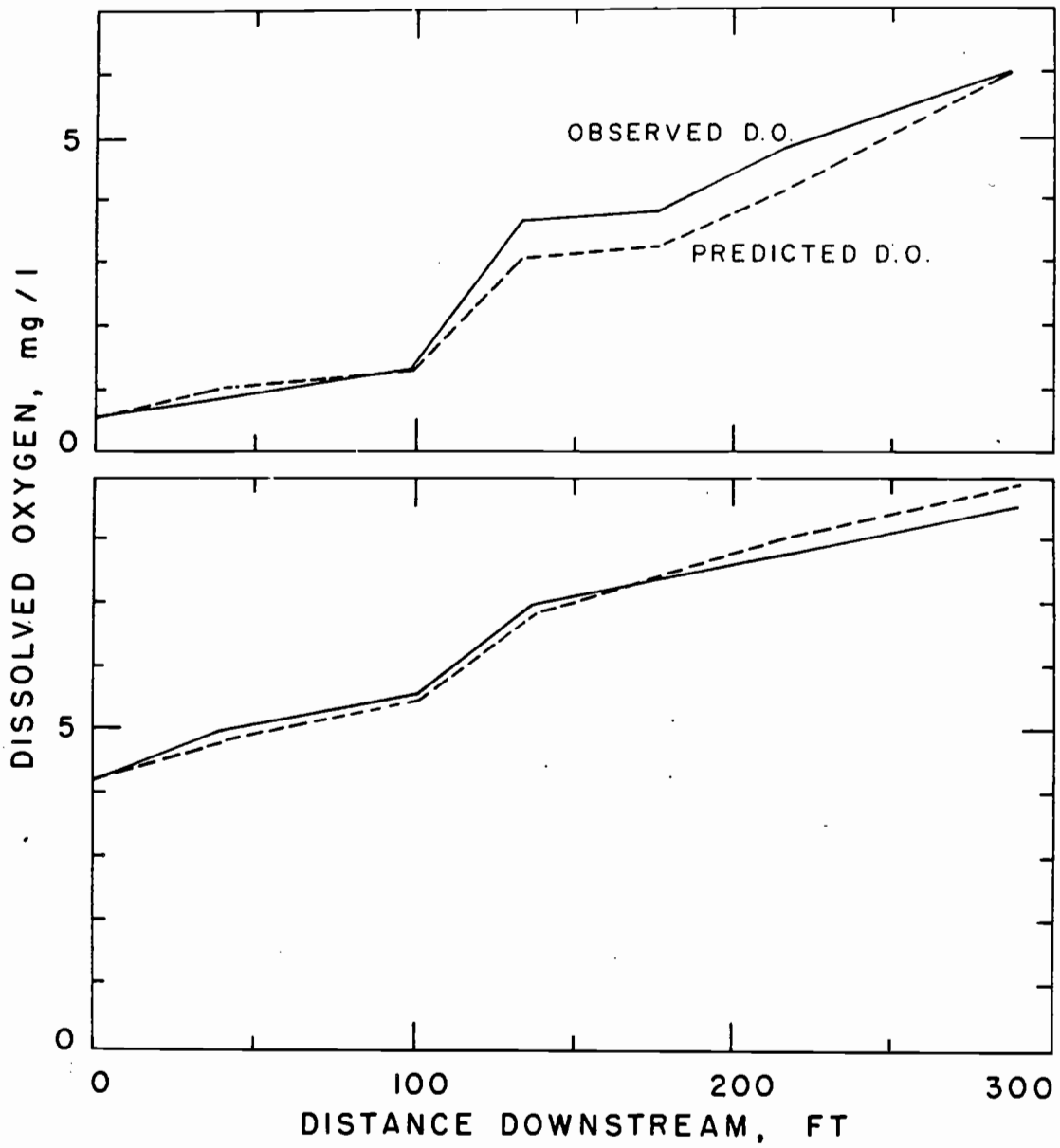

Figure 9. Measured and predicted values of dissolved oxygen using equation 155 for two field tests at Oak Creek.

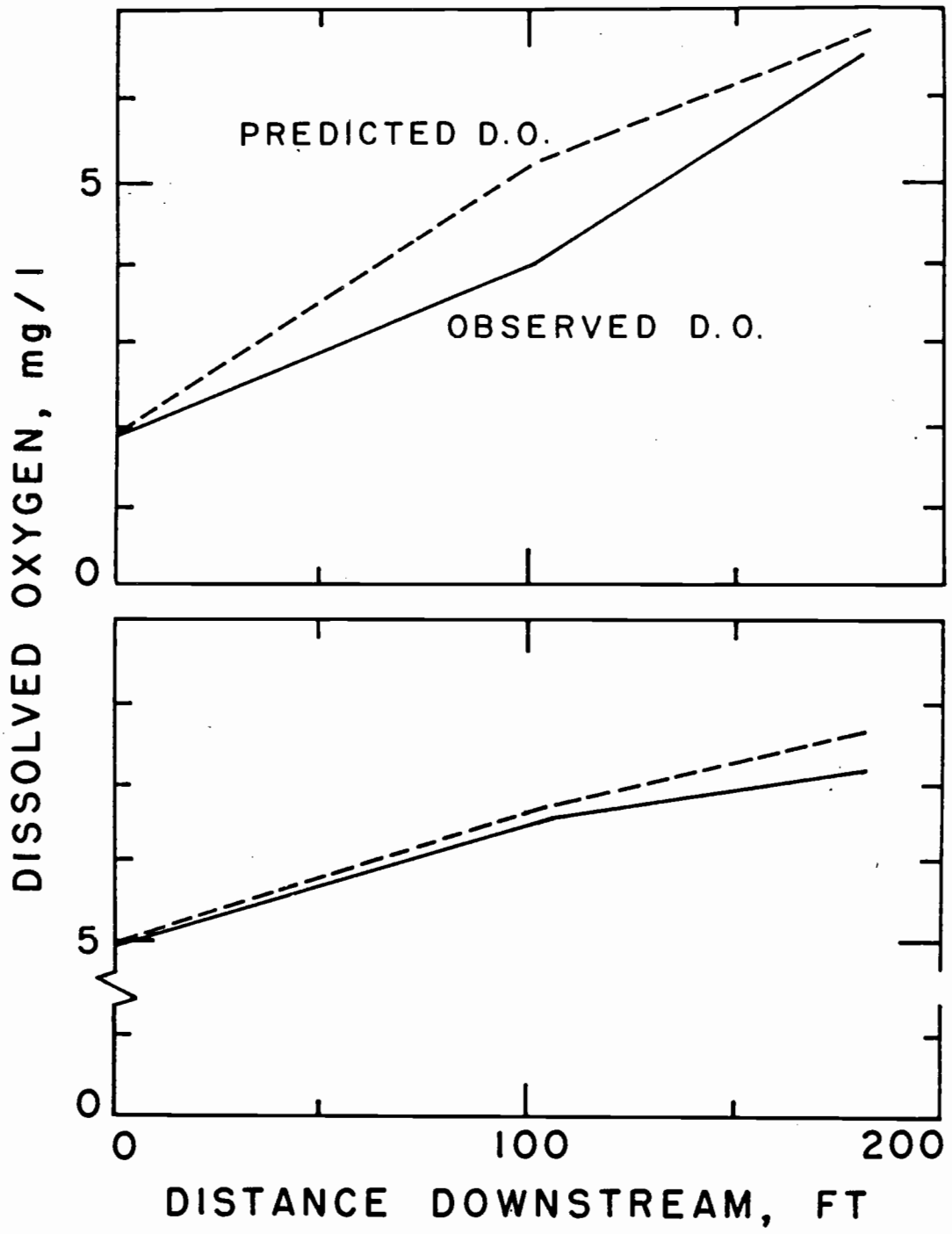

Figure 10. Measured and predicted values of dissolved oxygen using equation 155 for two field tests at Needle Branch.

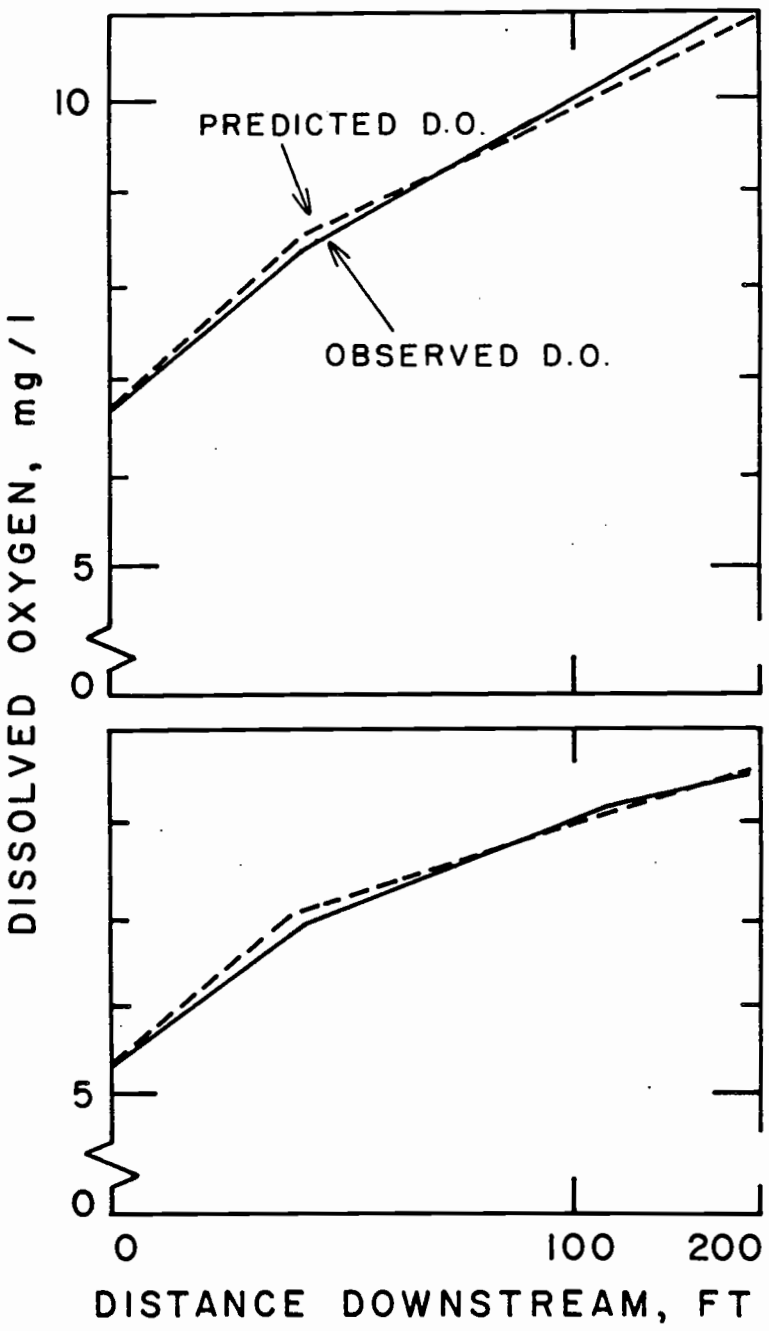

Figure 11. Measured and predicted values of dissolved oxygen using equation 155 for two field tests at Watershed 3.

Needle Branch Creek are shown as examples of streams with rapid and slow reaeration rates, respectively.

The reaeration rate coefficients for Needle Branch are several orders of magnitude smaller than those measured in the test segments of Watershed 3. Despite this large difference, the change in deficit per ft is very similar for the two streams. The seemingly rapid reaeration noted for Needle Branch is the result of slow velocities and a large initial deficit created by the artificial deoxygenation. When an instantaneous oxygen demand is used to deaerate a stream, as was done in this study, no residual demand is transported into the test segments. The source of oxygen demand under harvest impact conditions is submerged organic debris. An increase in the retention time within a segment will allow more leaching and BOD oxidation. Under these conditions, the larger reaeration rate coefficients would be more evident in the higher downstream oxygen concentrations. Examples of what might be expected when organic debris are deposited in a stream are presented in the discussion section.

Deviations of the predicted and observed oxygen concentrations for all 7 study streams exceeded 1 mg/l at only 3 points. More often, the divergence was less than 0.5 mg/l. Therefore, the model provides a very good estimate for field use and for evaluation of potential inputs from timber harvesting. Fitting errors were the greatest for very

long segments. Under these conditions, a small error in the calculated reaeration rate was maintained over a long distance. Where several segments were evaluated, the random value of the errors tended to offset each other. Perhaps more important than the fit of the individual points is the comparison of the recovery slopes for predicted and observed oxygen concentrations. As can be seen from the Oak Creek example, the recovery slopes were very accurately modeled.

DISCUSSION

During normal forest harvesting activities, organic debris can be deposited in small streams within or bordering the cutting site. If this deposited debris consists of green vegetation and it is in large enough quantities, the oxidation of that organic debris can reduce the dissolved oxygen in the stream to a level which is harmful for aquatic organisms. The magnitude of the oxygen deficit is dependent upon the quantity and characteristics of the organic debris, the stream environment, and the reaeration rate. The objective of this study has been to develop a predictive equation for this reaeration rate coefficient from field data for small Oregon streams. The applicability of this equation was then checked with oxygen sag curves for these streams. Using equation 155, together with estimates of organic loading and decay rate constants, a forester can predict where logging debris accumulations might reduce dissolved oxygen below acceptable levels. This approach will help identify the sites where harvesting practices should be modified to reduce potential impacts on the oxygen concentration of a stream.

The application of any fundamental theory to the highly variable conditions encountered in the field can be both difficult and inaccurate. Inaccuracies may arise from several sources of error. These include modeling errors

used in the physical description of the reaeration process and errors in field measurements of the variables that are required by the model structure. Ultimately, the prediction of impacts is tied not only to the physical system but also to the biological changes which occur. This chapter addresses the possible sources of error in the proposed model and provides an example of model application.

Comparing Reaeration Models

The reaeration model developed in this study has a simple structure and implies a simple reaeration process. In developing the predictive equation for reaeration in small streams, the roles of many factors including energy dissipation, depth, bed roughness, surface distortion, and bubble entrainment have been considered. The predictive equation which fits the observed data best, however, is a function of the stream segment slope, maximum velocity, width, and discharge. More complex models, designed to account for bubble entrainment and surface distortion, failed to provide as accurate a prediction as this simpler model. Some possible reasons for this incongruence are the use of incorrect models by other authors to account for surface area increases, the insensitivity of parameters in these more complex models to the conditions encountered in small streams, and errors in measuring the variables required in these models.

Model Errors

Many attempts have been made to develop a predictive equation for the reaeration rate coefficient. The approaches developed in this study seem to be consistent with known gas exchange phenomena. For turbulent conditions the reaeration rate should be proportional to the square root of both molecular diffusivity and energy dissipation. As the width of a segment increases and discharge decreases, the reaeration rate should increase. This model can be considered simple or incomplete in that it does not account for increases in surface area due to turbulence.

Models that were tested to account for increases in the surface area due to turbulence proved unsuccessful. These models used the Froude number and bed roughness to account for changes in the surface area exposed to gas exchange. Because film renewal and surface area distortion result from turbulent eddies at the surface, both should be strongly correlated to turbulence. If surface turbulence can be estimated using the unit energy dissipation rate, then the gas transfer coefficient (K_L) and the increase in surface area (C_A) should also be estimated by an energy dissipation term. However, the parameters used in these models were largely developed for steady, uniform flow. In contrast, the conditions in this study ranged from steady, gradually varied flow to rapidly varied flow. The application of parameters developed for uniform flow to these

conditions may lead to unaccountable errors. An example is the advection of relatively large amounts of kinetic energy between segments.

Several other problems arise from trying to use Manning's n and the Froude number to predict the ratio of the actual surface area to observed surface area (C_A). Two types of energy-dissipating systems are recognized in the streambed. The first type is the particle or skin roughness which describes the roughness resulting from the irregular shapes and sizes of particles on the streambed surface. This corresponds to the roughness caused by sand particles attached to the surface of sandpaper. The second type of roughness, called form resistance, represents the apparent roughness of the regular or irregular undulation of the streambed when measured against an assumed flat plane. With increased form roughness, energy is dissipated and less energy is available for mixing. The composite of these two roughness components is the total bed roughness.

In Graf's (1971) review of bedform mechanics, he notes the historical use of the Froude number to describe the importance of the two resistance components. When F is less than 1, form roughness predominates, resulting in the development of some vertical eddies and surface boils. At critical flow, F equals 1 and transitional conditions occur. When F is greater than 1, flow is supercritical. With supercritical flow conditions, the water surface flows

parallel to the bottom. Skin or particle roughness predominates during supercritical flow. For the small streams in this study, the Froude number was rarely greater than 1.0 and therefore form roughness dominated the energy dissipation mechanisms. This is further reflected in the very large Manning roughness coefficients developed in pool segments. The roughness coefficients in the rapids and riffles (where particle roughness contributes greatly to mixing) were often much lower than in these pools. From a visual inspection of the streams it is obvious that surface area distortion is the greatest in turbulent riffles.

In the Gangadharaiah (1970) study, form roughness was not a component of the resistance to flow. The flume used in the test was a flat chute. Because the Gangadharaiah relationship was developed with only surface roughness, it appears to be an inappropriate estimator of increased surface area where form roughness is important.

The simple model developed in this study has a structure similar to the equation developed by Krenkel and Orlob (1962) for a recirculating flume. Although the configuration of this testing apparatus is biased toward sidewall effects, it represents conditions similar to those found in small, dissected streams. Krenkel and Orlob did not attempt to model the role of increased surface area.

Measurement Errors

Errors in the measurement of stream characteristics and reaeration rates could also influence the model results. Possible sources of error in the field data include both incorrect estimations of stream hydraulic parameters and incorrect measurements of the oxygen concentration which is used to compute the reaeration rate coefficient. Composite variables such as the Froude number and Manning's n may be more susceptible to errors because of compounding inaccuracies.

Hydraulic Parameters

The measured hydraulic characteristics which were most often subject to error and had the greatest influence on the accuracy of the model were the slope, depth and discharge.

Slope measurements were usually quite accurate and reproducible. This was especially true for segments with a large change in elevation. However, for segments with very shallow slopes, such as the upper portions of Oak Creek and Berry Creek, the calculation was dependent on a measured drop of only 0.01 ft. Additional error was introduced from rippling on the surface. Independent measurements of the slopes of these two segments varied by 100 percent. These discrepancies may be partially attributed to changes in the surface profile at different discharges. For most segments,

where the slope of the stream surface was moderate, the measured slopes were very consistent.

The accuracy of the depth measurements was also dependent on the character of the individual segment. When the streambed character changed rapidly, it was necessary to sub-divide each segment. The relative errors were the greatest in the shallow segments, such as the bottom of Watershed 3. However, comparison of the cross-sectional areas measured at different discharges showed consistent relationships.

Discharge was determined by measuring the velocity and cross-section of the stream. Discharge could also be checked by measuring the deficit near the injection point. Where possible, the discharge was measured by recording the time required to fill a metal container. (See Field Measurements.) Measurements were repeated several times in order to establish reproducible results. The discharge estimated by using the collection method was usually slightly less than the results of the other techniques.

Discharge estimates using the artificial deficit created by a known injection rate are influenced by the downstream reaeration process. With this method, as the reaeration process continues, the estimated discharge becomes larger. Measurements of discharge that use the average cross section and mean velocity are also subject to errors. These errors can result from inadequate

adjustments for velocity variations in the cross section of the stream and overestimates of the active cross-sectional area. Velocity measurements made with a pygmy meter and drops of dye were compared to the collection method and found to yield similar results.

Although the discharge measured by the collection method was usually less than the values calculated from the other techniques, the difference was often less than 10%. In this case, the collection method value was used. If results were not within this range, the measurements were repeated until the disagreement could be resolved and a precise estimate of the discharge could be obtained.

Oxygen Concentration

The sources of error in measuring the concentration of oxygen include inaccuracies from the Winkler Test and instrument errors from the D.O. meter. "Standard Methods" reports that the Azide modification of the Winkler technique has a precision of 0.1 to 0.02 mg/l depending on the purity of the water. The two test samples collected prior to the addition of sodium sulfite to the stream always agreed within 0.05 mg/l. The calibrated meter was standardized to the results of the idometric determination and closely agreed with post-treatment idometric measurements. The manufacturers report that the meter has an accuracy of ±0.1 mg/l and precision of 0.05 mg/l. It was noted in

field applications that insufficient stream current could depress the oxygen concentration measured by the meter. Where possible, the stations were established at locations that provided adequate current. If the meter had to be agitated by hand, the reading may not have been as accurate.

An adjustment period was required for the meter to reach equilibrium with the oxygen concentration at each station. This time-lag has been previously reported (Holtje 1971). The delay period was reduced by transporting the meter probe in a container filled with deaerated water taken from the last measurement station. Not allowing the meter to reach equilibrium could introduce errors.

Care was taken to avoid the problems involved in measuring oxygen concentrations. Measurements were continuously monitored for extended periods and also were repeated in order to insure accurate and reproducible results. Repeated oxygen concentration measurements at each station agreed within 0.05 mg/l.

The reaeration rate was calculated from the observed oxygen recovery and the calculated mean velocity. The saturation concentration was assumed to be the concentration observed prior to injection of the reducing agent. This seemed to be appropriate because elevational and pressure variations made an accurate calculation of the solubility difficult. Calculated solubilities usually agreed closely with measured dissolved oxygen concentrations. The

low BOD concentrations measured during the tests confirmed the use of the initial dissolved oxygen concentration. An exception was the first test on Needle Branch. This site had an oxygen concentration which was 33% less than would have been expected from the temperature measured and barometric pressure reported. However, the reaeration rates measured in this test appear to be consistent with the other data. When the reaeration rates were calculated assuming an instrument error (i.e., reading too low), the results were not significantly different. Because this test provided data for the lowest flow conditions and had comparable results with the other data, it was retained in the analysis.

Examples of Model Applications

The capability of predicting reaeration rates allows foresters to estimate the position and magnitude of the oxygen deficits that will be created by logging slash. The reaeration rate constant can also be used to estimate the distance required for a stream to recover from a deficit. Berry (1975), using a finite difference model, simulated the oxygen demand and oxygen deficit created in streams draining a harvesting site. This section will present a few examples of simulated stream recovery under different conditions to illustrate the usefulness of predicted K_2 values in decision making.

Predicting Stream Deficits

Incorporating the predicted K_2 values into an estimate of the responses of a stream to organic debris would require the following steps:

Step 1: Divide the stream into segments of uniform hydraulic characteristics.

Step 2: Measure the stream discharge (Q) and the depth (H), width (W), slope (S), and maximum velocity (U_D) of each segment.

Step 3: Calculate the reaeration rate (K_2) using equation 155. Calculate U using equation 122.

Step 4: Estimate the potential quantity of debris (in mg/l of ultimate BOD) that will be deposited in the stream by a silvicultural procedure.

Step 5: Estimate the BOD rate constant (K_1), and leaching rate constant (K_4) from values reported by Berry (1975).

Step 6: Calculate the dissolved oxygen sag curve using the Berry finite difference oxygen model. The Berry oxygen model can account for longitudinal loading variations along the stream reach and can also adjust for temperature changes within a clearcut.

Step 7: Evaluate the consequences of the harvesting technique on water quality and fish populations in the stream.

Of these operations, step 4 will be the most difficult to quantiy with the present state of knowledge. The weight of organic debris which enters a stream channel due to logging has been shown to be highly variables (Dykstra and Froehlich, 1976). The ultimate BOD of that debris may vary even more due to differences in species, age, and season.

Some examples of stream recovery from an oxygen deficit are presented to demonstrate the use of the reaeration rate constant in oxygen modeling. These examples simulate the recovery of a stream from an oxygen deficit imposed upstream by a clearcut. It is assumed that no additional leaching of soluble BOD will occur through the downstream reaches. The temperature of the stream should also remain constant if the stream flows through undisturbed or re-vegetated sites (Brown et al., 1971). Under these simplified conditions, the downstream deficits can be modeled using equation 7 (rather than the Berry finite differences model) in step 6.

$$D = \frac{K_1 L_0}{K_2 - K_1} e^{-K_1 t} + [D_0 - \frac{K_1 L_0}{K_2 - K_1}] e^{-K_2 t} \qquad (7)$$

Equation 155 is used to define the reaeration rate coefficient (K_2) for the various stream conditions. Simplified to its basic parameters for field application and adjusted for temperature effects according to equation 118, equation 155 becomes:

$$K2_T = 1.016^{(T-20)} \; 37 \frac{W_D^{2/3} \, s^{1/2} \, g^{1/2} \, U_D^{7/6}}{Q^{2/3}} \qquad (158)$$

where $K2_T$ is the reaeration rate constant in $days^{-1}$ at temperature T in °C, W_D is the mean active stream width in ft, U_D is the maximum velocity in ft/s, g is the gravitational constant in ft/s^2, and Q is the discharge in ft^3/s. s: slope ft/ft

The mean velocity and maximum velocity are assumed to be equal for this approximation of the downstream oxygen recovery. This will result in a conservative estimate of the affected stream length. If the impact on the stream is shown to be significant using this simplification, then a more detailed evaluation using the measured mean velocity and maximum velocities would be warranted.

The stream characteristics for the simulations are listed in Table 7. In examples 1 and 2, it is assumed that

Table 7. Simulated stream conditions.

Test no.	Q ft^3/s	s ft/ft	U_D ft/s	W_D ft	H_D ft	K_2 1/day	K_1 1/day	L_0 mg/l	T °C
1	0.1	0.1	1.0	5	0.02	195	0.16	0	20
2	0.1	0.01	0.05	5	0.4	40	0.16	0	20
3	0.1	0.1	1.0	5	0.02	195	0.16	450	20
4	0.1	0.01	0.05	5	0.4	40	0.16	450	20

there is no soluble BOD in the stream. This simplifies the solution of the oxygen recovery but is not a realistic condition. Examples 3 and 4 assume a soluble BOD concentration

of 450 mg/l and a K_1 value of 0.16. The deficit is assumed to be 3 mg/l. K_1, L, and D are consistent with values that have been simulated for the downstream end of a 1000 ft clearcut (Berry 1975).

Figure 12 shows the oxygen sag curve for the four examples and compares these recoveries to water quality standards.

From the simulated oxygen recovery curves, it is apparent that the reaeration rate constant alone cannot be used to predict the distance required for a stream to recover from a deficit. The recovery distance is also dependent on the size of the deficit (D), concentration of the soluble oxygen demand (L), BOD rate constant (K_1), stream velocity (V), and the standard to be met. As the reaeration rate constant is reduced, the distance for recovery is extended. With more oxygen demand or larger K_1 values, the continuing removal of oxygen also extends the recovery distance. With a rapid stream velocity, the volume elements are transported downstream with less time available for changes in the oxygen concentration.

The recovery from the oxygen deficit behaves very differently for the examples with and without soluble BOD. In the case where no oxygen demand is present, the importance of the reaeration rate may be masked by velocity differences. For example, in cases 1 and 2 the stream with the larger reaeration rate takes a longer distance to recover

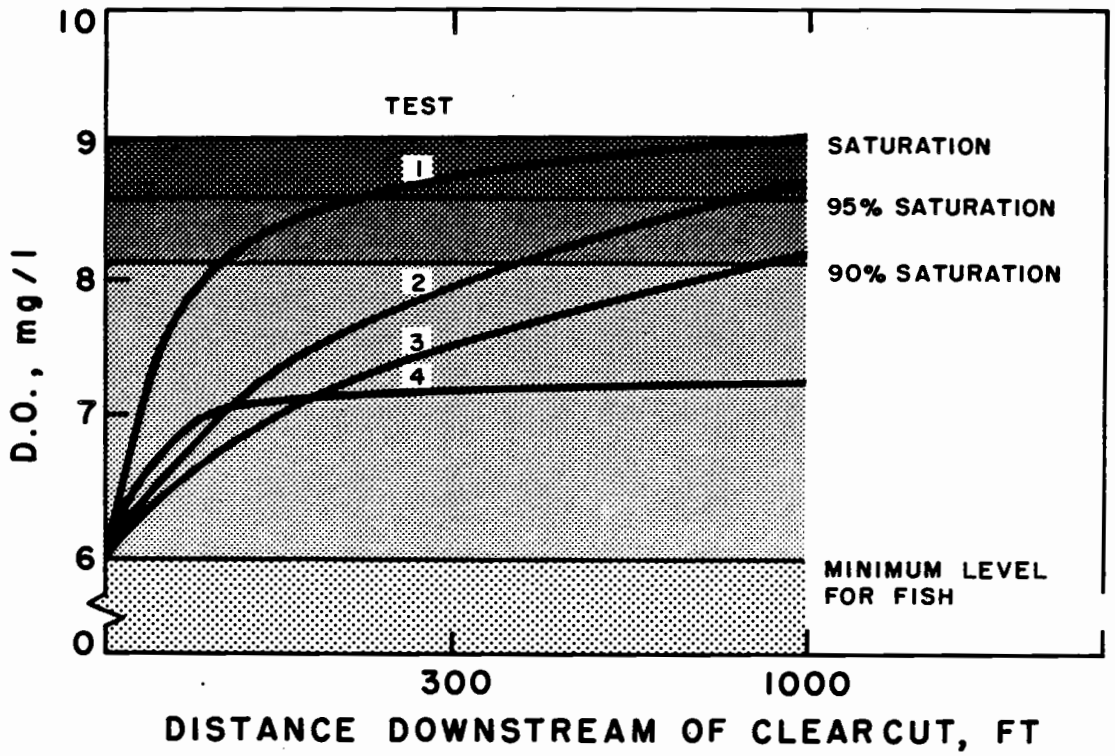

Figure 12. Hypothetical dissolved oxygen sag curves for various stream conditions.

because its velocity is much larger. However, when a significant continuous demand on the oxygen results from soluble BOD, the importance of the reaeration rate will become more evident as is shown in examples 3 and 4.

Debris contributions to some class II streams should be limited due to water quality requirements of a downstream class I stream with spawning sites. Under these conditions the dissolved oxygen at the confluence would be estimated as:

$$\frac{Q_1C_1 + Q_2C_2}{Q_1 + Q_2} = C_3 \qquad (159)$$

where C_1 and C_2, and Q_1 and Q_2 are the concentrations and discharges respectively for streams 1 and 2. C_3 is the oxygen concentration for the combined streams. Any oxygen sag routing downstream will be a function of the downstream conditions. Particular care should be taken where a class II stream discharges into a small class I stream with a relatively low reaeration rate.

Forest Practices to Control Dissolved Oxygen Impacts

Where the impacts of harvesting are expected to exceed the tolerable limits, forest practices must be implemented to avoid or ameliorate the detrimental influences of harvesting on the dissolved oxygen. Several forest practices can be used to either minimize solar inputs, reduce the

sources of organic debris, or avoid detrimental modification of the stream channel. All of these procedures may be costly to implement. Dykstra and Froehlich (1976) have shown that the costs of applying special harvesting practices are site-specific. The economic and sociologic impacts of these practices must be considered along with their effectiveness in maintaining dissolved oxygen goals.

Buffer strips are commonly used to maintain shade for temperature control. They also reduce the direct input of organic debris into the stream channels. Buffer strips can, however, sacrifice merchantable timber and isolate valuable timber growing sites. Where a class II stream is flowing into a sensitive class I stream, a lengthy buffer may be required near the confluence to avoid additions of deaerated water with high BOD concentrations into the class I stream.

Uphill, cable-assisted felling or full support felling can be used to reduce debris inputs. McGreer (1975) reports that uphill, cable-assisted felling reduces small debris in the streambed to 39% of the amount found during conventional felling. These special felling procedures are significantly more costly than conventional techniques.

Stream cleanup is an ameliorating procedure that is often required as a condition of a timber sale. The rationale is to remove organic debris that may influence dissolved oxygen, obstruct fish migration, or contribute to

a debris torrent. From the leaching and BOD equations, it is obvious that the highest oxygen demands occur very shortly after debris enters the stream. The small debris (needles, leaves, twigs) that contributes the most to the short term BOD concentrations in streams may also be the most difficult to remove. For these reasons, stream clean-up may not be effective in sensitive sites. Hand cleanup costs have been estimated to range from $100 to $500 per 100 ft of stream (Dykstra and Froehlich 1976).

Where organic debris is not detrimental to dissolved oxygen concentration, it serves as a food source. Large debris can also be a stabilizing component in the streams and provide valuable stream habitat.

Channel-bank breakdown can fill, widen, and dam the streambed; resultant reduced velocities decrease the reaeration rate. Where quiescent pools are created, the oxygen balance is disturbed by a decreased energy dissipation rate, an increase in the depth to width ratio, and an increase in the contact time available for leaching of organic debris. Yarding and tractor activities can be excluded from the streambed in order to maintain the stability of the streambed. Like special felling procedures, these restrictions may result in an increase in the cost of harvesting due to decreased productivity.

Where there is planning flexibility, cutting site boundaries can be oriented to minimize the stream reaches

exposed to uphill harvesting. Harvesting can also be planned for periods when the stream is the least sensitive. For example, harvesting may be scheduled for the winter when flows are high. The cold stream temperatures would also retard the rate of oxidation and result in higher saturation values. However, because this period coincides with the development of salmonid eggs in the streambed, this strategy may satisfy water quality requirements while sacrificing the real objective of protecting the fish.

Suggested Research

Preliminary studies have been made on the contributions of natural debris fall and logging activities to the accumulation of organic materials in streams. Additional information is needed on the amount of small debris that is entering forest streams and the oxygen demand it creates. This kind of information would be especially helpful if it could be used to evaluate the relative contributions expected from different management practices and forest types.

Reaeration directly influences the oxygen concentration of surface waters. In locations where rearing habitat is limiting, the surface oxygen concentration is one valid parameter for assessing the stream habitat for fish populations. Where spawning beds are limiting, it is the intragravel oxygen concentration that must be evaluated. Intragravel oxygen concentrations are indirectly influenced by

reaeration through exchanges with surface waters. The concentrations of oxygen in intragravel waters have reportedly been depressed by logging activities and may be slow in recovering. This problem requires continued investigation. Specifically, the reasons for the delay in recovery must be determined.

Additional development of the roles of bubble entrainment, surface distortion, and turbulence could improve the reaeration model. These factors are all very difficult to measure because of their transient nature. The use of hot-wire current detectors might be one method for estimating stream turbulence. The extreme variability of natural streams makes these components difficult to evaluate in reaeration studies.

Finally, the predictive equation for reaeration rates and the oxygen models cited in this study should be validated for debris induced deficits. The accuracy and sensitivity of K_1, K_2, and K_4 values must be evaluated under natural conditions.

SUMMARY

Reaeration is the physical process of oxygen moving into solution. An equation based on hydraulic parameters has been developed to estimate the reaeration rate coefficient for small streams. The model was developed from data collected in seven small Oregon streams. A total of 45 test segments were used in the analysis. Oxygen was artificially depleted by injecting sodium sulfite into the streams. The reaeration rates were determined by monitoring the recovery of the oxygen concentrations in the stream segments.

Simplified to its basic parameters for field application, the reaeration rate equation is:

$$K_{2_T} = 1.016^{(T-20)} \; 37 \; \frac{W_D^{2/3} \; s^{1/2} \; g^{1/2} \; U_D^{7/6}}{Q^{2/3}} \qquad (158)$$

where K_{2_T} is the reaeration rate coefficient in $days^{-1}$ at temperature T (in °C), W_D is the mean active stream width in ft, U_D is the maximum velocity in ft/s, g is the gravitational constant in ft/s^2, and Q is the discharge in ft^3/s.

The maximum unit energy dissipation rate (sU_Dg) was found to be an important composite parameter. The energy dissipation rate was used to estimate turbulence. Turbulence promotes reaeration by maintaining an oxygen gradient

at the surface. The width of the stream provides information on the contact area available for molecular diffusion. The discharge of the stream describes the volume that is receiving the flux of molecules. As the discharge increases, a greater flux of molecules is required to reaerate the stream.

The model provides a precise and accurate fit throughout the range of reaeration rates measured. This is particularly important for the low reaeration rates where oxygen problems would be expected to occur. The overall R^2 for the model was 0.99.

This model is relatively easy to apply and requires a minimum amount of data. The measurements that are needed are uncomplicated. This simplicity may aid in the implementation of this model for predicting impacts on water quality.

In general, the reaeration rates for the selected forest streams were rapid. Most streams could assimilate large amounts of organic debris without incurring large oxygen deficits.

Future research is needed to establish the quantity and characteristics of debris that will result from various harvesting procedures.

BIBLIOGRAPHY

Adeney, W. E., and H. G. Becker. 1919. Determination of the rate of solution of atmospheric nitrogen and oxygen by water. Philosophical Magazine, Vol. 38, pp. 317-338.

Atkinson, S. W. 1971. BOD and toxicity of log leachates. M. S. Thesis, Oregon State University, Corvallis, Oregon. 97p.

Baird, M. H. I., and J. F. Davidson. 1962. Annular jets--II; gas adsorption. Chemical Engineering Science, Vol. 17, No. 87, pp. 473-480.

Banks, R. B. and F. F. Herrera. 1977. Effects of wind and rain on surface reaeration. Proceedings of the American Society of Civil Engineers, Journal of the Environmental Engineering Division, Vol. 103, No. EE3, pp. 489-504.

Benedek, A. 1971. Problems with the use of sodium sulfite in aerator evaluation. Proceedings of the 26th Industrial Waste Conf., Purdue University, Engineering Bulletin, Engineering Extension Service No. 140, pp. 947-956.

Bennett, J. P. and R. E. Rathbun. 1972. Reaeration in open-channel flow. U. S. Geological Survey, Geological Survey Professional Paper No. 737. 75p.

Berry, J. D. 1975. Modeling the impact of logging debris on the dissolved oxygen balance of small mountain streams. M. S. Thesis, Oregon State University, Corvallis, Oregon. 163p.

Brown, E. C. 1974. Statistical evaluation of reaeration prediction equations. Proceedings of the American Society of Civil Engineers, Journal of the Environmental Engineering Division, Vol. 100, No. EE5, pp. 1051-1068.

Brown, G. W. 1967. Temperature prediction using energy budget techniques on small mountain streams. Ph.D. Thesis, Oregon State University, Corvallis, Oregon. 120p.

Brown, G. W. 1969. Predicting temperatures of small streams. Water Resources Research, Vol. 5, pp. 68-75.

_____. 1972. An improved temperature prediction model for small streams. Water Resources Research Institute, Report WRRI-16, Oregon State University, Corvallis. 132p.

_____. 1972. Forestry and water quality. Oregon State University Bookstore, Corvallis, Oregon. 74p.

_____. 1972. The Alsea watershed study. In: 1972 Loggers Handbook. Vol. 32. (Pacific Logging Congress).

Calderbank, P. H. and A. C. Lochiel. 1964. Mass transfer coefficients, velocities and shapes of carbon dioxide bubbles in free rise through distilled water. Chemical Engineering Science, Vol. 19, No. 7, pp. 485-503.

Camp, T. R. 1963. Water and Its Impurities. Reinhold Publishing Corp., New York. 355p.

Carver, C. E. 1969. Oxygen transfer from falling water droplets. Proceedings of the American Society of Civil Engineers, Journal of the Sanitary Engineering Division, Vol. 95, No. SA2, pp. 239-251.

Chen, K. Y. and J. C. Morris. 1972. Oxidation of sulfide by O_2: catalysis and inhibition. Proceeding of the American Society of Civil Engineers, Journal of the Sanitary Engineering Division, Vol. 98, No. SA1, pp. 215-227.

Chow, V. T. 1959. Open-Channel Hydraulics. McGraw-Hill Book Company, New York. 680p.

Church, P. C. and W. G. Pond. 1974. Basic Animal Nutrition and Feeding. Albany Printing Company, Albany, Oregon. 300p.

Churchill, M. A., R. A. Buckingham and H. L. Elmore. 1962. The prediction of stream reaeration rates. Chattanooga, Tennessee Valley Authority, Division of Health and Safety. 98p.

Churchill, M. A., H. L. Elmore and R. A. Buckingham. 1962. The prediction of stream reaeration rates. Proceedings of the American Society of Civil Engineers, Journal of the Sanitary Engineering Division, Vol. 88, No. SA4, pp. 1-46.

Clark, G. L. 1957. The Encyclopedia of Chemistry. Reinhold Publishing Corp., New York. 1037p.

Danckwerts, P. V. 1951. Significance of liquid-film coefficients in gas absorption. Industrial and Engineering Chemistry, Vol. 43, No. 6, pp. 1460-1467.

Dean, J. A. 1973. Lange's Handbook of Chemistry. 11th Edition. McGraw-Hill Book Company, New York.

Deindoerfer, F. H. and A. E. Humphrey. 1961. Mass transfer from individual gas bubbles. Industrial and Engineering Chemistry, Vol. 53, No. 9, pp. 755-759.

Dobbins, W. E. 1956. The nature of the oxygen transfer coefficient in aeration systems. In: Biological Treatment of Sewage and Industrial Wastes. Reinhold Book Corp., New York, pp. 141-253.

_____. 1964. BOD and oxygen relationships in streams. Proceedings of the American Society of Civil Engineers, Journal of the Sanitary Engineering Division, Vol. 90, No. SA3, pp. 53-78.

_____. 1964. BOD and oxygen relationships in streams--closure. Proceedings of the American Society of Civil Engineers, Journal of the Sanitary Engineering Division, Vol. 91, No. SA5, pp. 49-55.

Doudoroff, P. and D. L. Shumway. 1967. Dissolved oxygen criteria for the protection of fish. American Fisheries Society, Special Publication No. 4, pp. 13-19.

Dykstra, D. P. and H. A. Froehlich. 1976. Cost of stream protection during timber harvest. Journal of Forestry, Vol. 74, No. 10, pp. 684-687.

Edwards, R. W. and M. Owens. 1962. The oxygen balance of a chalk stream, part IV of: The effects of plants on river conditions. Journal of Ecology, Vol. 50. No. 1, pp. 207-220.

Fortescue, G. E. and J. R. A. Pearson. 1967. On gas absorption into a turbulent liquid. Chemical Engineering Science, Vol. 22, No. 9, pp. 1163-1176.

Gameson, A. L. H. and M. J. Barrett. 1958. Oxidation, reaeration, and mixing in the Thames estuary. In: Oxygen relations in streams. Cincinnati. U.S. Public Health Service, Robert A. Taft Sanitary Engineering Center, Technical Report no. W 58-2, pp. 63-93.

Gangadharaiah, T., N. S. Lakshmana Rao and K. Seetharamiah. 1970. Inception and entrainment in self-aerated flows. Proceedings of the American Society of Civil Engineers, Journal of the Hydraulics Division. Vol. 96, No. SA6, pp. 549-565.

Graf, W. H. 1971. Hydraulics of Sediment Transport. McGraw-Hill Book Company, New York. 513p.

Guthrie, D., C. Avery and K. Avery. 1973. Statistical interactive programming system: users reference manual. Technical Report No. 36, Department of Statistics, Oregon State University, Corvallis. 111p.

Haberman, W. L., and G. I. Morton. 1954. An experimental study of bubbles moving in liquids. Proceedings of the American Society of Civil Engineers, Vol. 80, No. 387, pp. 1-25.

Haney, P. D. 1954. Theoretical principles of aeration. Journal of the American Water Works Association, Vol. 46, No. 4, pp. 353-376.

Higbie, R. 1935. The rate of absorption of a pure gas into a still liquid during short periods of exposure. Transactions of the American Institute of Chemical Engineering. Vol. 36, No. 2, pp. 365-389.

Holtje, R. K. 1971. Reaeration in small mountain streams. Ph.D. Thesis, Oregon State University, Corvallis, Oregon. 146p.

Ippen, A. T., Campbell, L. G., and C. E. Carver. 1952. The determination of oxygen absorption in aeration processes. M.I.T. Hydrodynamics Laboratory Report No. 7.

Isaacs, W. P. and A. K. Gaudy. 1968. Atmospheric oxygenation in a simulated stream. Proceedings of the American Society of Civil Engineers, Journal of the Sanitary Engineering Division, Vol. 94, No. SA2, pp. 319-344.

Isaacs, W. P. and J. A. Maag. 1969. Investigation of the effects of channel geometry and surface velocity on the reaeration rate coefficient. Purdue University, Engineering Bulletin, LIII.

Isaacs, W. P., P. Chularachana, and R. Bogart. 1969. An experimental study on the effects of channel surface roughness on the reaeration rate coefficient. Proceeding of the 24th Annual Purdue Industrial Waste Conference. Purdue University, Lafayette, Indiana, pp. 1464-1476.

Isaacs, W. P. and A. K. Gaudy. 1970. Atmospheric oxygenation in a simulated stream--closure. Proceeding of the American Society of Civil Engineers, Journal of the Sanitary Engineering Division, Vol. 96, No. SA1, pp. 171-178.

Johnson, A. I., F. Besik, and A. E. Hamielec. 1969. Mass transfer from a single rising bubble. The Canadian Journal of Chemical Engineering, Vol. 47, No. 6, pp. 559-564.

Krenkel, P. A. 1960. Turbulent diffusion and the kinetics of oxygen absorption. Ph.D. Thesis, University of California, Berkeley.

Krenkel, P. A. and G. T. Orlob. 1962. Turbulent diffusion and the reaeration coefficient. Proceedings of the American Society of Civil Engineers, Journal of the Sanitary Engineering Division, Vol. 88, No. SA2, pp. 53-84.

Lakshmana Rao, N. S., K. Seetharamiah, and T. Gangadharaiah. 1970. Characteristics of self-aerated flows. Proceeding of the American Society of Civil Engineers, Journal of the Hydraulic Division, Vol. 96, No. HY2, pp. 331-356.

Lamont, J. C. and D. S. Scott. 1970. An eddy cell model of mass transfer into the surface of a turbulent liquid. Journal of the American Institute of Chemical Engineers, Vol. 16, No. 4, pp. 513-519.

Landine, R. C. 1971. A note on the solubility of oxygen in water. Water and Sewage Works, Vol. 118, No. 8, pp. 242-244.

Leonard, J. H. and G. Houghton. 1963. Mass transfer and velocity of rise phenomena for single bubbles. Chemical Engineering Science, Vol. 18, No. 2, pp. 133-142.

Lewis, W. K. and W. G. Whitman. 1924. Principles of gas absorption. Industrial and Engineering Chemistry, Vol. 16, No. 128, pp. 215-220.

Maham, B. H. 1966. College Chemistry. Addison-Wesley Publishing Company, Reading, Massachusetts. 666p.

Maron, S. H. and C. F. Prutton. 1958. Principles of Physical Chemistry. The MacMillan Company, New York.

McGreer, D. J. 1975. Stream protection and three timber falling techniques: a comparison of costs and benefits. M.S. Thesis. Oregon State University, Corvallis, Oregon. 92p.

Metzger, I. and W. E. Dobbins. 1967. Role of fluid properties in gas transfer. Environmental Science and Technology. Vol. 1, No. 1, pp. 57-67.

Metzger, I. 1968. Surface effects in gas absorption. Environmental Science and Technology, Vol. 2, No. 10, pp. 784-786.

Miyamoto, S. 1932. A theory of the rate of solution of gas into liquid. Chemistry Society of Japan Bulletin, Vol. 7, pp. 8-17.

Montgomery, H. A. C., N. S. Thom, and A. Cockburn. 1964. Determination of dissolved oxygen by the Winkler method and the solubility of oxygen in pure water and sea water. Journal of Applied Chemistry, Vol. 14, pp. 280-296.

O'Connor, D. J. and W. E. Dobbins. 1956. The mechanism of reaeration in natural streams. Proceedings of the American Society of Civil Engineers, Journal of the Sanitary Engineering Division. Vol. 32, No. SA6. 30p.

Owens, M., R. Edwards, and J. W. Gibbs. 1964. Some reaeration studies in streams. International Journal Air and Water Pollution, Vol. 8, pp. 469-486.

Owens, M. and R. W. Edwards. 1966. Some chemical aspects of water quality in relation to minimum acceptable flows. Association of River Authorities Annual Conference, Great Yarmouth, England. pp.3-22.

Parkhurst, J. D. and R. D. Pomeroy. 1972. Oxygen absorption in streams. Proceedings of the American Society of Civil Engineers, Journal of the Sanitary Engineering Division, Vol. 98, No. SA1, pp. 101-123.

Ponce, S. L. 1973. The biochemical oxygen demand of Douglas-fir needles and twigs, western hemlock needles and red alder leaves in stream water. M. S. Thesis, Oregon State University, Corvallis, Oregon. 141p.

Ratcliff, G. A. and J. G. Holdcroft. 1963. Diffusivity of gases in aqueous electrolyte solutions. Transactions of the Institute of Chemical Engineers, Vol. 4, pp. 315-319.

Rothacher, J. 1967. Hydrologic and related characteristics of three small watersheds in the Oregon Cascades. Pacific Northwest Forest and Range Experiment Station. 54p.

Sawyer, C. N. and P. L. McCarty. 1967. Chemistry for Sanitary Engineers. McGraw-Hill Book Company, New York. 518p.

Schaumburg, F. D. and S. W. Atkinson. 1970. BOD_5 and toxicity associated with log leachates. Paper read before the meeting of the Western Division of the American Fisheries Society, Victoria, British Columbia.

Straub, L. G. and A. G. Anderson. 1958. Experiments on self-aerated flow in open channels. Proceedings of the American Society of Civil Engineers, Journal of the Hydraulic Division, Vol. 84, No. HY7, pp. 1-35.

Streeter, H. W. and Phelps, E. B. 1925. A study of pollution and natural purification of the Ohio River. U.S. Department of Health, Education and Welfare. Public Health Bulletin, No. 146, Government Printing Office, Washington, D.C., 75p.

Tebbutt, T. H. Y. 1972. Some studies on reaeration in cascades. Water Research, Vol. 6, No. 3, pp. 297-304.

Thackston, E. L. and P. A. Krenkel. 1969. Reaeration prediction in natural streams. Proceedings of the American Society of Civil Engineers, Journal of the Sanitary Engineering Division, Vol. 95, No. SA1, pp. 65-93.

Thames Survey Committee and the Water Pollution Research Laboratory. 1964. Effects of polluting discharges on the Thames Estuary. Water Pollution Research Tech. Paper No. 11. Her Majesty's Stationery Office, London, England, pp. 371-372.

Trewartha, G. T. 1954. An Introduction to Climate. McGraw-Hill Book Company, Inc., New York. 402p.

Truesdale, G. A., A. L. Downing, and G. F. Lowden. 1955. The solubility of oxygen in pure water and sea water. Journal of Applied Chemistry, Vol. 5, No. 2, pp. 53-62.

Tsivoglou, E. C. 1967. Tracer measurement of stream reaeration. Federal Water Pollution Control Administration, U.S. Department of the Interior, Washington, D.C. 86p.

Tsivoglou, E. C. and J. R. Wallace. 1972. Characterization of stream reaeration capacity. Office of Research and Monitoring, U.S. Environmental Protection Agency, EPA-R3-72-012.

Warren, C. E. and P. Doudoroff. 1971. Biology and Water Pollution Control. W. B. Saunders Company, Philadelphia. 434p.

Whipple, G. C. and M. C. Whipple. 1911. Solubility of oxygen in sea water. Journal of the American Chemical Society, Vol. 33, No. 3, pp. 362-365.

Whitman, W. G. 1923. Two-film theory of gas absorption. Chemical and Metallurgical Engineering, Vol. 29, No. 4, pp. 146-148.

Wilson, G. T. and N. Macleod. 1974. A critical appraisal of empirical equations and models for the prediction of the coefficient of reaeration of deoxygenated water. Water Research, Vol. 8, No. 6, pp. 341-366.

Wonnacott, T. H. and R. J. Wonnacott. 1972. Introductory Statistics, 2nd Edition. John Wiley and Sons, Inc., New York, 510p.

APPENDICES

APPENDIX I. LIST OF TERMS

Symbol	Definition	SI Units*	Other Units*	Dimensions**
a	Rate of photosynthesis	$kg/m^3/s$	mg/l/day	$M/L^3/T$
a_s	Activity of gas in solution	-	-	-
A	Surface or interface area	m^2	ft^2	L^2
A_D	Surface area with dye	m^2	ft^2	L^2
A_W	Cross sectional area of stream	m^2	ft^2	L^2
b	Percent of molecules lost from h	-	-	-
b_f	Coefficient for fall pattern of cascades	-	-	-
c	Coefficient or constant	-	-	-
C	Gas or solute concentration	kg/m^3	mg/l	M/L^3
C_A	Surface area increase coefficient	-	-	-
C_L	Concentration of gas in bulk flow	kg/m^3	mg/l	M/L^3
C_s	Saturation concentration	kg/m^3	mg/l	M/L^3
C_s'	Saturation concentration at P_{st}	kg/m^3	mg/l	M/L^3
C_W	Concentration of gas at surface	kg/m^3	mg/l	M/L^3
d	Diameter of a molecule	m	A	L
d_e	Equivalent diameter of a bubble	m	cm	L
d_T	Transitional depth	m	ft	L
D	Gas deficit (C_s-C)	kg/m^3	mg/l, ppm	M/L^3
D_L	Longitudinal mixing coefficient	m/s	ft/day	L/T

Appendix I (continued)

Symbol	Definition	SI Units*	Other Units*	Dimensions**
D_m	Molecular diffusivity	m^2/s	ft^2/s	L^2/T
D_{ox}	Rate of O_2 transfer through the surface	$kg/m^2/s$	$g/m^2/day$	$M/L^2/T$
D_x	Longitudinal dispersion coefficient	m^2/T	$miles^2/day$ ft^2/s	L^2/T
E	Rate of energy dissipation per unit mass	m^2/s^3	ft^2/s^3	L^2/T^3
E_D	Maximum rate of energy dissipation per unit mass	m^2/s^3	ft^2/s^3	L^2/T^3
f	Fugacity of gas above solution	Pascal	mm Hg	M/L·T
f_{ox}	Exchange coefficient	m/s	m/day	L/T
F	Froude number	-	-	-
F_D	Froude number with dye measurements	-	-	-
g	Gravitational constant (32.2 ft/s^2)	m/s^2	ft/s^2	L/T^2
h	Thickness of liquid available for gas loss	m	ft	L
H	Hydraulic depth of a stream	m	ft	L
H_D	Active depth of stream	m	ft	L
H_L	Henry's Law constant	$kg·m^3$/ Pascal	$mg·cm^3$/ mm Hg	L^2/T^2
H_m	Depth above minimum flow	m	ft	L
Ht	Elevation	m	ft	L
I	Injection rate	m^3/s	ml/min	L^3/T
J	Flux of molecules per unit area	-	-	-
k_2	Reaeration coefficient (base 10)	s^{-1}	$days^{-1}$	T^{-1}

Appendix I (continued)

Symbol	Definition	SI Units*	Other Units*	Dimensions**
k_L	Liquid film coefficient (base e)	m/s	ft/day	L/T
k_G	Gas film coefficient (base e)	m/s	ft/day	L/T
k_y	Average eddy diffusivity	m^2/s	ft^2/day	L^2/T
K_1	BOD rate constant (base e)	s^{-1}	$days^{-1}$	T^{-1}
K_2	Reaeration coefficient (base e)	s^{-1}	$days^{-1}$	T^{-1}
K_3	BOD settling rate constant (base e)	s^{-1}	$days^{-1}$	T^{-1}
K_4	Leaching rate constant (base e)	s^{-1}	$days^{-1}$	T^{-1}
K_D	Droplet oxygen transfer coefficient (base e)	s^{-1}	$days^{-1}$	T^{-1}
K_G	Overall gas film coefficient (base e)	s^{-1}	$days^{-1}$	T^{-1}
K_H	Weir drop reaeration coefficient (base e)	s^{-1}	$days^{-1}$	T^{-1}
K_I	Impeller oxygen transfer coefficient (base e)	s^{-1}	$days^{-1}$	T^{-1}
K_L	Overall liquid film coefficient (base e)	m/s	ft/day	L/T
κ	Boltzmann's constant	-	-	-
κ_o	von Karman's constant ($\simeq .4$)	-	-	-
l	mixing length	m	ft	L
L	Ultimate BOD concentration	kg/m^3	mg/l	m/L^3
L_e	Size of square rolling cell	m	cm	L
m	Mass	kg	grams	M
M	Molecular weight of a gas	kg/mole	grams/mole	M

Appendix I (continued)

Symbol	Definition	SI Units*	Other Units*	Dimensions**
M_s	Surface compression modulus	-	-	-
n	Manning's n	-	-	-
n_s	Number of fresh surfaces at the interface	-	-	-
N	Net flux of oxygen per unit area of film	$kg/m^2/s$	$mg/cm^2/s$	$M/L^2/T$
N_o	Avagadro's number (6.023 x 10^{23}) molecules/mole	-	-	-
p	Vapor pressure of water	Pascal	mm Hg	$M/L \cdot T^2$
p_{gas}	Partial pressure of a gas at saturation	Pascal	mm Hg	$M/L \cdot T^2$
p_G	Partial pressure of a gas in the gas phase	Pascal	mm Hg	$M/L \cdot T^2$
p_i	Partial pressure of a gas at the interface	Pascal	mm Hg	$M/L \cdot T^2$
P	Barometric pressure	Pascal	mm Hg	$M/L \cdot T$
P_B	Rate of photosynthesis production by bottom plants	$kg/m^2/s$	$g/m^2/day$	M/L/T
P_{ox}	Rate of oxygen production by photosynthesis	$kg/m^2/s$	$g/m^2/day$	$M/L^2/T$
P_p	Rate of oxygen production by phytoplankton	$kg/m^2/s$	$g/m^2/day$	$M/L^2/T$
P_r	Power of rainfall	$ergs/s \cdot m^2$	watts	$M/L^2/T^3$
P_{st}	Standard barometric pressure	101,308 Pascal	760 mm Hg	$M/L \cdot T^2$
q	Unit discharge	m^2/s	ft^2/s	L^2/T
Q	Discharge	m^3/s	ft^3/s	L^3/T
Q_{ox}	Rate change of dissolved oxygen	$kg/m^2/s$	$g/m^2/day$	$M/L^2/T$

Appendix I (continued)

Symbol	Definition	SI Units*	Other Units*	Dimensions**
r	Renewal rate of surface volume elements	s^{-1}	$days^{-1}$	T^{-1}
r_D	Deficit ratio	-	-	-
r_e	Rate of gas molecules entering fluid	kg/s	-	M/T
r_o	Rate of gas molecules leaving the fluid	kg/s	-	M/T
R	Ideal gas constant	-	l·atm/°K	-
R_h	Hydraulic radius	m	ft	L
R_m	Rate oxygen is respired by bottom deposits	$kg/m^2/s$	$g/m^2/day$	$M/L^2/T$
R_{ox}	Rate oxygen is used for respiration	$kg/m^2/s$	$g/m^2/day$	$M/L^2/T$
R_p	Rate oxygen is respired by unattached photosynthetic organisms	$kg/m^2/s$	$g/m^2/day$	$M/L^2/T$
R_r	Rainfall rate	m/s	cm/s	L/T
R_B	Rate oxygen is respired by bottom plants	$kg/m^2/s$	$g/m^2/day$	$M/L^2/T$
R	The Reynolds number	-	-	-
s	Slope	-	-	-
s'	Sine function of the slope angle	-	-	-
S	slash BOD (unleached)	kg/m^3	mg/l	M/L^3
t	Time	s	days	T
t_D	Time of flow measured by dye	s	days	T
t_e	Contact period	s	days	T
T	temperature	°C	°F, °K	t

Appendix I (continued)

Symbol	Definition	Si Units*	Other Units**	Dimensions**
T_i	Titrant used to gain break-point	l	ml	L^3
T_r	Tebbutt's deficit ratio	-	-	-
u	Deviation of instantaneous velocity from the mean velocity	m/s	ft/s	L/T
u_m	Minimum escape velocity	m/s	ft/s	L/T
U	Mean downstream velocity	m/s	ft/s	L/T
U*	Shear velocity	m/s	ft/s	L/T
U_b	Velocity of a rising bubble	m/s	ft/s	L/T
U_d	Velocity of a falling drop	m/s	ft/s	L/T
U_D	Velocity of dye in stream	m/s	ft/s	L/T
v	Velocity of a molecule	m/s	ft/s	L/T
V	Volume of fluid	m^3	l, ft^3	L^3
V_o	Volume of fluid and air	m^3	l, ft^3	L^3
ω	Weight of a water column	kg	lbs	M
W	Stream width	m	ft	L
W_c	Weir reaeration constant	m^{-1}	ft^{-1}	L^{-1}
W_D	Stream width influenced by dye	m	ft	L
W_p	Wetted perimeter	m	ft	L
X	Distance in longitudinal direction	m	ft	L
χ	Film thickness	m	ft	L
y	Depth from the surface	m	ft	L
ϕ	Surface age distribution function	-	-	-

Appendix I (continued)

Symbol	Definition	SI Units*	Other Units**	Dimensions**
ϕ_F	Coefficient adjusting for general fit	-	-	-
ϕ_s	Coefficient adjusting for channel shape	-	-	-
ϕ_p	Coefficient adjusting for water purity effects	-	-	-
ϕ_T	Coefficient for temperature effects	-	-	-
ϕ_U	Coefficient for velocity distribution	-	-	-
ϕ_{UN}	Coefficient for adjusting units	-	-	-
θ	Age of surface volume elements	s	days	T
ρ	Density	kg/m^3	$slug/ft^3$	M/L^3
σ	Surface tension	Pascal·m	$slug/s^2$	M/T^2
μ	Viscosity of water	Pascal·s	slug/ft·s	M/L·
ν	Kinematic viscosity of water	m^2/s	ft^2/s	L^2/T
ε_y	Momentum transfer coefficient	m^2/s	ft^2/day	L^2/T

*Abbreviations

Symbol	Definition	Symbol	Definition
ft	feet	mm Hg	millimeter mercury
g	grams	s	seconds
kg	kilogram	°C	degrees centigrade
l	liter	°F	degrees fahrenheit
lbs	pounds	°K	degrees Kelvin
m	meters		
mg	milligrams		

** Dimensions

Symbol	Definition
L	Length
M	Mass
T	Time
t	Temperature

APPENDIX II. THE RELATIONSHIP BETWEEN THE OVERALL LIQUID FILM COEFFICIENT AND PARTIAL LIQUID FILM COEFFICIENT

The total drop in concentration across the two phase films can be expressed as:

$$(C_s - C_L) = (C_s - C_i) + (C_i - C_L) \qquad \text{(II-1)}$$

where C_s is the saturation concentration (dependent on the partial pressure of oxygen in the atmosphere) in mg/l, C_L is the concentration in the bulk flow in mg/l, and C_i is the concentration in the interface in mg/l.

The flux of molecules (N) across the gradients can be defined as:

$$N = k_L(C_i - C_L) \qquad \text{(II-2)}$$

$$N = k_G(p_G - p_i) \qquad \text{(II-3)}$$

$$N = K_L(C_s - C_L) \qquad \text{(II-4)}$$

where k_L is the liquid film coefficient in ft/day, k_G is the gas film coefficient in ft/day, K_L is the overall liquid film coefficient in ft/day, N is the flux of molecules in mg/ft^2/day, and p_G and p_i are the partial pressures of oxygen in the atmosphere and at the interface in mm Hg.

Henry's Law constant H (in mg·cm^2/mm Hg) can be used to show that:

Appendix II (continued)

$$p_G = H\ C_s \qquad \text{(II-5)}$$

$$p_i = H\ C_i \qquad \text{(II-6)}$$

Substituting equations 5 and 6 with equation 3 results in the equation:

$$N = k_G\ H(C_s - C_i) \qquad \text{(II-7)}$$

Equations 2, 3, and 7 can be rearranged and substituted into equation 1 to yield the equation:

$$\frac{N}{K_L} = \frac{N}{Hk_G} + \frac{N}{k_L} \qquad \text{(II-8)}$$

Dividing both sides by N simplifies the equation to the form:

$$\frac{1}{K_L} = \frac{1}{Hk_G} + \frac{1}{k_L} \qquad \text{(II-9)}$$

When H is large, as in a sparingly soluble gas like oxygen, the relationship simplifies to the equation:

$$\frac{1}{K_L} = \frac{1}{k_L} \qquad \text{(II-10)}$$

From this development it can be concluded that for sparingly soluble gases, the transfer across the film is dependent on transfer through the liquid volume rather than the gas phase.

APPENDIX III. SOLUBILITY OF DISSOLVED OXYGEN IN PURE WATER AT 760 mm Hg PRESSURE

Temperature °C	Churchill[1]	Montgomery[2]	Truesdale[3]	Whipple & Whipple[4]
0	14.65	14.81	14.16	14.6
1	14.25	14.36	13.77	14.2
2	13.86	13.93	13.40	13.8
3	13.49	13.53	13.05	13.5
4	13.13	13.15	12.70	13.1
5	12.79	12.79	12.37	12.8
6	12.46	12.45	12.06	12.5
7	12.14	12.12	11.76	12.5
8	11.84	11.82	11.47	11.9
9	11.55	11.52	11.19	11.6
10	11.27	11.25	10.92	11.3
11	11.00	10.99	10.67	11.1
12	10.75	10.73	10.43	10.8
13	10.50	10.49	10.20	10.6
14	10.26	10.26	9.98	10.4
15	10.03	10.04	9.76	10.2
16	9.82	9.83	9.56	10.0
17	9.61	9.63	9.37	9.7
18	9.40	9.44	9.18	9.5
19	9.21	9.25	9.01	9.4
20	9.02	9.07	8.84	9.2
21	8.84	8.90	8.68	9.0
22	8.67	8.73	8.53	8.8
23	8.50	8.57	8.38	8.7
24	8.33	8.42	8.25	8.5
25	8.18	8.26	8.11	8.4
26	8.02	8.13	7.99	8.2
27	7.87	7.99	7.86	8.1
28	7.72	7.85	7.75	7.9
29	7.58	7.72	7.64	7.8
30	7.44	7.60	7.53	7.6

[1]Churchill *et al.* (1962): $C_s = 14.652 - 0.41022(T) + 0.0079910(T)^2 - 0.000077774(T^3)$

[2]Montgomery (1964): $C_s = 468/(31.6 + T)$

[3]Truesdale (1955): $C_s = 14.161 - 0.3943(T) + 0.007714(T^2) - 0.0000646(T^3)$

[4]Whipple & Whipple (1911): $C_s = (P - p)\ [(0.678)/(35 + T)]$

APPENDIX IV. VAPOR PRESSURES FOR WATER AT DIFFERENT TEMPERATURES

Temperature °C	Bars	mm of Hg	Pascal
0	0.006,107	4.581	15,511
1	0.006,566	4.925	16,676
2	0.007,055	5.292	17,918
3	0.007,576	5.683	19,242
4	0.008,131	6.099	20,651
5	0.008,721	6.542	22,151
6	0.009,349	7.012	23,743
7	0.010,016	7.513	25,439
8	0.010,725	8.045	27,240
9	0.011,478	8.609	29,150
10	0.012,277	9.209	31,182
11	0.013,124	9.844	33,332
12	0.014,022	10.518	35,614
13	0.014,974	11.231	38,028
14	0.015,982	11.988	40,591
15	0.017,049	12.788	43,300
16	0.018,178	13.635	46,168
17	0.019,373	14.531	49,202
18	0.020,635	15.478	52,409
19	0.021,969	16.478	55,795
20	0.023,378	17.535	59,374
21	0.024,866	18.651	63,152
22	0.026,435	19.828	67,138
23	0.028,091	21.070	71,343
24	0.029,836	22.379	75,775
25	0.031,676	23.759	80,448
26	0.033,613	25.212	85,368
27	0.035,653	26.742	90,548
28	0.037,800	28.352	96,000
29	0.040,058	30.046	101,736
30	0.042,433	31.827	107,766

Source: American Institute of Physics, 1972. American Institute of Physics Handbook. McGraw-Hill Book Company.

APPENDIX V. FIELD DATA

Test Number	Temperature T °C	Calculated Solubility C_s mg/l	Predeaeration Concentration C_s mg/l	Observed Concentration C mg/l	Deficit D mg/l	Length X ft	Mean Velocity U ft/s	Maximum Velocity U_D ft/s	K_{2_T} base e $days^{-1}$	$K_{2_{20}}$ base e $days^{-1}$
				Berry Creek						
	8.00	11.75	10.70	3.20	7.50					
1	8.00	11.75	10.70	3.80	6.90	20	0.030	0.154	10.71	12.96
2	8.00	11.75	10.70	6.10	4.60	90	0.099	0.321	38.43	46.49
	8.00	11.75	10.70	8.90	1.80					
3	8.00	11.75	10.70	9.90	0.80	120	0.141	0.316	82.22	99.48
	11.90	10.72	10.50	0.40	10.10					
4	11.90	10.72	10.50	1.10	9.40	20	0.022	0.115	6.92	7.87
5	11.90	10.72	10.50	6.10	4.40	90	0.081	0.346	59.35	67.49
	11.90	10.72	10.50	9.00	1.50					
6	11.90	10.72	10.50	9.50	1.00	50	0.130	0.321	90.99	103.48
7	11.90	10.72	10.50	10.00	0.50	70	0.162	0.342	138.29	157.27
				Needle Branch						
	8.00	11.66	8.60	1.80	6.80					
8	8.00	11.66	7.90	3.90	4.00	100	0.030	0.067	13.62	16.48
9	8.00	11.66	8.30	6.45	1.85	80	0.017	0.048	14.24	17.22
	11.20	10.85	10.00	6.00	4.00					
10	11.20	10.85	10.00	7.60	2.40	100	0.094	0.177	41.30	47.49
11	11.20	10.85	10.00	8.22	1.78	80	0.044	0.111	14.34	16.48
				Deer Creek						
	9.00	11.47	11.20	3.70	7.50					
12	9.00	11.47	11.40	4.80	6.60	40	0.284	0.800	78.41	93.38
13	9.00	11.47	11.40	5.30	6.10	30	0.229	0.526	51.86	61.76
14	9.00	11.47	11.20	6.40	4.80	80	0.310	0.615	80.29	95.61
15	9.00	11.47	11.00	7.10	3.90	35	0.096	0.219	49.10	58.46
16	9.00	11.47	11.00	7.75	3.25	60	0.089	0.286	23.34	27.80

Appendix V (continued)

Test Number	Temperature T °C	Calculated Solubility C_s mg/l	Predeaeration Concentration C_s mg/l	Observed Concentration C mg/l	Deficit D mg/l	Length X ft	Mean Velocity U ft/s	Maximum Velocity U_D ft/s	K_{2_T} base e $days^{-1}$	$K_{2_{20}}$ base e $days^{-1}$
	11.10	10.82	11.60	3.10	8.50					
17	11.10	10.82	11.60	4.00	7.60	40	0.503	1.081	121.59	140.04
18	11.10	10.82	11.60	4.30	7.30	30	0.486	0.667	56.42	64.98
19	11.10	10.82	11.60	5.50	6.10	80	0.305	0.630	59.21	68.19
20	11.10	10.82	11.60	6.30	5.30	36	0.098	0.330	33.21	38.25
21	11.10	10.82	11.60	7.00	4.60	50	0.116	0.312	28.48	32.81
				Andrews #1						
	12.50	10.00	10.90	4.80	6.10					
22	12.50	10.00	10.90	8.15	2.75	90	0.325	0.732	248.33	279.73
	6.00	11.58	11.50	5.36	6.14					
23	6.00	11.58	11.50	8.18	3.32	90	0.257	0.529	151.36	189.03
				Watershed #3						
	7.00	11.38	12.30	6.60	5.70					
24	7.00	11.38	12.30	8.40	3.90	40	0.496	1.000	406.24	499.35
25	7.00	11.38	12.30	10.20	2.10	65	0.181	0.417	149.24	183.44
26	7.00	11.38	12.30	11.00	1.30	30	1.030	1.667	1422.34	1748.33
	17.60	8.94	9.60	5.40	4.20					
27	17.60	8.94	9.60	6.90	2.70	40	0.546	1.290	521.00	541.23
28	17.60	8.94	9.60	8.12	1.48	65	0.219	0.439	174.75	181.54
29	17.60	8.94	9.60	8.50	1.10	30	1.413	1.579	1207.07	1253.94
				Oak Creek						
	12.10	10.65	9.86	4.21	5.65					
30	12.10	10.65	9.86	5.00	4.86	40	0.030	0.133	9.85	11.17
31	12.10	10.65	9.86	5.65	4.21	61	0.027	0.087	5.37	6.08
32	12.10	10.65	9.86	7.05	2.81	37	0.261	0.551	246.54	279.47

Appendix V (continued)

Test Number	Temperature T °C	Calculated Solubility C_s mg/l	Predeaeration Concentration C_s mg/l	Observed Concentration C mg/l	Deficit D mg/l	Length X ft	Mean Velocity U ft/s	Maximum Velocity U_D ft/s	K_{2_T} base e $days^{-1}$	$K_{2_{20}}$ base e $days^{-1}$
33	12.10	10.65	9.86	7.90	1.96	80	0.090	0.274	34.92	39.58
34	12.10	10.65	9.86	8.60	1.26	70	0.147	0.526	79.95	90.63
	10.00	11.18	11.30	0.60	10.70					
35	10.00	11.18	11.30	1.00	10.30	40	0.053	0.124	4.32	5.06
36	10.00	11.18	11.30	1.40	9.90	61	0.070	0.090	3.92	4.59
37	10.00	11.18	11.30	3.70	7.60	37	0.441	0.738	272.65	319.55
38	10.00	11.18	11.30	3.80	7.50	20	0.168	0.308	9.59	11.23
39	10.00	11.18	11.30	4.80	6.50	60	0.168	0.235	34.61	40.56
40	10.00	11.18	11.30	5.90	5.40	70	0.283	0.737	64.71	75.84
				Andrews #2						
	6.00	11.58	11.10	5.80	5.30					
41	6.00	11.58	11.10	6.50	4.60	50	0.304	0.472	74.44	92.97
	6.00	11.58	11.10	7.60	3.50					
42	6.00	11.58	11.10	7.80	3.30	30	0.271	0.588	45.86	57.28
43	6.00	11.58	11.10	8.10	3.00	10	0.197	0.667	161.86	202.14
	13.10	9.86	10.00	2.80	7.20					
44	13.10	9.86	10.00	3.50	6.50	50	0.453	0.735	80.13	89.40
	13.10	9.86	10.00	5.50	4.50					
45	13.10	9.86	10.00	5.90	4.10	40	0.310	0.755	62.33	69.55

Appendix V (continued)

Test Number	Slope s ft/ft	Mean Unit Energy Dissipation E ft^2/s^3	Maximum Unit Energy Dissipation E_D ft^2/s^3	Depth H ft	Dye Depth H_D ft	Hydraulic Radius R_h ft	Froude Number F	Manning n	Width W ft	Discharge Q ft^3/s
1	0.001	0.001	0.005	0.530	0.127	0.470	0.007	0.961	6.67	0.13
2	0.017	0.055	0.178	0.149	0.068	0.147	0.045	0.559	5.95	0.13
3	0.030	0.136	0.305	0.154	0.125	0.143	0.063	0.508	3.30	0.13
4	0.0005	0.0004	0.002	0.466	0.104	0.465	0.006	0.902	7.55	0.09
5	0.016	0.042	0.178	0.140	0.040	0.141	0.038	0.634	6.55	0.09
6	0.024	0.099	0.244	0.130	0.056	0.121	0.064	0.438	5.03	0.09
7	0.035	0.180	0.380	0.121	0.066	0.103	0.082	0.381	3.97	0.09
8	0.012	0.011	0.025	0.212	0.150	0.212	0.011	1.958	3.00	0.03
9	0.012	0.006	0.018	0.340	0.221	0.277	0.005	4.905	2.85	0.03
10	0.013	0.039	0.074	0.151	0.083	0.139	0.043	0.494	4.08	0.06
11	0.012	0.017	0.042	0.248	0.136	0.305	0.016	1.660	4.00	0.06
12	0.035	0.316	0.888	0.266	0.124	0.268	0.097	0.409	4.83	0.48
13	0.011	0.079	0.181	0.289	0.133	0.278	0.075	0.289	6.88	0.48
14	0.021	0.207	0.411	0.221	0.114	0.204	0.116	0.243	6.86	0.48
15	0.051	0.157	0.358	0.337	0.219	0.427	0.029	1.999	10.01	0.48
16	0.008	0.022	0.069	0.458	0.170	0.490	0.023	0.906	9.88	0.48
17	0.035	0.559	1.201	0.165	0.083	0.156	0.219	0.161	6.25	0.56
18	0.011	0.167	0.229	0.131	0.122	0.131	0.237	0.083	6.87	0.56
19	0.021	0.204	0.421	0.239	0.126	0.232	0.110	0.268	7.08	0.56
20	0.049	0.157	0.526	0.408	0.156	0.435	0.027	1.944	10.87	0.56
21	0.009	0.034	0.091	0.490	0.204	0.515	0.029	0.784	8.81	0.56
22	0.107	1.121	2.524	0.217	0.105	0.196	0.123	0.512	3.53	0.27
23	0.106	0.873	1.801	0.165	0.134	0.158	0.112	0.558	3.52	0.25
24	0.091	1.444	2.914	0.087	0.044	0.086	0.297	0.179	4.33	0.19
25	0.100	0.581	1.335	0.249	0.134	0.213	0.064	0.935	3.41	0.19
26	0.222	7.373	11.932	0.027	0.022	0.026	1.104	0.061	5.13	0.19

Appendix V (continued)

Test Number	Slope s ft/ft	Mean Unit Energy Dissipation E ft^2/s^3	Maximum Unit Energy Dissipation E_D ft^2/s^3	Depth H ft	Dye Depth H_D ft	Hydraulic Radius R_h ft	Froude Number F	Manning n	Width W ft	Discharge Q ft^3/s
27	0.091	1.591	3.760	0.098	0.043	0.097	0.307	0.176	4.34	0.24
28	0.100	0.701	1.408	0.228	0.137	0.232	0.081	0.819	4.00	0.24
29	0.223	10.112	11.304	0.027	0.029	0.026	1.511	0.045	5.33	0.24
30	0.002	0.002	0.009	0.944	0.202	0.759	0.006	1.835	7.48	0.20
31	0.002	0.001	0.005	0.872	0.258	0.755	0.005	1.876	8.94	0.20
32	0.041	0.341	0.721	0.070	0.037	0.065	0.174	0.190	9.73	0.20
33	0.014	0.040	0.121	0.320	0.109	0.309	0.028	0.898	6.68	0.20
34	0.016	0.076	0.274	0.217	0.063	0.214	0.056	0.466	6.02	0.20
35	0.002	0.003	0.008	1.045	0.438	0.860	0.009	1.140	7.76	0.42
36	0.001	0.003	0.004	0.811	0.566	0.652	0.014	0.575	8.20	0.42
37	0.043	0.607	1.018	0.106	0.057	0.081	0.239	0.133	10.03	0.42
38	0.003	0.014	0.025	0.429	0.235	0.393	0.045	0.240	5.81	0.42
39	0.018	0.097	0.136	0.343	0.265	0.316	0.051	0.557	6.74	0.42
40	0.016	0.146	0.380	0.213	0.086	0.210	0.108	0.238	6.60	0.42
41	0.079	0.772	1.197	0.162	0.231	0.181	0.133	0.445	3.68	0.40
42	0.06	0.049	0.107	0.244	0.221	0.249	0.097	0.166	3.08	0.40
43	0.077	0.487	1.653	0.276	0.123	0.263	0.066	0.872	4.88	0.40
44	0.078	1.145	1.856	0.303	0.193	0.262	0.145	0.380	3.39	0.48
45	0.025	0.252	0.614	0.281	0.123	0.277	0.103	0.328	5.19	0.48